Document No. 78SD4218

August 1977

ANALYSIS OF THE

PASSIVE STABILIZATION OF THE

LONG DURATION EXPOSURE FACILITY (LDEF)

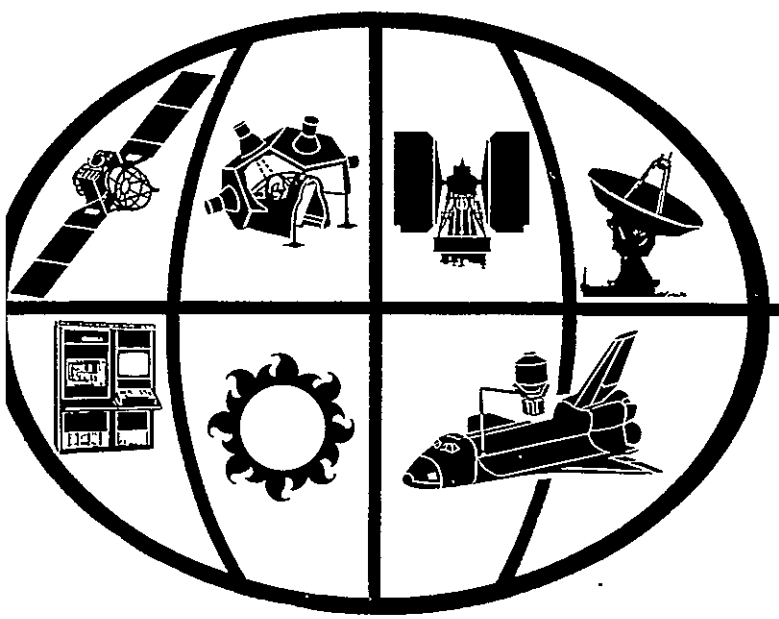

space division

GENERAL ELECTRIC

Document No. 78SD4218

August 1977

ANALYSIS OF THE PASSIVE STABILIZATION OF THE LONG DURATION EXPOSURE FACILITY (LDEF)

Prepared Under

Contract NAS 1-14674

for

Langley Research Center

Prepared by:

S. H. Siegel

N. S. Vishwanath

Approved by:

T. D. McLay
Program Manager

TABLE OF CONTENTS

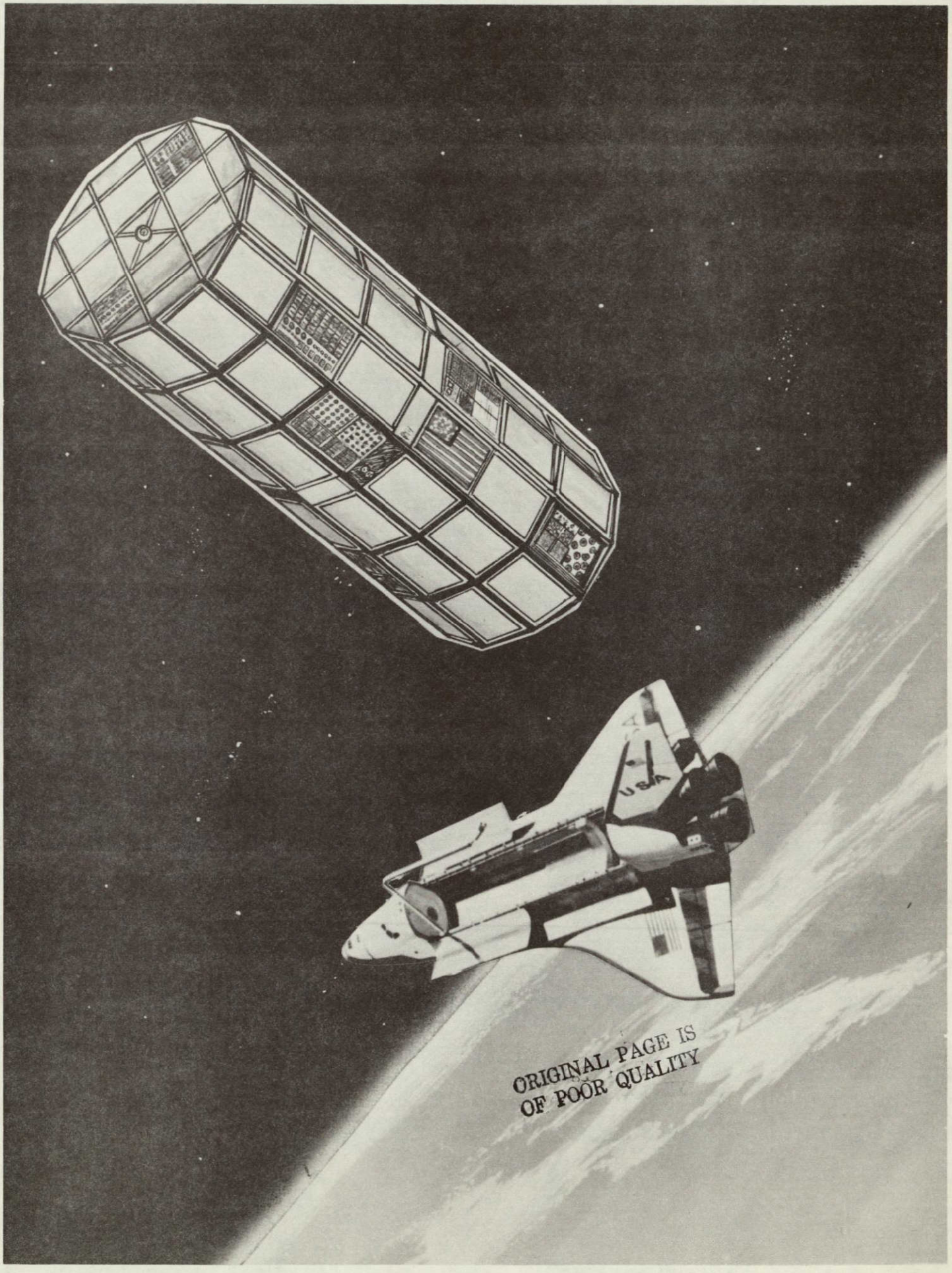

SECTION 1.0

INTRODUCTION

This report, "Analysis of the Passive Stabilization of the Long Duration Exposure Facility", has been prepared for Langley Research Center under contract number NAS 1-14674. It presents the results of a four-month study of the application of an existing design of the Magnetically Anchored Rate Damper to gravity gradient stabilization of the Long Duration Exposure Facility (LDEF). The objectives of this study were to perform the analyses and simulations required to investigate the use of an existing viscous magnetic rate damper for rate stabilizing the LDEF. A wide range of spacecraft mass properties, orbit altitudes and inclinations and disturbance torques was considered with primary emphasis on the spacecraft and mission parameters for the first LDEF flight. The study is divided into two main tasks: (1) Linear Analysis and (2) Simulation. Under the first task linear analyses were performed to determine steady-state errors and transient error time constants as a function of key system parameters. A design range damping constant was selected based upon these results. In the second task a three-axis non-linear digital simulation was used to verify the results of the linear analyses.

All of the measurement values in this study are expressed in English units. The following table is provided for use in conversion to the International System of Units (SI).

SECTION 2.0

SUMMARY AND CONCLUSIONS

2.1 SUMMARY

The nominal LDEF configurations and the anticipated orbit parameters are given in Section 3.1. Using these parameters, a linear steady state analysis was performed. In this analysis the effects of orbit eccentricity, solar pressure, aerodynamic pressure, magnetic dipole, and the magnetically anchored rate damper were evaluated to determine the configuration sensitivity to variations in these parameters. The worst case conditions for steady state errors were identified, and the performance capability calculated.

Garber instability bounds (a linear instability associated with gravity gradient stabilized spacecraft) were evaluated for the range of configurations and damping coefficients under consideration.

The transient damping capabilities of the damper were evaluated, and the time constant as a function of damping coefficient and spacecraft moment of inertia determined. The capture capabilities of the damper were calculated, and the results combined with the steady state, transient, and Garber instability analyses to select damper design parameters.

After completion of the linearized analyses, the performance of the selected configuration (LDEF First Flight) and damper design was simulated on a large three axis digital computer program for the complete non-linear equations of motion. Both steady-state and transient performances were simulated.

2.2 CONCLUSIONS

The LDEF spacecraft can be three-axis stabilized to satisfy (with minor exceptions) specified performance requirements. This is accomplished using the existing design of the Magnetically Anchored Rate Damper. Adequate stability is achieved for the full range of orbit altitudes and for a worst-case set of disturbances. The single requirement that is not met is the yaw pointing requirement. The 30-degree pointing requirement is exceeded by 1.4 degrees for nominal disturbances and by 5.7 degrees for worst-case disturbances. The 10-degree yaw oscillation about a bias position for shuttle retrieval is exceeded by 2 degrees for nominal disturbances and by 3 degrees for worst-case disturbances. Neither of these exceptions are intolerable. All rate requirements are met. The results of the steady-state simulation study are summarized in Table 2.2.1. The first column lists the total range of performance values observed for a nominal set of disturbances and within the nominal range of altitudes. The second column lists the maximum values observed for the total range of altitudes and with worst-case disturbances.

MOTION PARAMETER	BODY AXIS								
	PITCH			ROLL			YAW		
	Altitude, n-mi			Altitude, n-mi			Altitude, n-mi		
	175	215	235	175	215	235	175	215	235
Maximum * Bias Angle -Deg	+1.55 to +1.75	+.55 to +1.1	+.45 to +.95	-.05 to +.1	+.05 to -.2	-.15 to +.05	+31.75 to +32.95	+18.25 to +21.0	+13.9 to +17.8
Maximum * Oscillation about the bias -Deg	1.55 to 1.95	.85 to 1.3	+.75 to +1.05	2.35 to 9.0	+3.25 to +8.2	+3.25 to +7.35	3.35 to 10.15	10.75 to 10.4	+ 8.3 to 11.3
Maximum * Angular Rate -Deg/Sec	.0022 to .0027	.0015 to .0044	.001 to .0013	.0040 to .0179	.0061 to .0143	.0064 to .0146	.0014 to .0065	.0042 to .0069	.0026 to .0070

* The range of value corresponds to a range of damping constant values varying from 1.0 lb-ft-sec to 5.5 lb-ft-sec.

SUMMARY OF STEADY STATE SIMULATION RESULTS

TABLE 2.2.1

The damping constant was specified to be a minimum of 0.9 lb-ft-sec over the entire temperature range of 0-140° F. This specification is based on avoiding the region of Garber instability in the presence of a 2-inch yaw axis CP-CM offset at a 175 nm altitude. The corresponding damping constant is approximately 2.0 lb.-ft.-sec. at 70°F and 5.5 lb.-ft.-sec. at 0°F.

The major sources of both attitude and rate errors are given below. Values are listed in Table 3.2.1.

1) Aerodynamics. Pitch and yaw errors which are caused by yaw and pitch axis offsets between the center-of-pressure and the center-of-mass. These errors vary sharply with altitude.
2) Magnetic dipole. This disturbance causes a yaw error of several degrees. Pitch and roll errors due to this disturbance are insignificant.
3) Rate Damper. At the higher values of damping constant the damper torques are a significant source of error in all three axes.

Capture simulation results are summarized in Table 2.2.2. For maximum anticipated separation rates (.04 deg./sec about all axes) the spacecraft is captured upright. Maximum capture time, with capture arbitrarily defined as that time after which pitch and roll errors remain less than 10 degrees, is 85 hours. For initial rates of 0.1 deg/sec about all axes the upright capture rate is exceeded and the spacecraft tumbles. For the minimum damping constant case tumbling is stopped in 60 hours, and a normal capture occurs. However, for maximum damping, the spacecraft continues to tumble about the pitch axis. This run was continued for 150 hours at which time roll and yaw had settled out but pitch rate remained approximately constant. It is believed this occurs because the damper magnet is nearly aligned with the LDEF pitch axis. As a result, there is no damping about the damper magnet axis. The damper magnet cannot maintain its orientation with respect

to the Earth's field because of the high damping torques which are caused by high initial rates and high damping constant. However, this occurs at low temperatures only and as the temperature increases, damping would decrease and capture would occur.

CAPTURE PARAMETER	TIME PARAMETER	
	Damping	
	Minimum	Maximum
Time to Stop Tumbling - Hours (Initial rates = 0.1 deg/sec on all axes)	60	*
Capture Time - Hours (Initial rates = 0.04 deg/sec on all axes)	85	46
Roll Decay Time Constant - Orbits	20	56
Pitch Decay Time Constant - Orbits	43	21

* Did not capture

SUMMARY OF CAPTURE SIMULATION RESULTS

TABLE 2.2.2

SECTION 3.0

ANALYSIS

The linear analysis is divided into six sections.

1. System Definition. Provides the ground rules of the study such as coordinate systems, spacecraft configuration, performance requirements, damper design, etc.

2. Steady-State Performance. Parameter study for a range of spacecraft mass properties, orbit altitudes, inclinations and disturbance torques.

3. Garber Instability. Describes this dynamic instability and defines the areas in which it will occur.

4. Upright Capture Conditions. Defines the rate-and-attitude requirements for upright capture.

5. Spacecraft Disturbances. Provides an estimate of spacecraft attitude error caused by arbitrary disturbances.

6. Selection of Damping Constant. Gives the step-by step procedure used to select the damping constant.

3.1 System Definition

3.1.1 Coordinate Reference Frames

Orbital Reference Frame

X_R - local vertical, positive up

Y_R - velocity vector, positive forward

Z_R - normal to X_R and Y_R , positive in the direction of orbital rate

Spacecraft Reference Frame

X_S - yaw

Y_S - roll

Z_S - pitch

Notes: (1) When the spacecraft is in its nominal orientation XsYsZs coincide with $X_RY_RZ_R$.

(2) Order of Euler angle rotations are pitch (θ), roll (ϕ), yaw (ψ).

(3) W_x, W_y, W_z are components of the spacecraft rate with respect to the XsYsZs frame.

3.1.2 Spacecraft Mass Properties

Four spacecraft were considered in this study. Three general configurations were designated "light", "nominal" and "heavy". Midway through the study it was decided to place primary emphasis on the first flight spacecraft, and the mass properties for this spacecraft were determined as accurately as possible. This spacecraft was designated "final". Mass properties are listed in Table 3.1.1. All products of inertia were assumed to be zero.

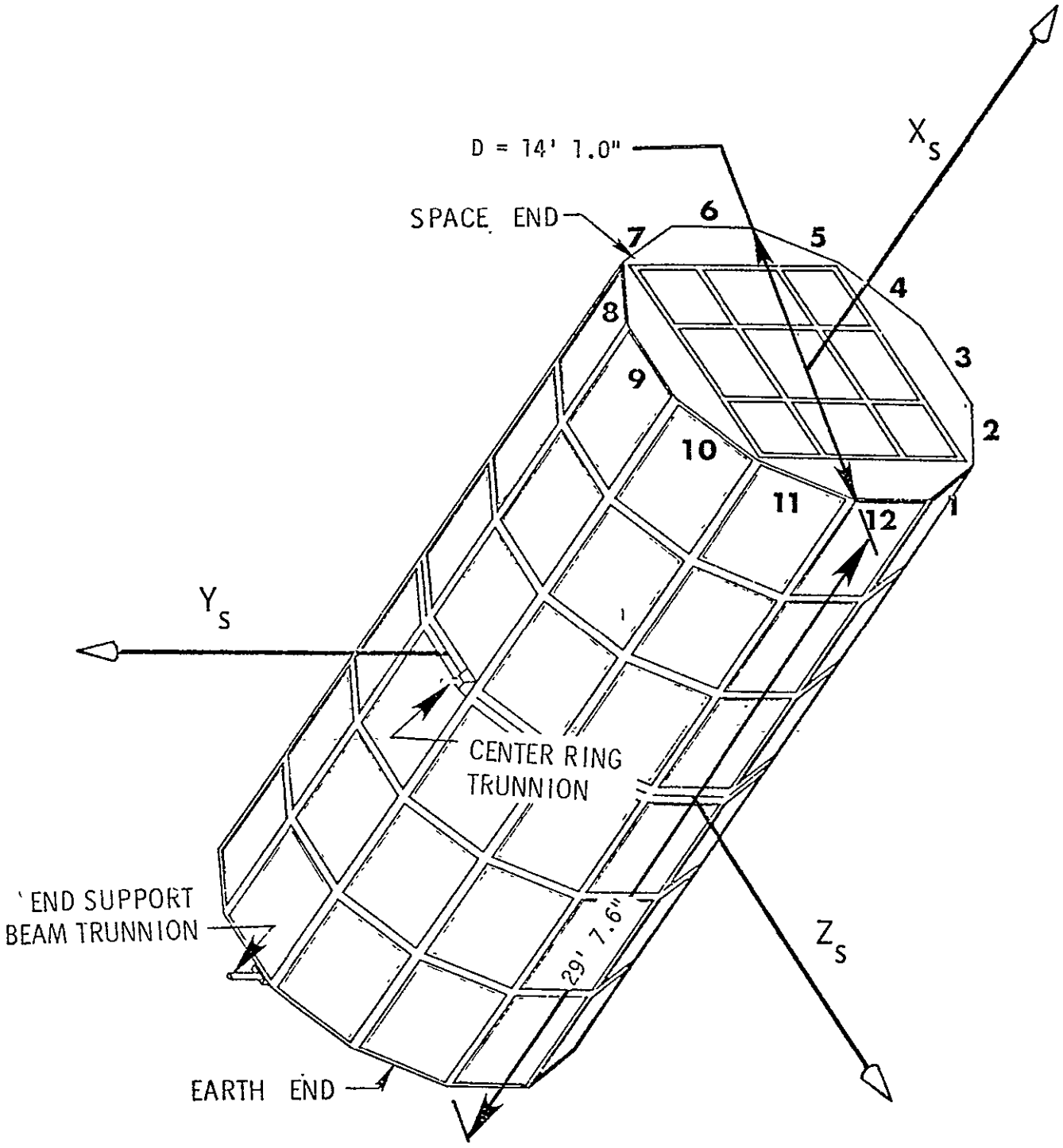

Figure 3.1.1.- LDEF Configuration.

Spacecraft	Weight	Moments of Inertia (slug-Ft^2 x 10^{-3})		
	(Lbs.)	Yaw	Roll	Pitch
Min (Light)	12000	14	40	40.8
Nominal	18000	20	65	66.3
Max (Heavy)	32000	40	115	117.3
Design (Final)	16200	19.2	53.7	54.8

LDEF Mass Properties

Table 3.1.1

3.1.3 Spacecraft Configuration

The LDEF configuration is defined in Figure 3.1.1. For the purposes of this study it was assumed to be a symmetrical closed cylindrical shape consisting of twelve side plates and two end plates. The nominal center-of-mass (CM) location is assumed to be at the geometric center. The end support beam and the trunnions were ignored. Their only effect would be to cause a small shift in the center-of-pressure for solar pressure and aerodynamic torques. It will be shown that solar pressure torque is insignificant. The aerodynamic torque caused by this shift will also be minimized by locating the CM at the calculated value of the CP instead of the geometric center.

Solar energy reflection coefficients for all fourteen plates were assumed to be the following values:

P_A (absorption) = 0.2

P_S (specular reflection) = 0.5

P_D (diffuse reflection) = 0.3

3.1.4 Performance Requirements

Performance requirements are divided among the following items: initial acquisition, experiment pointing and shuttle retrieval. Steady-state performance requirements are listed in Table 3.1.2.

Requirement	Pitch (Deg.)	Roll (Deg.)	Yaw (Deg.)	Rates (Deg./Sec.)
Experiment Pointing	± 10	± 10	0 ± 30 or 180 ± 30	No Requirement
Shuttle Retrieval	± 10	± 10	± 10 with respect to any bias position	.034 for each axis

LDEF Steady-State Performance Requirements

Table 3.1.2

The acquisition requirement is that the LDEF shall reach steady-state retrieval conditions within three months. It is desirable but not mandatory to reach the steady-state experiment pointing conditions within 10 days. Maximum initial rate errors and attitude errors are specified to be 0.04 deg./sec. and 15 degrees respectively per axis.

3.1.5 Orbit Definition

Orbit altitude (nm)

Total Range 175-300

First LDEF flight

Release 235 (min.)

Nominal Retrieval 215

Contingency Retrieval 175

Orbit Inclination (deg.)

Total Range 28.5 - 57

First LDEF Flight 28.5

Eccentricity 0.002

The argument of perigee and the right ascension of the ascending node are unrestricted and can assume any value.

3.1.6 Spacecraft Natural Frequencies

It is useful to determine the natural frequency and coefficient of damping in each axis considering the equations of motion to be a damped single-axis spring-mass system. The equation of motion is

$$I\ddot{\theta} + b\dot{\theta} + K\theta = 0$$

where I = moment of inertia

b = damping constant

K = gravity - gradient spring constant

The characteristic equation of this system is

$$S^2 + \frac{b}{I} s + \frac{K}{I} = 0$$

The natural frequency, damping coefficient and time constant are respectively:

$$Wn = \sqrt{\frac{K}{I}}$$

$$\zeta = \frac{b}{2IW_n}$$

$$\tau = \frac{1}{\zeta W_n}$$

These values have been calculated for the first flight configuration and are listed in Table 3.1.3 for damping constants from 1-6 lb-ft/rad./sec.

Parameter	Body Axis		
	Pitch	Roll	Yaw
Natural Frequency/Orbit Rate	1.374	1.628	0.239
Period of Natural Frequency a) Hours b) Orbits	 1.12 0.73	 0.94 0.61	 6.43 4.18
Damping Coefficient a) B = 1 Ft-lb-sec b) B = 6 Ft-lb-sec	 .00585 .0351	 .00504 .0302	 .0959 .575
Time Constant (orbits) a) B = 1 Ft-lb-sec b) B = 6 Ft-lb-sec	 19.80 3.30	 19.40 3.24	 6.93 1.16
Stiffness (Lb-ft/deg.) at 215 nm	.00233	.00320	2.47×10^{-5}

CHARACTERISTICS OF LDEF MOTION FOR

FIRST FLIGHT CONFIGURATION

TABLE 3.1.3

3.2 Steady-State Performance

There are five sources of attitude error for the LDEF gravity gradient stabilized spacecraft; the magnetically anchored rate damper, solar torque, magnetic torque, orbit eccentricity, and aerodynamic torque. The magnitude and nature of the torques, in conjunction with the spacecraft parameters, determine the pointing accuracy and capture capability of the spacecraft. A linear analysis program was used to perform a parameter variation study. The effects of each of these disturbances on steady-state attitude error was determined for a range of spacecraft and orbit parameters values.

The analysis program calculates disturbance torques at equal increments around the orbit. The frequency components of the torque are computed by Fourier analysis. Three torque coefficients are calculated for each axis; static, orbital, and twice orbital. Higher harmonics are not calculated since they produce negligible attitude errors. Steady-state damper torques are calculated assuming the spacecraft is perfectly oriented, and that the damper magnet exactly follows the earth's magnetic field. For simplicity, the earth's magnetic field is assumed to be a simple dipole field oriented along the spin axis of the earth. The rate of change of the magnetic field vector with respect to the orbiting coordinate system is determined, and the instantaneous torque calculated. Attitude error is calculated for each harmonic by dividing the total torque applied to the spacecraft by the stiffness at the frequency of interest. Although the program calculates individual errors for each harmonic the results in most cases have been combined into a single root-sum-square value. This

has been done to present the results in a more concise, and therefore more meaningful manner. Where an individual component of error is important (for example, pitch bias caused by aerodynamics) that component is presented separately. The following sections describe each of the disturbance torques, and their effect upon the spacecraft performance.

3.2.1 Magnetically Anchored Rate Damper Torque

The magnetically anchored rate damper is a GE developed component designed to damp large amplitude oscillations of gravity gradient stabilized spacecraft. The viscous fluid version of the damper is shown in Figure 3.2.1. It consists of an inner sphere, which contains a permanent magnet and bellows; and an outer sphere that is constructed of pyrolitic graphite (for diamagnetic centering) and aluminum. The space between the spheres, and inside the bellows, is filled with Silicone oil, with a viscosity selected to provide the required damping coeffient.

The mechanism of damping depends upon the relative rate of rotation of the inner sphere of the damper, and the outer sphere; which is rigidly attached to the spacecraft. During spacecraft acquisition and capture, the relative motion is largely the result of motions of the spacecraft. After the spacecraft has stabilized, however, relative motion continues to exist because the magnet follows the Earth's magnetic field, not the local vertical. The damping torques then become disturbance torques to the spacecraft and contribute to the overall pointing inaccuracy. The amplitude of this error is a linear function of the damping constant, and decreasing the damping level will

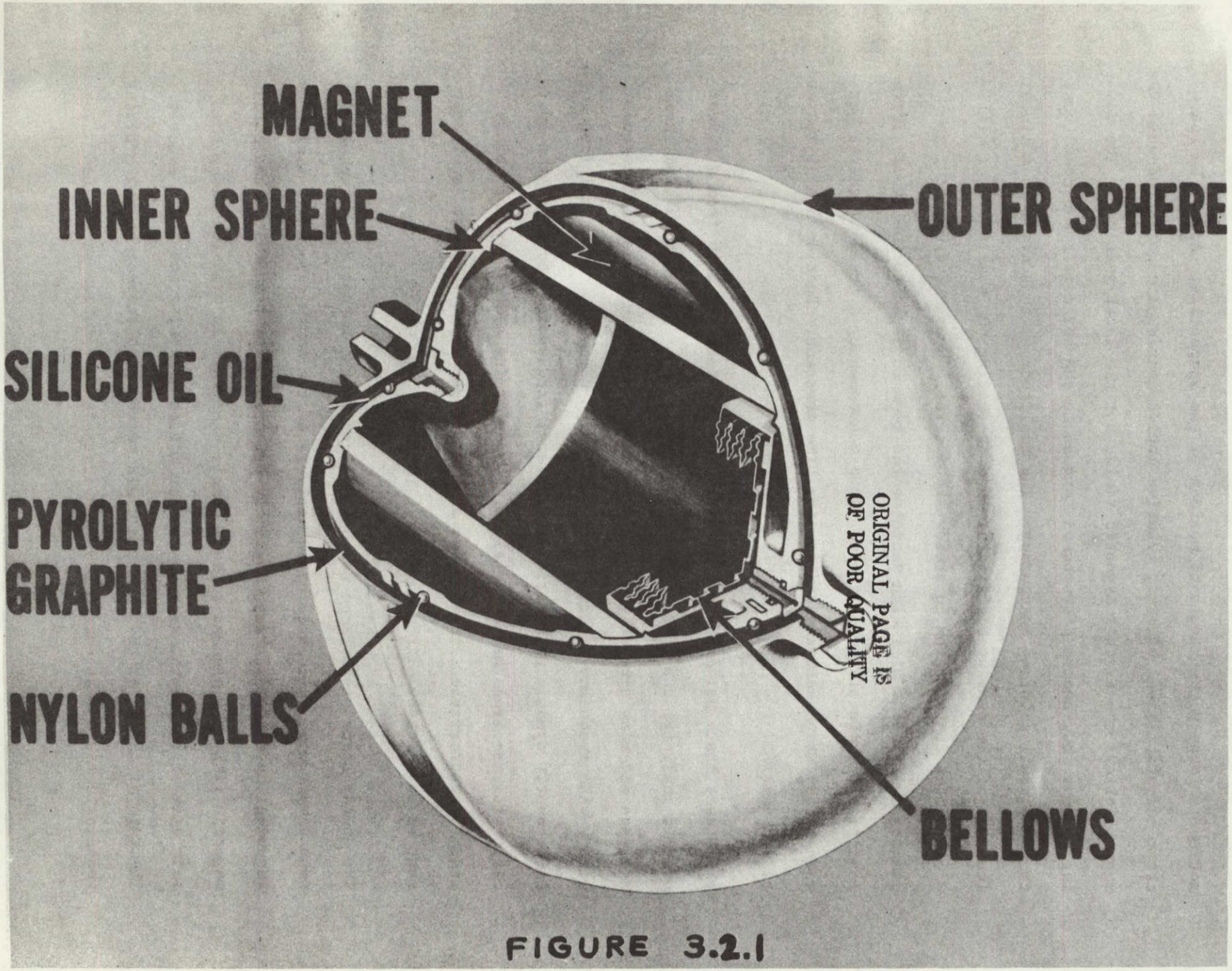
MAGNET
INNER SPHERE
OUTER SPHERE
SILICONE OIL
PYROLYTIC GRAPHITE
NYLON BALLS
BELLOWS
ORIGINAL PAGE IS OF POOR QUALITY

FIGURE 3.2.1

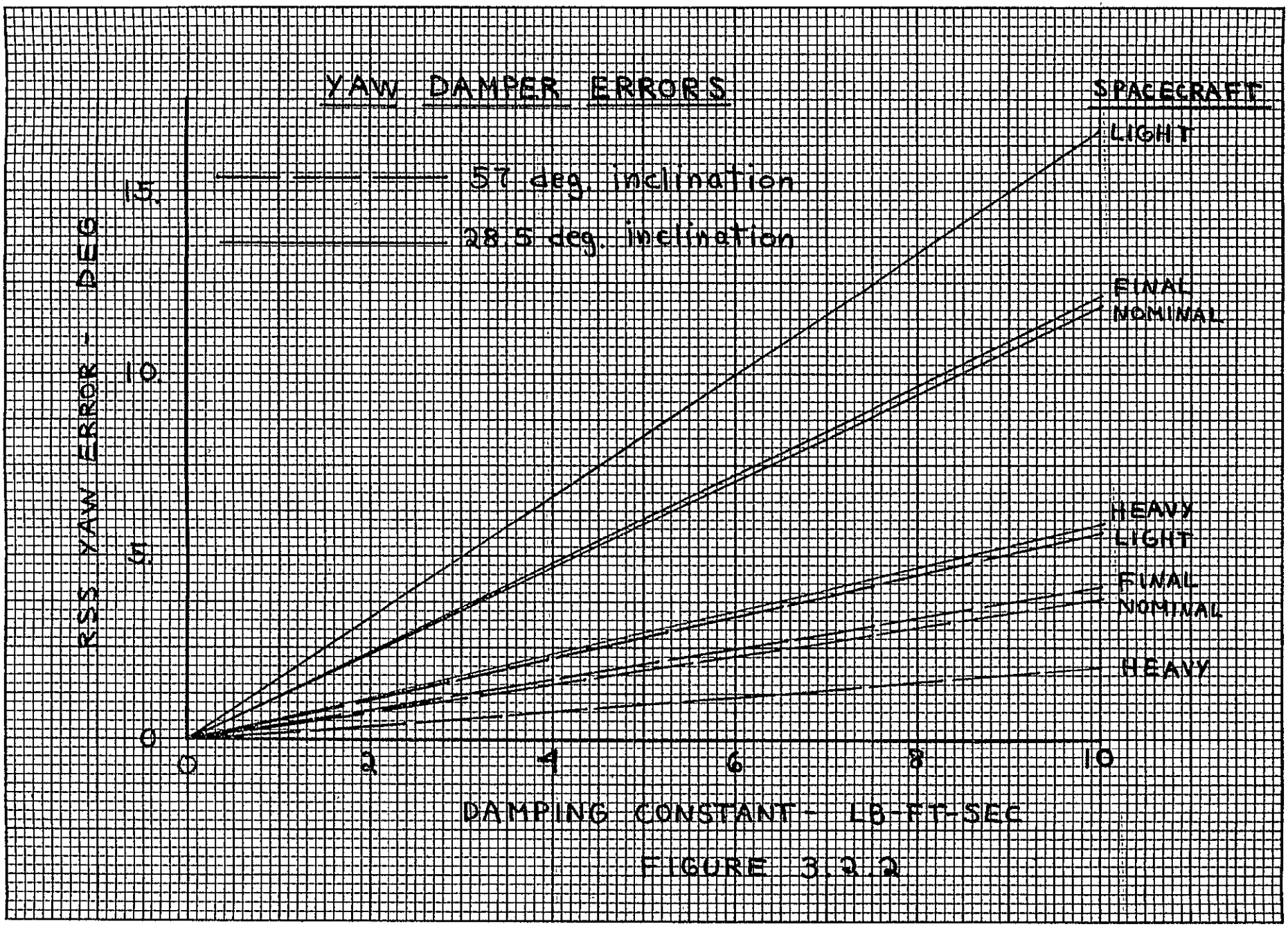
YAW DAMPER ERRORS
57 deg. inclination
28.5 deg. inclination
SPACECRAFT
LIGHT
FINAL NOMINAL
HEAVY LIGHT
FINAL NOMINAL
HEAVY
RESULTANT YAW ERROR - DEG
15.
10.
5.
0
0
2
4
6
8
10
DAMPING CONSTANT - LB-FT-SEC

FIGURE 3.2.2

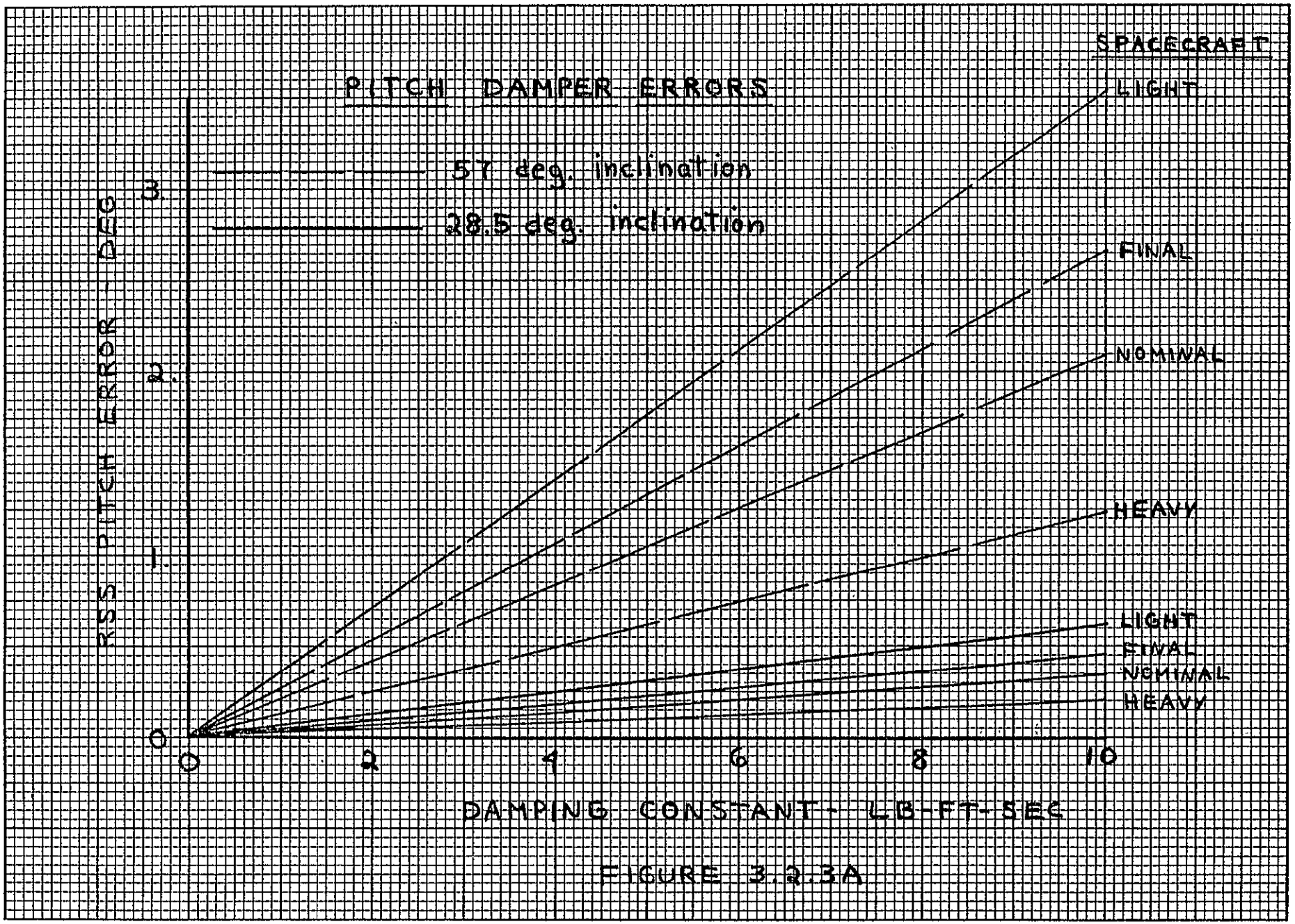

FIGURE 3.2.3A

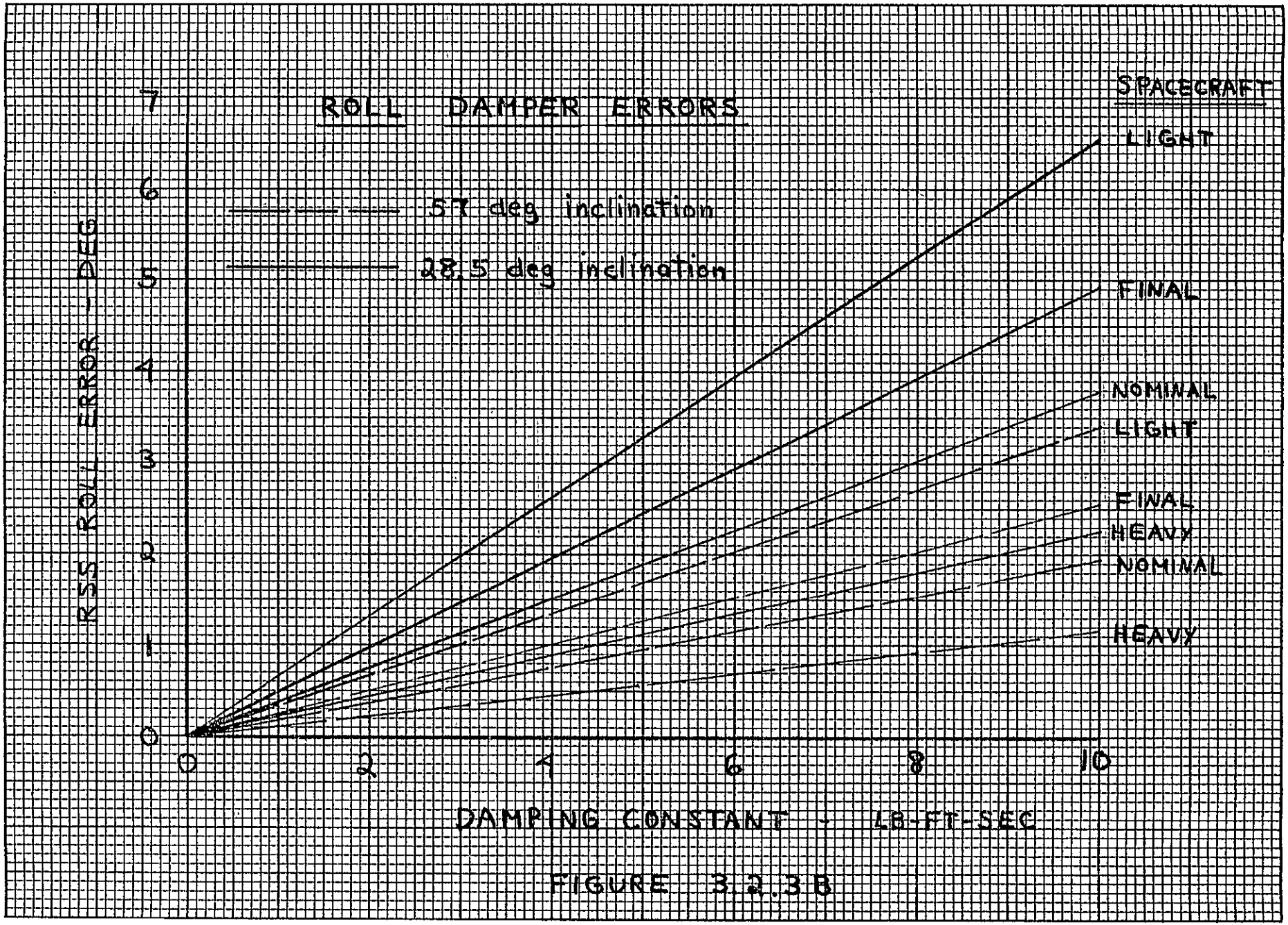
ROLL DAMPER ERRORS
57 deg inclination
28.5 deg inclination
SPACECRAFT
LIGHT
FINAL
NOMINAL
LIGHT
FINAL
HEAVY
NOMINAL
HEAVY
RSS ROLL ERROR - DEG
0
1
2
3
4
5
6
7
0
2
4
6
8
10
DAMPING CONSTANT - LB-FT-SEC

FIGURE 3.2.3 B

3.2.2 Aerodynamic Torque

At altitudes of between 175 and 300 nm, the earth's atmosphere is a major source of disturbance to the LDEF. The dynamic pressure (the familiar $1/2\ \rho v^2$) caused by the spacecraft's passage through the rarified atmosphere can exceed solar pressure by a factor of over 200. Aerodynamic pressure is directly proportional to the aerodynamic density, and to estimate the density, a model of the earth's atmosphere is required. There are several atmospheric models in existence the most widely used being that of JACCHIA [1]. This model defines the atmospheric density as a function of altitude, solar sun spot cycle (F 10.7 cm solar flux) and diurnal bulge. The diurnal bulge is a "thickening" of the earth's atmosphere due to the earth temperature increase associated with solar heating. Typically, the greatest density occurs at 2 p.m. local time, where the density may be a factor of three higher than on the opposite side of the earth (at this altitude). The density difference is greater at higher altitudes.

Aerodynamic torques, like solar torques, are dependent upon the spacecraft configuration, but are particularly sensitive to orbit altitude, solar activity, orbit eccentricity, argument of perigee, and position of the orbit with respect to the diurnal bulge.

A general aerodynamic study was performed for LDEF, since it was anticipated that aerodynamic effects would be the largest source of disturbance torque. Four factors considered in the analysis were spacecraft configuration, orbit eccentricity, argument of perigeee, and ascending node. The 10.7 cm solar flux index was selected to be 200, which is approximately the maximum 2 σ value for the 1978-1989 time period. A plot of this index is shown in Figure 3.2-4 (Reference 2). Drag coefficient is a function of several variables including altitude, exospheric temperature, type of reflection and shape. Calculations were made based upon equations

presented in Reference 3 and are plotted in Figure 3.2-5. A drag coefficient value of 2.2 provides a conservative result..

Figure 3.2.4(a) shows the variation of atmospheric density with respect to the orbital position.

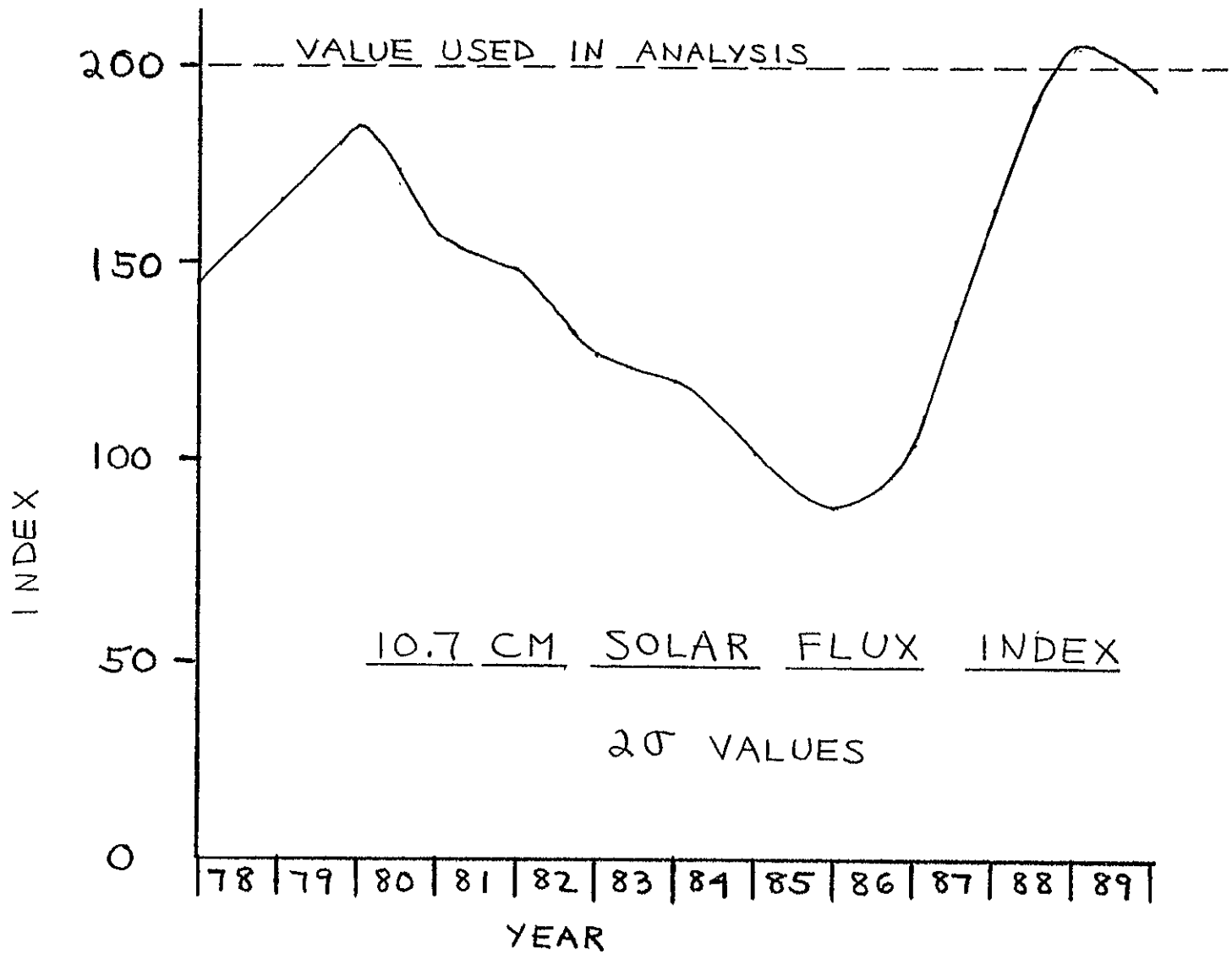
VALUE USED IN ANALYSIS
200
150
100
50
0
INDEX
10.7 CM SOLAR FLUX INDEX
2σ VALUES
78
79
80
81
82
83
84
85
86
87
88
89
YEAR

fig 3.2.4

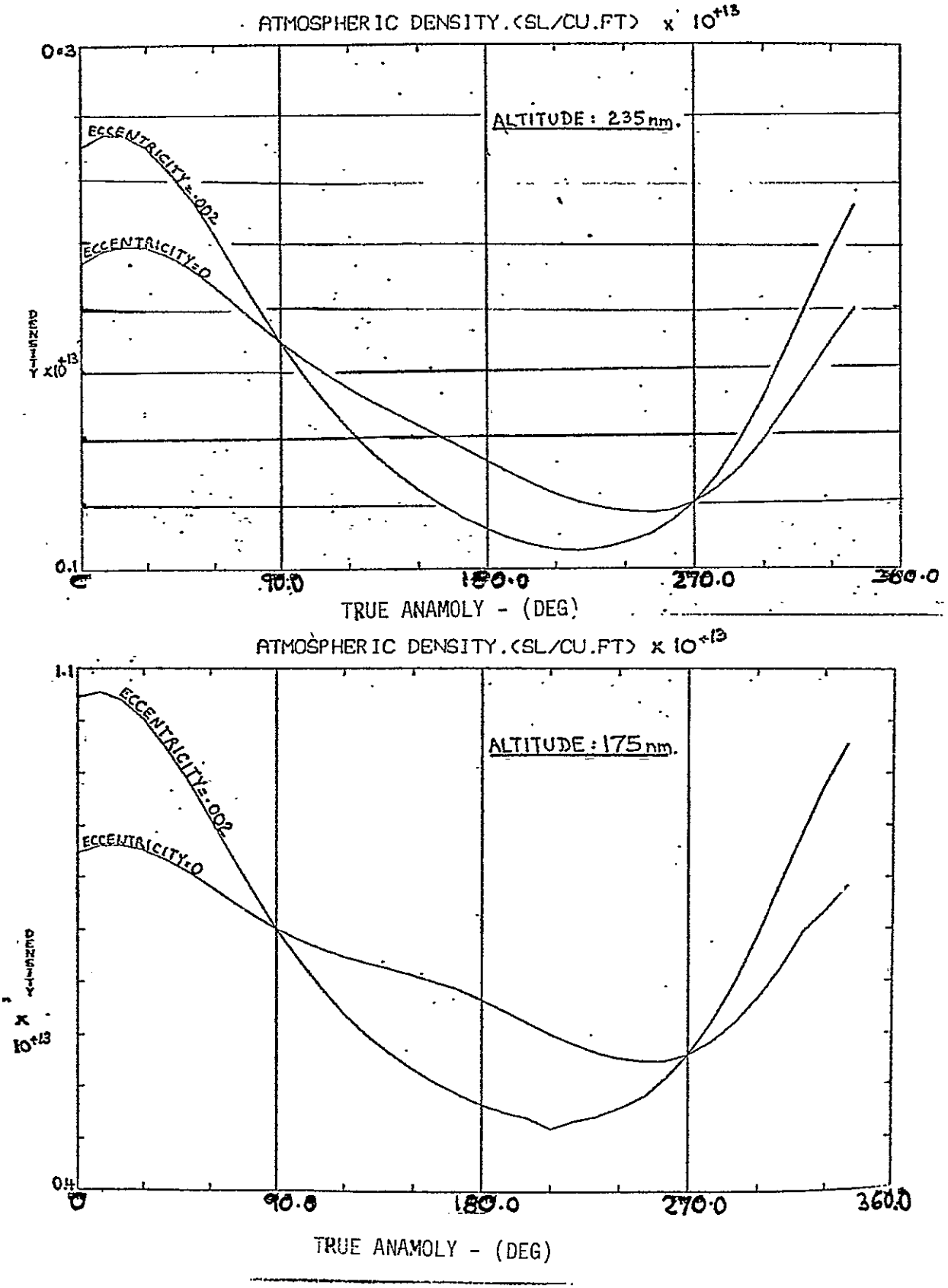

FIGURE 3.2.4-(a) ATMOSPHERIC DENSITY VARIATION

AERODYNAMIC DRAG COEFFICIENT

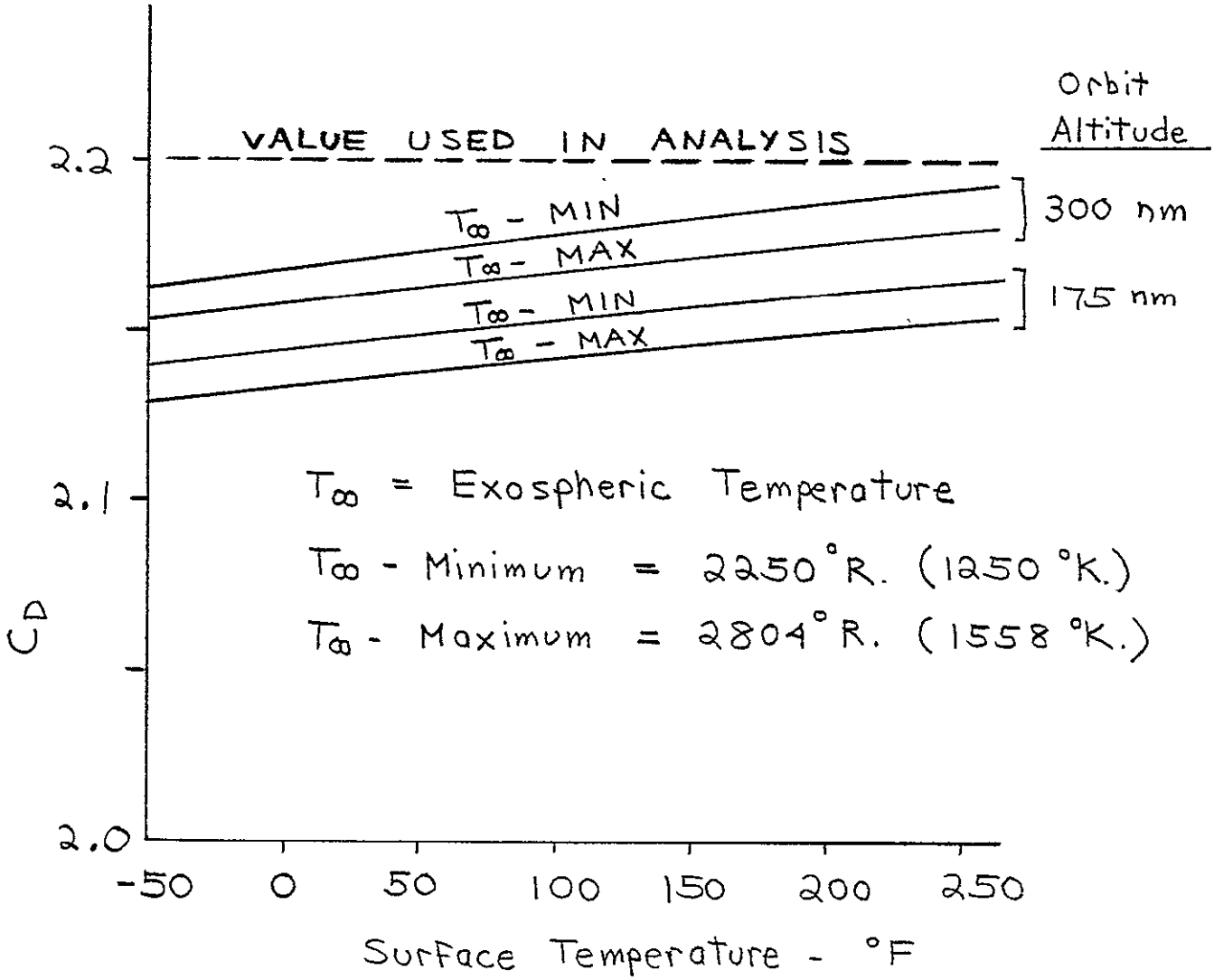

fig. 3.2.5

The LDEF spacecraft is symmetrical, and the aerodynamic torques would be negligible if the center of aerodynamic pressure coincided with the center of mass. The effect of angle of attack between the aerodynamic stream and the spacecraft, is insignificant because the angle of attack is relatively constant. Any shift in the center of mass from the center of geometry will, however, produce an aerodynamic torque, and hence an attitude error.

The effects of an offset between the center-of-pressure (CP) and the center-of-mass (CM) are shown in Figures 3-2.6 to 3-2.12 inclusive. Torques were calculated for an orbit eccentricity of 0.002 with an ascending node position of 2 P.M. Perigee was located at the 2 P.M. position to provide maximum disturbance torque. Figure 3-2.13 shows how errors vary with ascending node position.

The primary effects of aerodynamic torques are:

1) Pitch bias caused by a yaw axis CP-CM offset. (Figure 3-2.7).
   It can be seen that at the minimum altitude of 175 nm a 1" CP-CM offset results in a 1-degree pitch bias. Pitch bias must be limited to prevent Garber instability (See Section 3.3).

2) Yaw error caused by a pitch axis CP-CM offset. (Figure 3.2-10).
   Because yaw stiffness is much lower than roll or pitch, small CP-CM offsets produce large errors. For example at nominal retrieval altitude of 215 nm a 1-inch CP-CM offset causes a peak yaw error of 35 degrees. (This result is obtained by noting the final spacecraft configuration lies midway between the light and nominal spacecraft.)

Other aerodynamic errors are relatively small. It should be pointed out that the yaw errors that result from a roll axis CP-CM offset are caused by the atmosphere rotating with the earth (Figures 3-2.8 and 3-2.12).

3.2.3 Magnetic Dipole Torque

In addition to indirectly causing a spacecraft torque through the magnetically anchored rate damper, the earth's magnetic field can produce a direct magnetic torque. Any magnetic dipole, caused by magnetic materials mounted on the spacecraft, will attempt to align itself to the earth's magnetic field and will torque the spacecraft. The magnitude of the torque is proportional to the strength of the magnetic dipole moment, the orientation of the dipole within the spacecraft, and the location of the spacecraft with respect to the earth. The magnetic field strength decreases with the cube of the orbit radius (exactly the same as gravity gradient), and is twice as strong at the poles (north and south) as at the equator.

Hence, a spacecraft in a high inclination orbit has more magnetic torque on it than a spacecraft in a low inclination orbit, and similarly a spacecraft at a high altitude has less torque on it than a spacecraft at low altitude.

To quantitatively determine the magnitude of the attitude errors, the frequency of the magnetic disturbance torques must be known. At low altitudes, the magnetic field in S/C frame changes as the spacecraft moves in orbit, and the magnetic torque changes as a function of time. For orbit periods short compared to earth's rotational period, the torques (pitch, roll and yaw) are largely constant (zero frequency) and sinusoidal at orbital frequency, depending upon dipole orientation and orbit inclination.

A magnetic analysis was performed with the same magnetic field assumptions as those of Section 3.2.1 except direct magnetic torques were considered. Torques are present on all axes, being exclusively sinusoidal at orbital frequency on pitch, and constant plus sinusoidal at orbital frequency on roll and yaw. In low inclinations the roll and yaw magnetic dipoles are the most effective, producing static torque on yaw and roll (respectively), with the pitch axis dipole producing only small sinusoidal roll and yaw torques.

The magnitudes of the magnetic torques are directly proportional to the size of the spacecraft magnetic moment. In general, this dipole is not known in advance of the spacecraft construction, and varies with payload.

Attitude error as a function of dipole are shown in Figures 3-2.14 and 3-2.15. Errors can be considered to be independent of altitude for the range of 175-300 nm. For dipoles below 10,000 pole-cm about each axis pitch and roll errors are insignificant. However, yaw error is approximately 7 degrees.

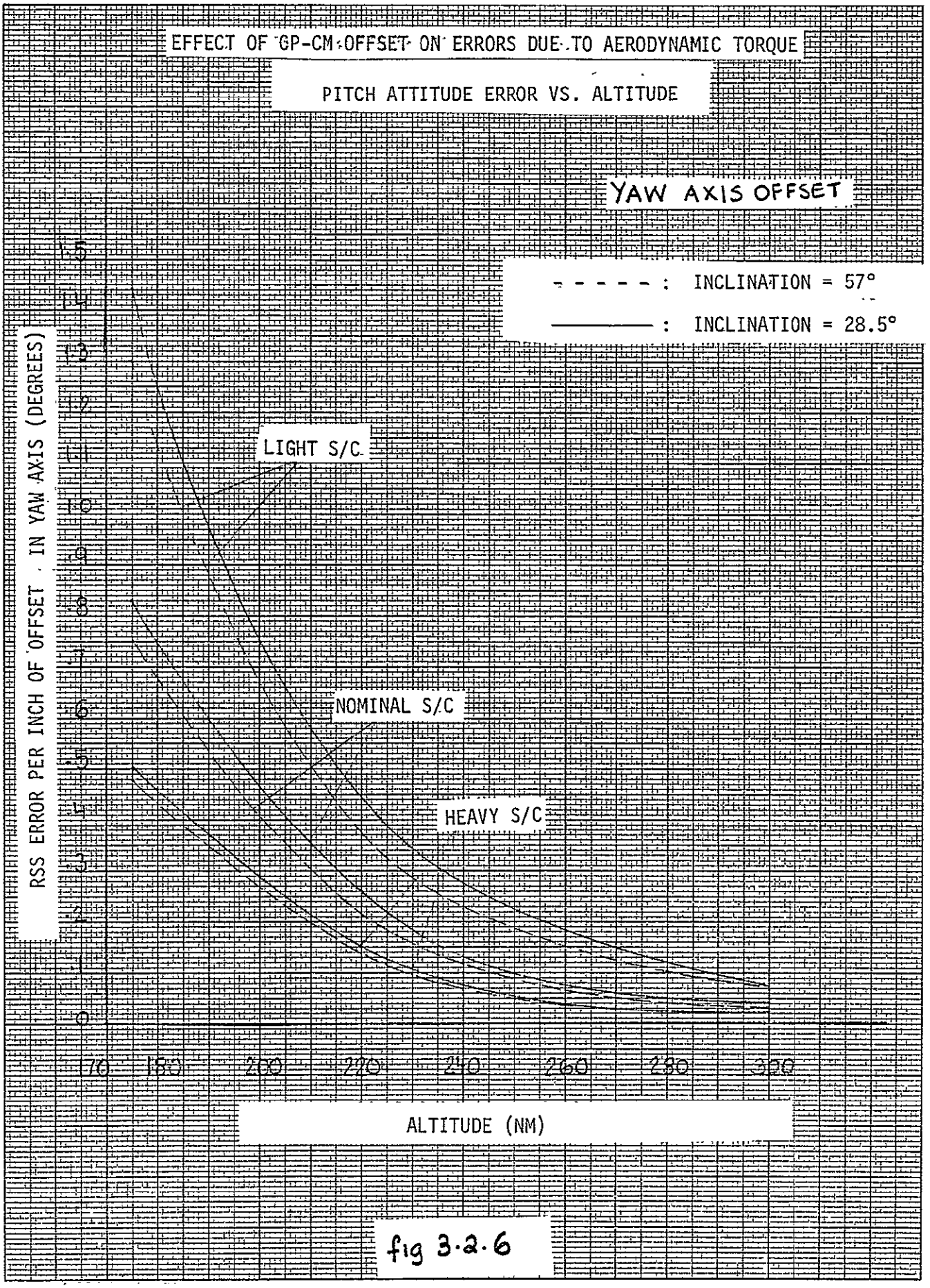

fig 3.2.6

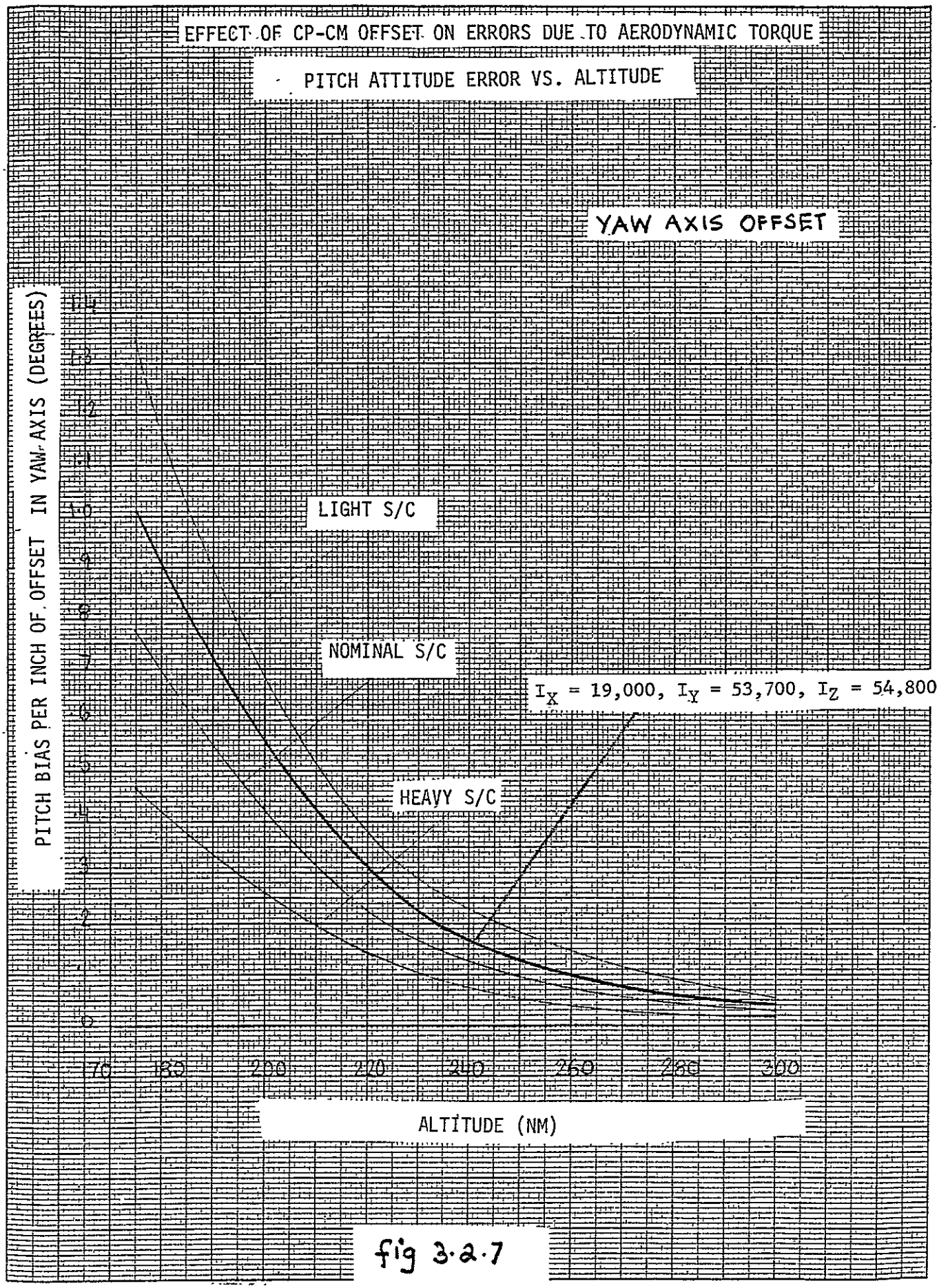

fig 3.2.7

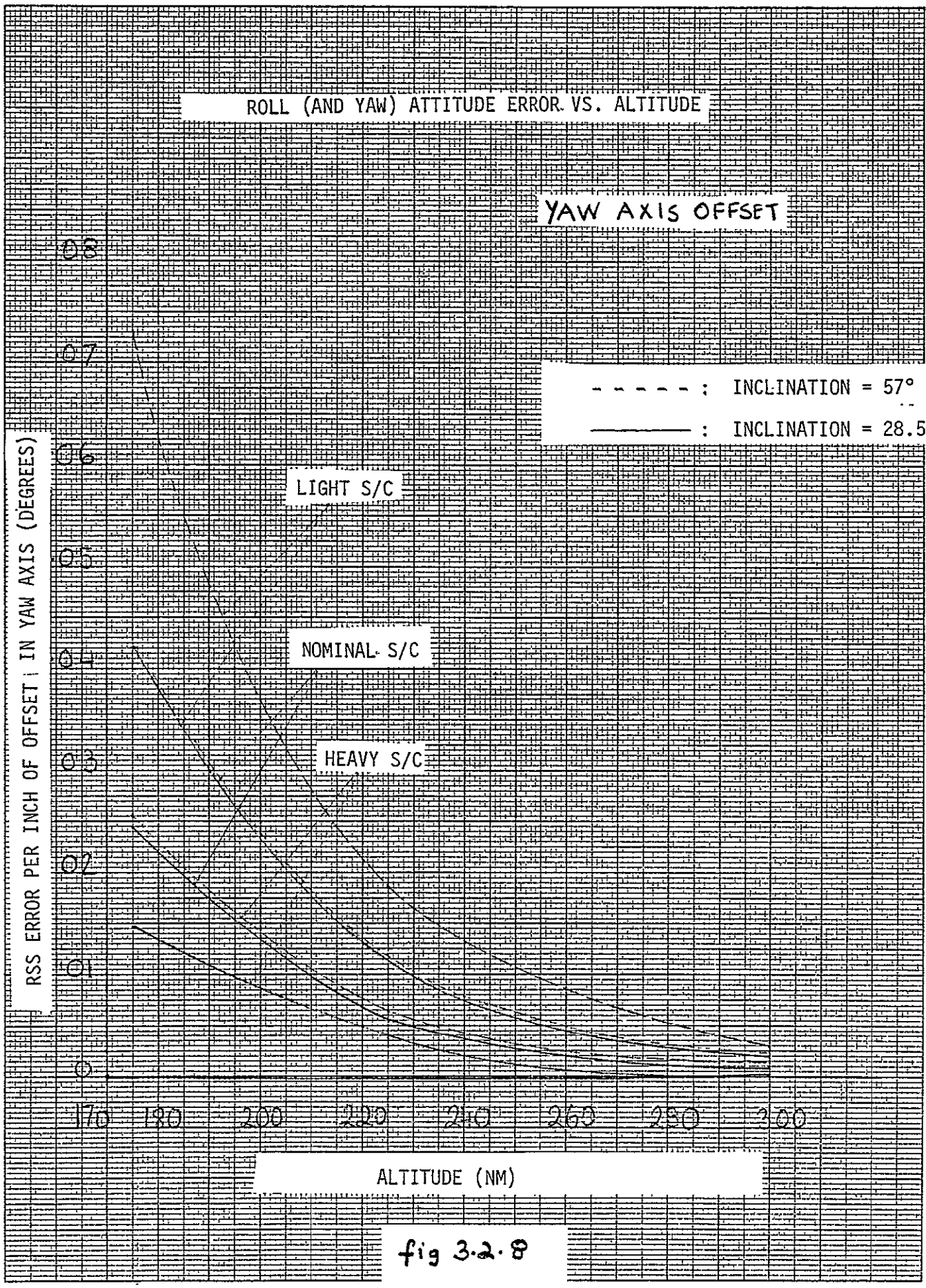

fig 3.2.8

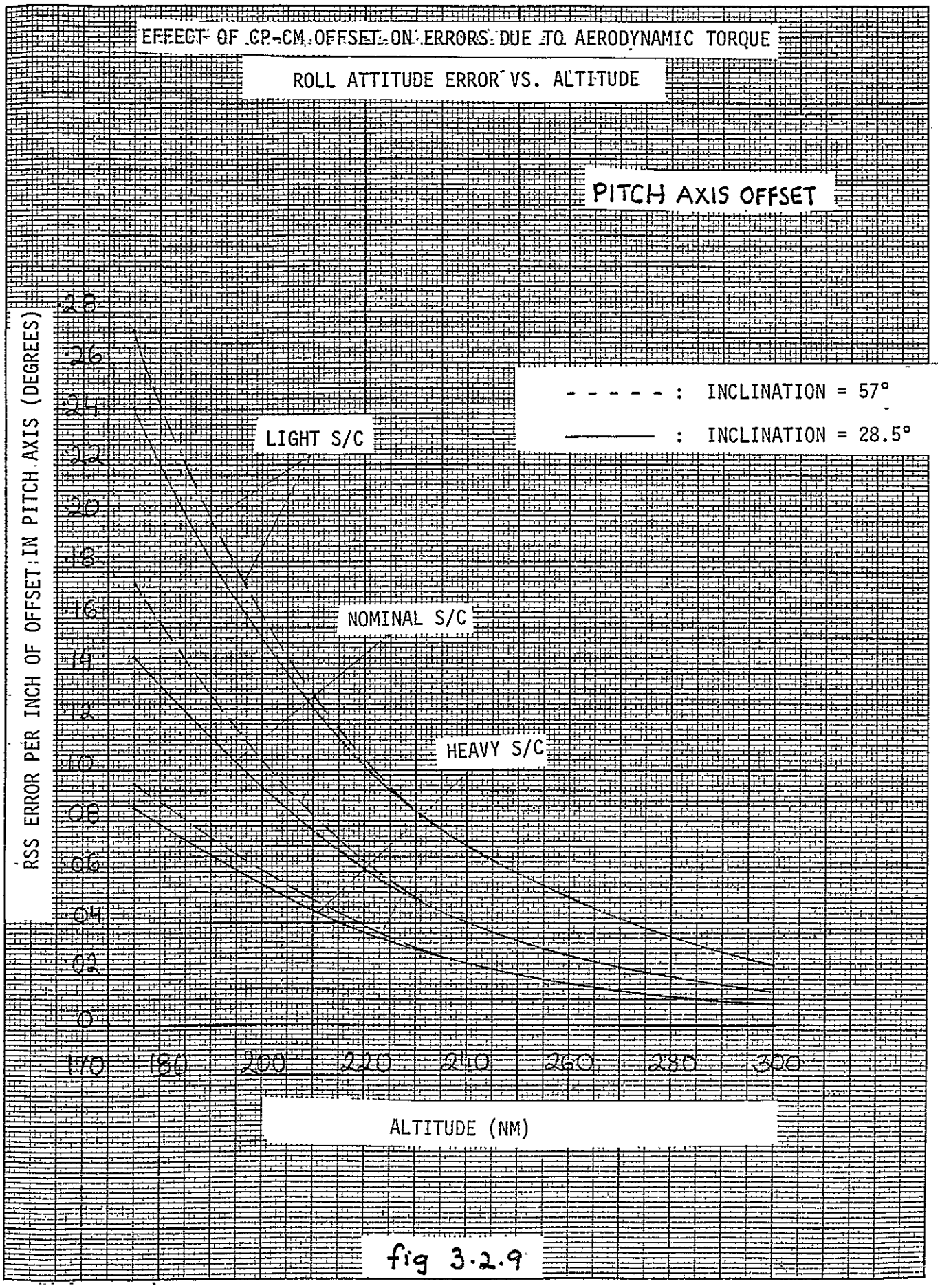

fig 3.2.9

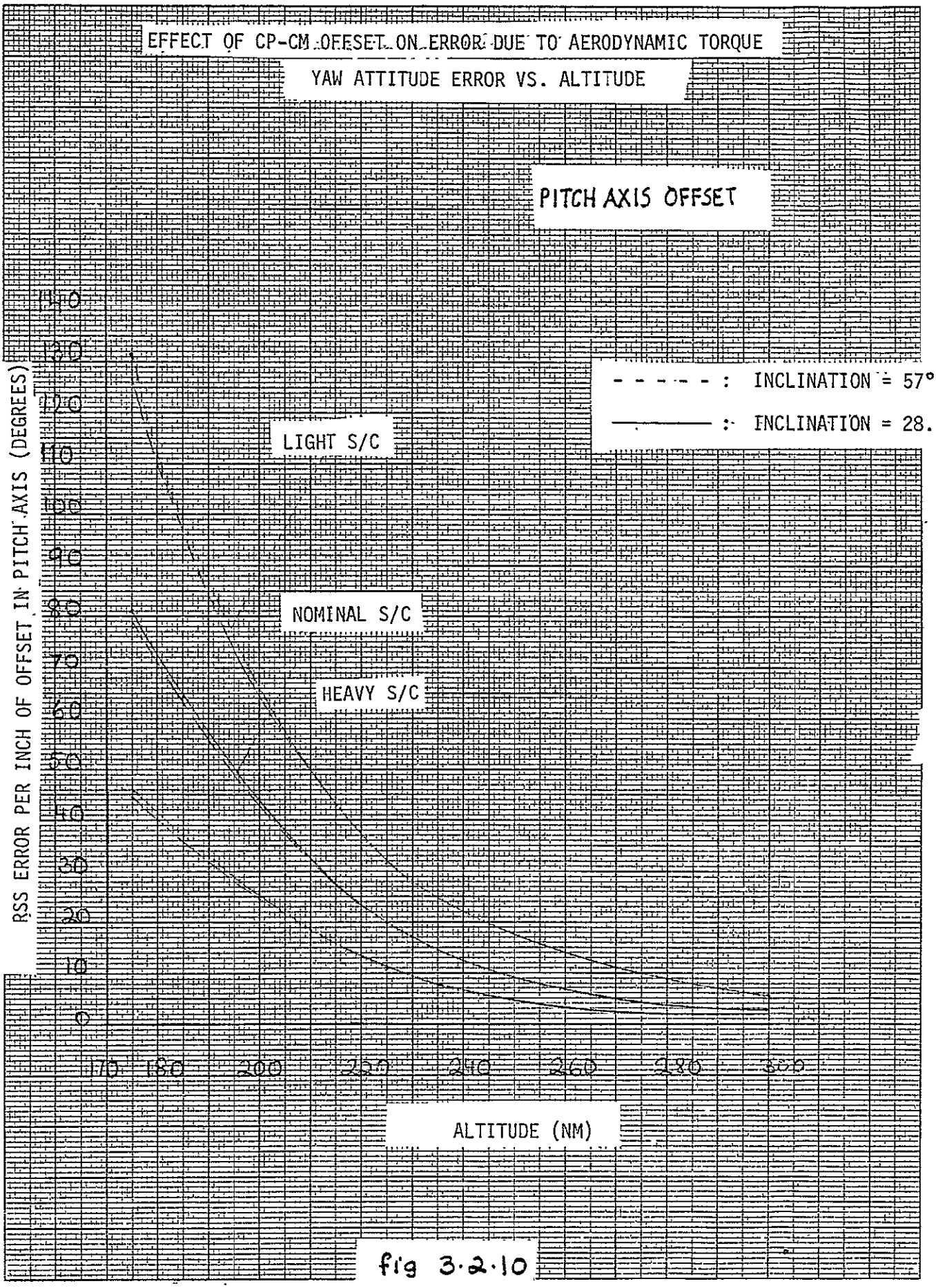
EFFECT OF CP-CM OFFSET ON ERROR DUE TO AERODYNAMIC TORQUE
YAW ATTITUDE ERROR VS. ALTITUDE
PITCH AXIS OFFSET
- - - - - : INCLINATION = 57°
——— : INCLINATION = 28.5°
LIGHT S/C
NOMINAL S/C
HEAVY S/C
RSS ERROR PER INCH OF OFFSET IN PITCH AXIS (DEGREES)
140
130
120
110
100
90
80
70
60
50
40
30
20
10
0
170
180
200
220
240
260
280
300
ALTITUDE (NM)

fig 3.2.10

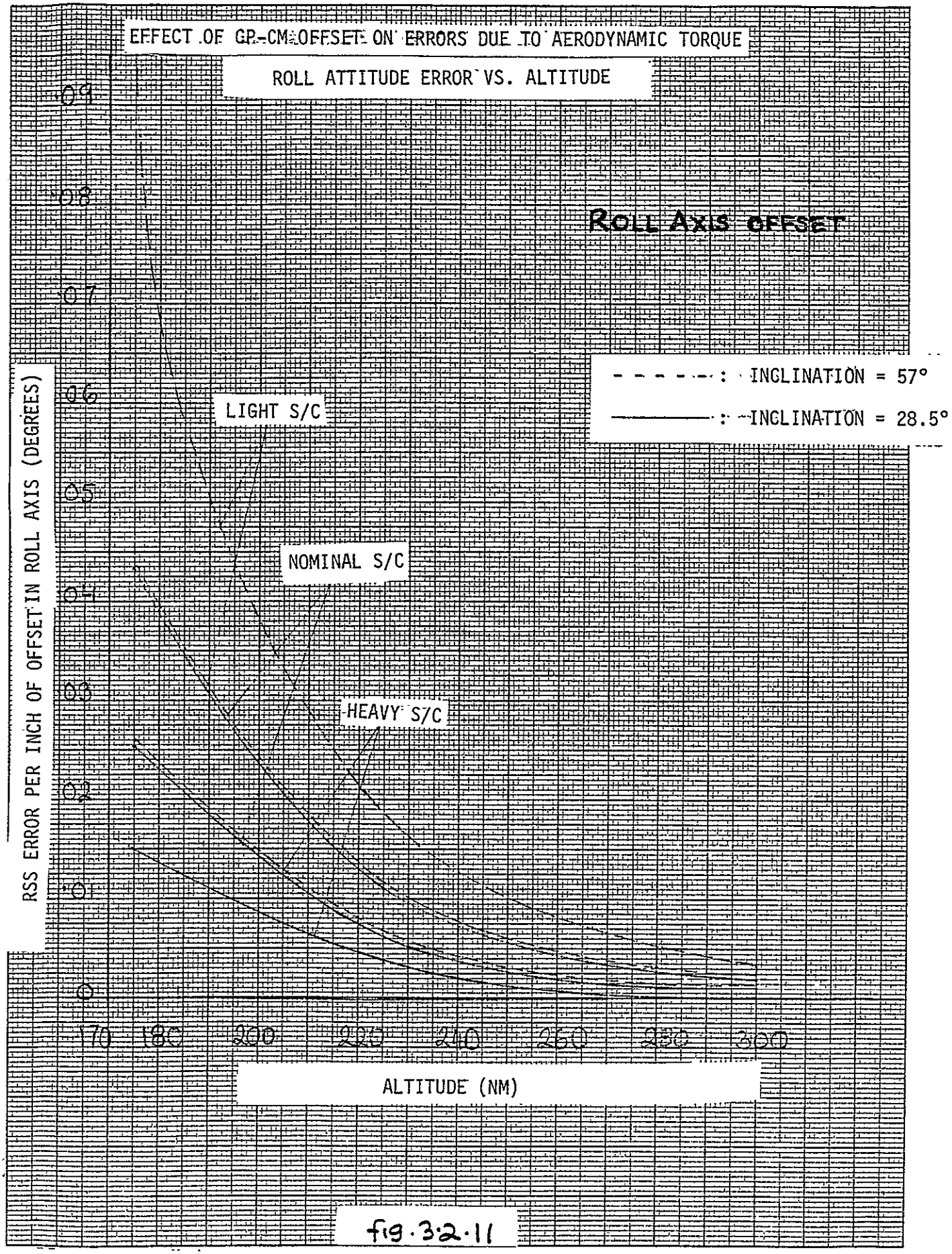

fig·3·2·11

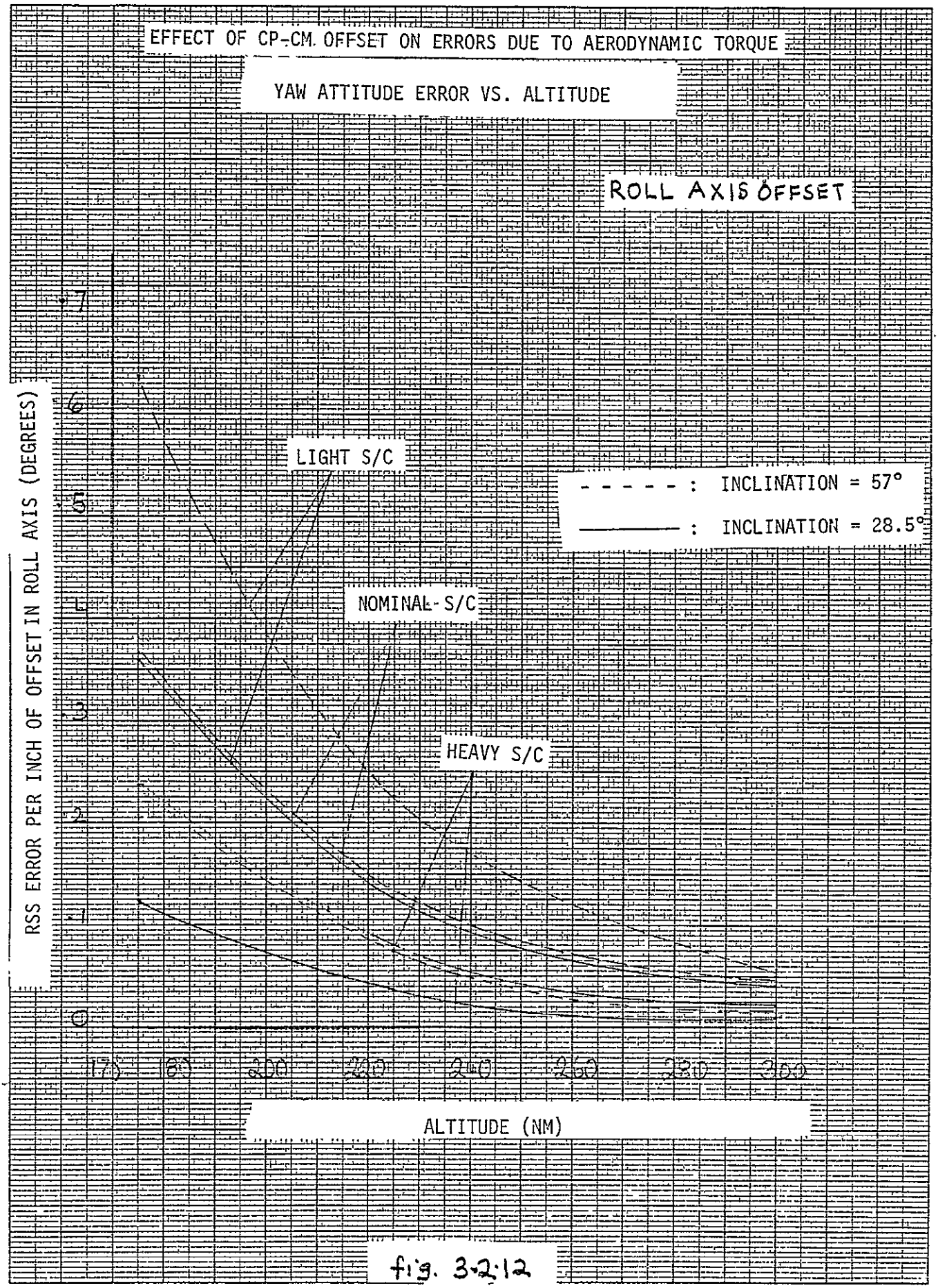

fig. 3-2-12

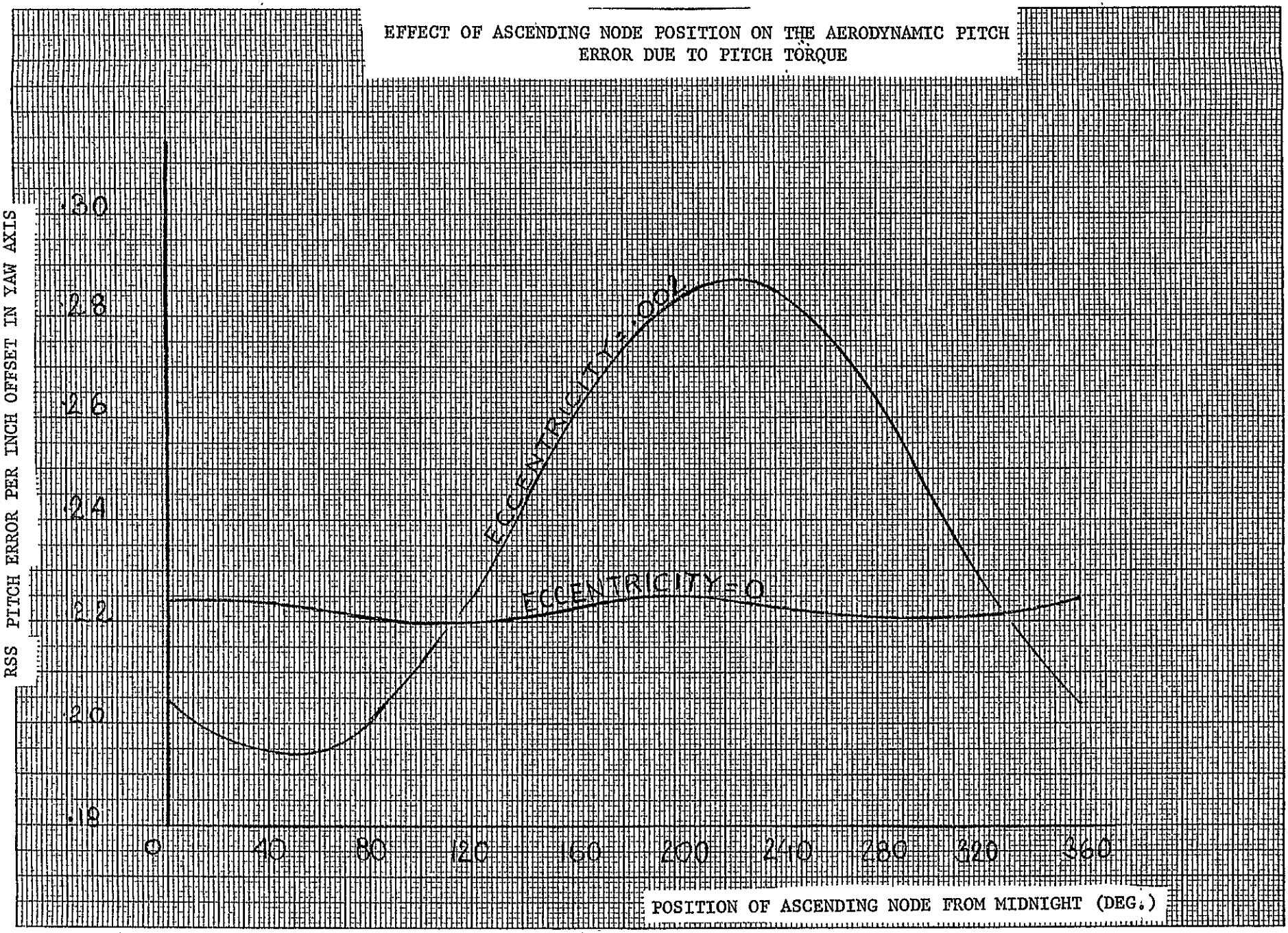
EFFECT OF ASCENDING NODE POSITION ON THE AERODYNAMIC PITCH ERROR DUE TO PITCH TORQUE
RSS PITCH ERROR PER INCH OFFSET IN YAW AXIS
.30
.28
.26
.24
.22
.20
.18
ECCENTRICITY = .002
ECCENTRICITY = 0
0
40
80
120
160
200
240
280
320
360
POSITION OF ASCENDING NODE FROM MIDNIGHT (DEG.)

fig 3.2.13

An estimate of LDEF dipole was made based upon experience with the Nimbus/Landsat spacecraft. Five of these spacecraft have been launched, and their pitch axis constant dipoles calculated by observing roll and yaw wheel speed growth over a period of time. The purpose of this was to command a compensating magnet strength to cancel this dipole. A value of dipole per pound of spacecraft, excluding the primary aluminum structure was found. These are listed below

Spacecraft	Dipole/Spacecraft Weight Pole-CM/Lb.
Landsat 1	1.72
Landsat 2	0.28
Nimbus 4	1.73
Nimbus 5	0.0
Nimbus 6	0.85

LDEF weight (first flight configuration) is 16200 lbs. Structure (including trays) is approximately 12,000 lbs. The estimate of the LDEF dipole, based on the maximum of the Nimbus/Landsat dipole/lb. values is

$$(16{,}200 - 12{,}000) \times 1.73 \ \frac{\text{pole-cm}}{\text{lb.}} = 7300 \text{ pole-cm per axis.}$$

Note however, that to achieve these values on Nimbus and Landsat required strict control of magnetic materials and current loops. An uncontrolled payload could far exceed these values.

3.2.4 Orbit Eccentricity Torques

One of the characteristics of a circular orbit is the constant rate of rotation of the radius vector (a vector from the center of the earth to the orbiting body). For a spherical earth the radius vector is parallel to the local vertical, and a gravity gradient spacecraft will align itself with the local vertical and acquire the average rate of rotation.

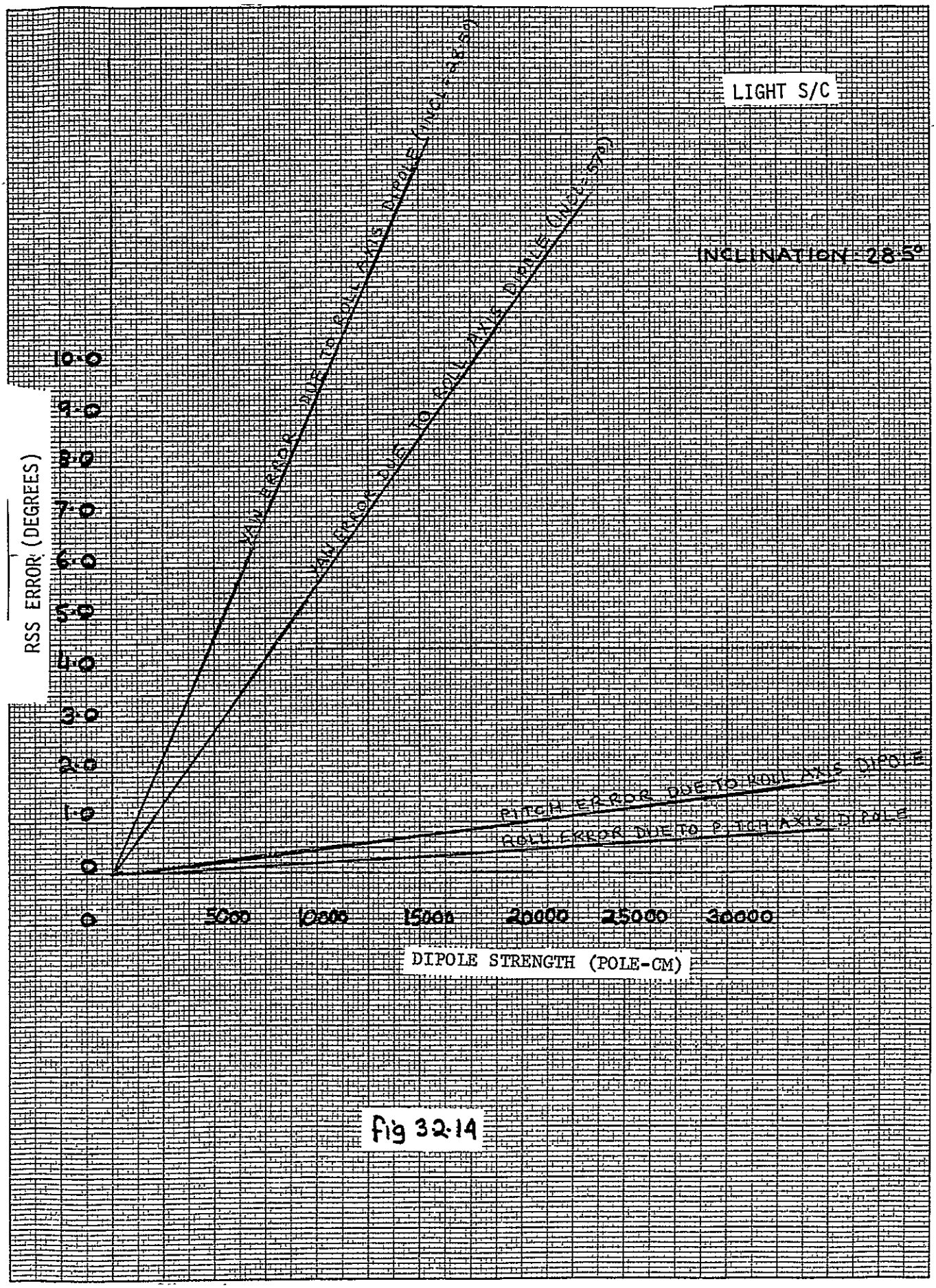

Fig 32.14

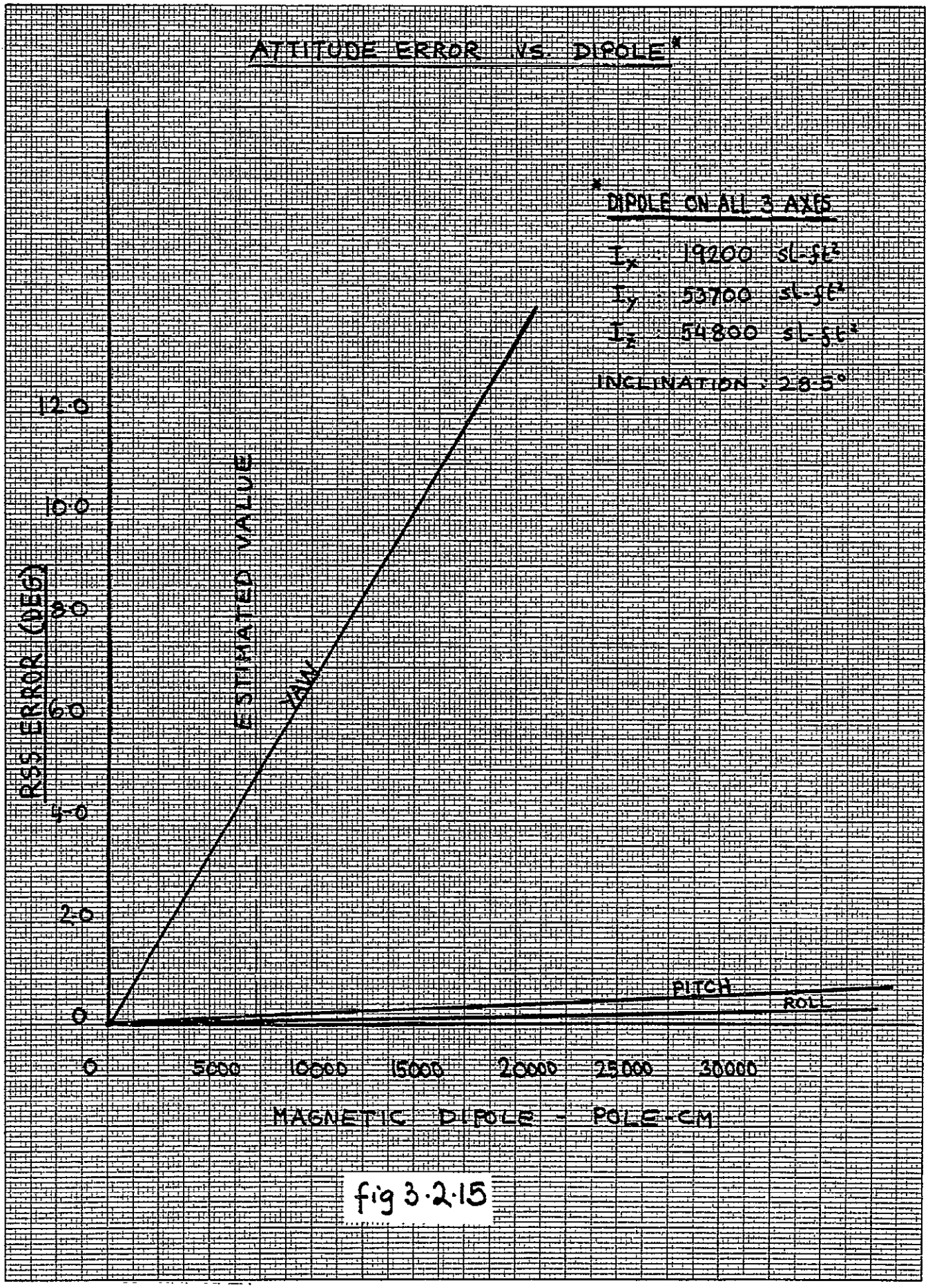

fig 3.2.15

The rate of rotation of the radius vector is not uniform for an eccentric orbit, however, but varies from a minimum at apogee to a maximum at perigee. The spacecraft will acquire the average rate of rotation of the eccentric orbit, but cannot respond to the variations in rate. Consequently errors will develop between the axis of minimum moment of inertia and the local vertical. The spacecraft will therefore be torqued sinusoidally by gravity gradient, with peak torque at apogee and perigee. Since the disturbance torque is a gravity gradient torque, absolute moments of inertia are irrelevant, and the attitude error is dependent only upon moment of inertia relationships, and orbit eccentricity.

The attitude error resulting from orbit eccentricity is only a pitch error. For an eccentricity of 0.002 the error is 0.23 degrees. The error is linearly proportional to the eccentricity. Neither the orbit altitude, nor the orbit inclination, affect eccentricity errors.

3.2.5 Solar Pressure Torque

Solar pressure torque is the result of the solar force vector, caused by the pressure of the sunlight (approximately 9.65×10^{-8} lb/ft^2), not passing through the spacecraft center of mass. The location of the center of mass is well defined, but the effective point of application of the solar force (i.e., the center of pressure) is not invariant, but moves as a function of sun angle. For a spacecraft as large as the LDEF, solar torque will be a strong function of sun angle, since the solar force vector is close to the surface of the spacecraft and the center of mass is on or near the axis of symmetry.

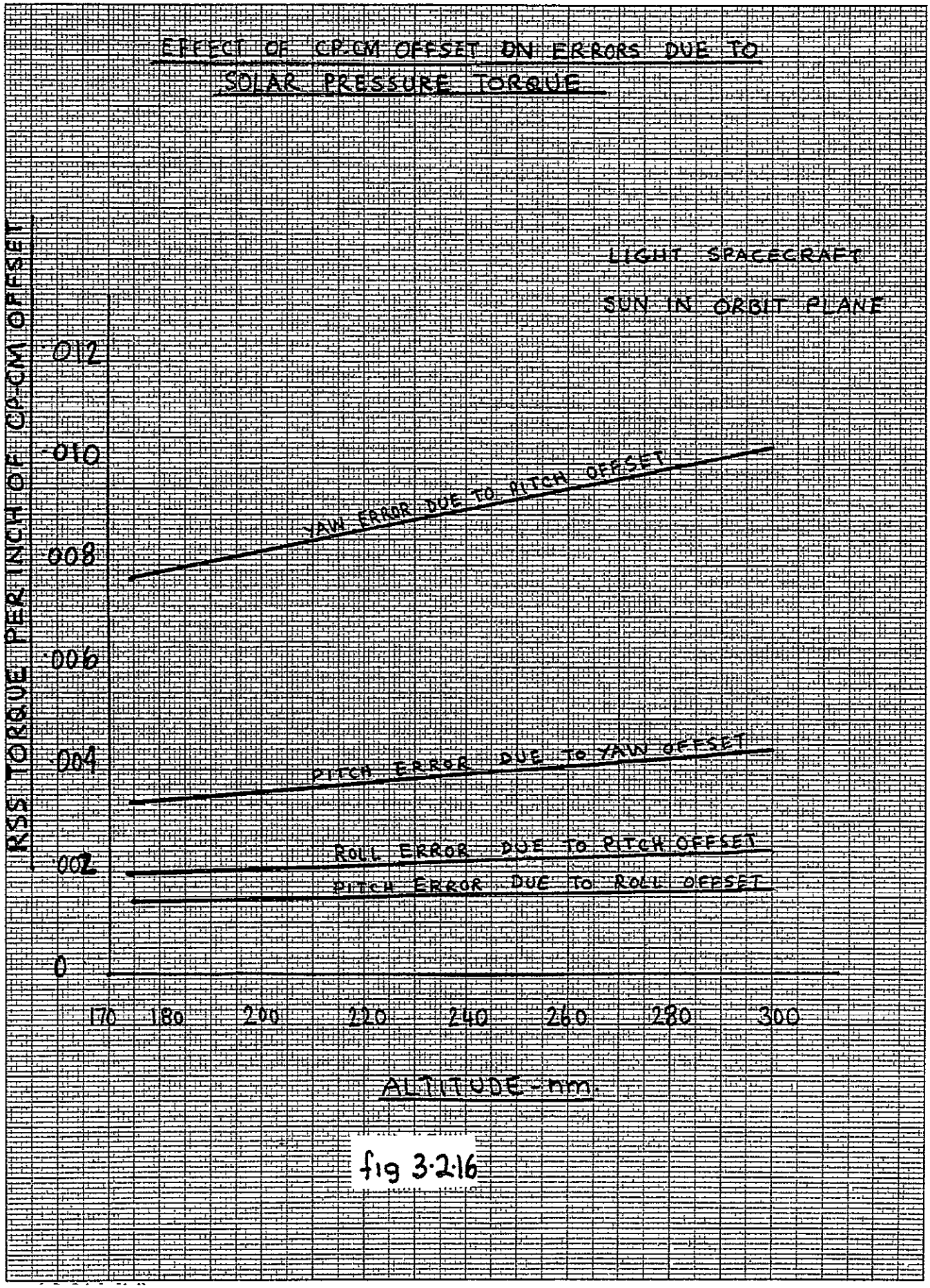

fig 3.2.16

Solar pressure torque on LDEF is an insignificant disturbance. This results because the solar pressure is weak (orders of magnitude below the aerodynamic pressure) and the symmetrical shape of the vehicle limits the CP-CM offset to small values.

The results of the solar torque analysis are shown in Figure 3.2-16 . For this evaluation, the sun was assumed to be in the orbit plane, which places the torque primarily on the pitch and yaw axes. This is the worst sun orientation since "out of plane" torque will affect the roll axis, which is stronger than the pitch axis, and would produce less local vertical pointing error. Only the light spacecraft was considered since its stiffness is lowest and therefore has the largest attitude errors for a given value of disturbance torque. The errors increase slightly with altitude because the stiffness decreases with altitude. It is obvious from these data that solar pressure torque is insignificant.

3.2.6 Summary

The results of the linear analysis are summarized in Table 3.2.1. These results are based on the first-flight LDEF configuration and the following parameter values:

Orbit altitude = 175-235 nm

Orbit inclination = 28.5 deg.

Orbit Eccentricity = 0.002

Damping Constant = 1 to 6 lb.-ft.-sec.

Magnetic Dipole = 7300 pole-cm per axis

CP-CM Offset = 1 inch along pitch and roll axes

= 2 inches along yaw axis

Disturbance	Error (Deg.)		
	Pitch	Roll	Yaw
Aerodynamics	0.4-2.0	0.1 - 0.2	20 - *
Damper	0.05-0.3	0.5 - 3.0	1.2 - 7.2
Magnetic Dipole	0.3	0.2	5.0
Orbit Eccentricity	0.23	0	0
Solar Pressure	0	0	0

SUMMARY OF LINEAR ANALYSIS RESULTS FOR LDEF

FIRST FLIGHT SPACECRAFT

TABLE 3.2.1

*These are results of a linear analysis and therefore errors greater than 20 degrees fail to have a meaningful significance. Hence they are shown here as an asterisk.

3.3 Garber Instability

All gravity gradient spacecraft have a first order instability which was identified by T. Garber (Ref. 4). This instability is caused by a pitch bias, and causes the roll motion to go unstable. This condition is predicted by the linearized equations of motion when the linearization is performed about biased pitch, roll and yaw positions. Only pitch biases produce the instability, however.

The pitch bias at which the spacecraft goes unstable is a function of configuration and damping. Figure 3.3.1 shows this behavior. The analysis on which the results are based appears in Appendix A.

The lowest level of damping for the LDEF mission was chosen to be 0.9. Corresponding to this value the pitch bias causing a 'Garber Instability' situation is 3.35^{o}. A further discussion on Garber Instability appears in Section 4.3 where the simulation of such a condition is discussed.

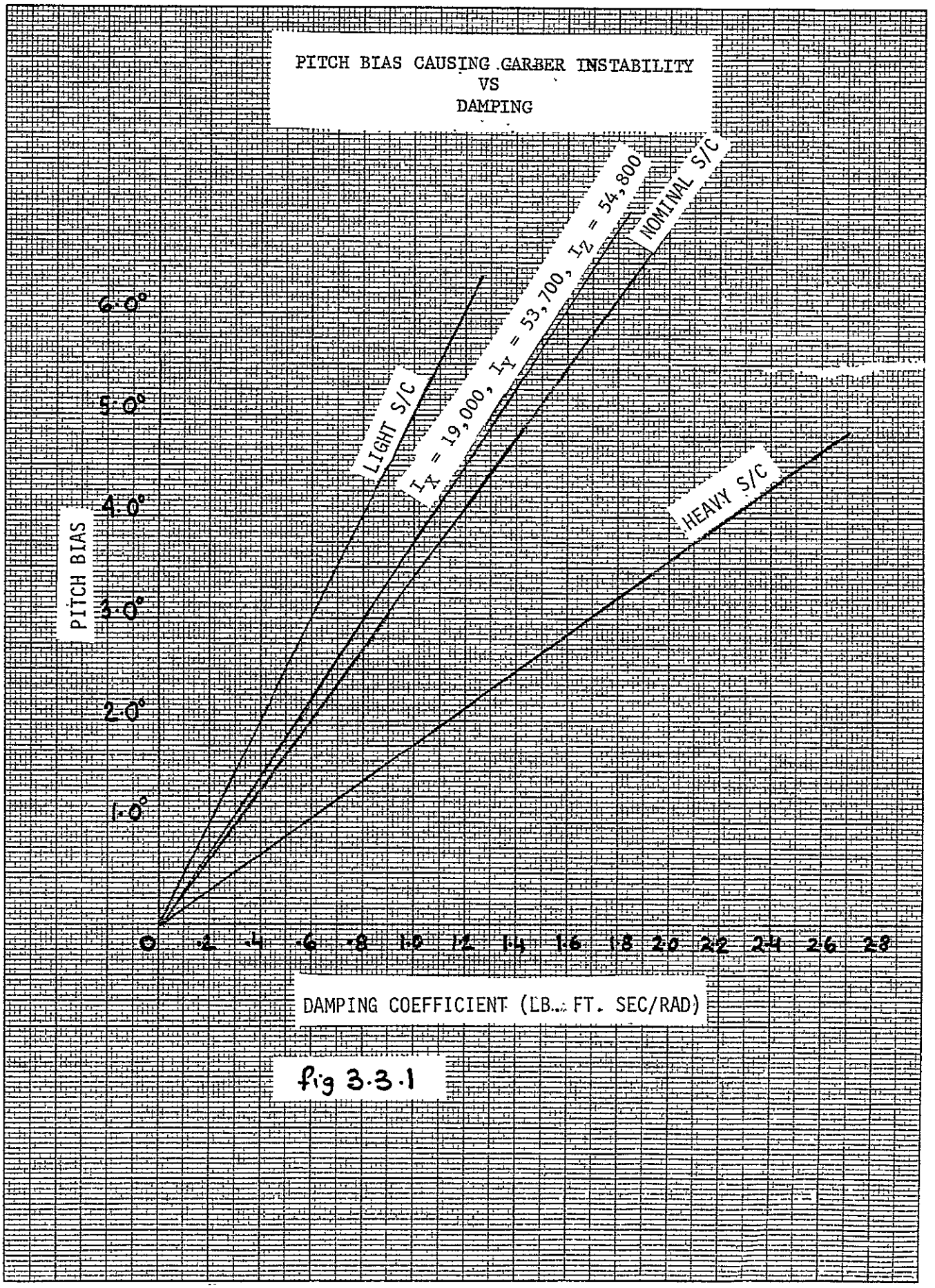
PITCH BIAS CAUSING GARBER INSTABILITY
VS
DAMPING
PITCH BIAS
6.0°
5.0°
4.0°
3.0°
2.0°
1.0°
LIGHT S/C
Ix = 19,000, Iy = 53,700, Iz = 54,800
NOMINAL S/C
HEAVY S/C
0
.2
.4
.6
.8
1.0
1.2
1.4
1.6
1.8
2.0
2.2
2.4
2.6
2.8
DAMPING COEFFICIENT (LB.. FT. SEC/RAD)

fig 3.3.1

3.4 Upright Capture Conditions

The requirements for right-side-up capture of the spacecraft following separation are (Reference 6):

1) $I_p > I_R > I_y$ (1)

and

2) The initial-energy H is such that

$$H \leq \frac{3}{2}\dot{\eta}^2 (I_R - I_y) \quad (2)$$

These conditions assure right-side-up capture but not a fly-forward capture. To realize both right-side-up and fly-forward conditions requires that

$$H \leq \min \left[\frac{3}{2}\dot{\eta}^2 (I_R - I_y) \; ; \; \frac{1}{2}\dot{\eta}^2 (I_p - I_R) \right] \quad (3)$$

Where $\dot{\eta}$ = orbital rate

The total energy of the spacecraft is given

$$H = \frac{1}{2}\left[I_R \omega_R^2 + I_y \omega_y^2 + I_p \omega_p^2 \right] +$$

$$\frac{3}{2}\dot{\eta}^2 \left[(I_R - I_y)\gamma^2 + (I_p - I_y)\gamma''^2 \right]$$

$$+ \frac{1}{2}\dot{\eta}^2 \left[(I_p - I_R)\beta^2 + (I_p - I_y)\beta''^2 \right]$$

(4)

where W_p, W_R, W_y = pitch roll and yaw body rates respectively and

$$\gamma = \sin\theta_R \sin\theta_y - \cos\theta_R \sin\theta_p \cos\theta_y$$

$$\gamma' = \sin\theta_R \cos\theta_y + \cos\theta_R \sin\theta_p \sin\theta_y$$

$$\beta = \cos\theta_R \sin\theta_y + \sin\theta_R \sin\theta_p \cos\theta_y$$

$$\beta'' = -\sin\theta_R \cos\theta_p$$

$\gamma, \gamma', \beta', \beta''$ are elements of a coordinate transformation Matrix

$$\begin{Bmatrix} \alpha & \beta & \gamma \\ \alpha' & \beta' & \gamma' \\ \alpha'' & \beta'' & \gamma'' \end{Bmatrix}$$

corresponding to an ordered set of rotations (the order of rotation being roll-pitch-yaw) relating the orbital coordinate frame to the S/C body frame.

θ_p, θ_r, θ_y are the Euler angles in pitch, roll and yaw.

Equation 4 was evaluated for the first flight LDEF configuration for a range of initial body rates, and several combinations of initial attitude errors. The results are presented in Figures 3.4.1 and 3.4.2.

Figure 3.4.1 is a plot of W_y vs W_R (= W_p) for various energy levels and for initial attitude errors of 15 degrees/axis. It can be seen that at the 50% energy level :

$$W_R = W_p = W_y = 0.034 \text{ deg./sec.}$$

The maximum limit (100% energy level, and therefore no safety margin) is

$$W_R = W_p = W_y = 0.053 \text{ deg./sec.}$$

Figure 3.4.2 is a plot of W_y vs W_R (= W_p) for various combinations of initial attitude errors, but for only the 50% energy level

The plots in both figures are symmetrical about the W_y and W_R axes and, therefore, only the first quadrant is shown.

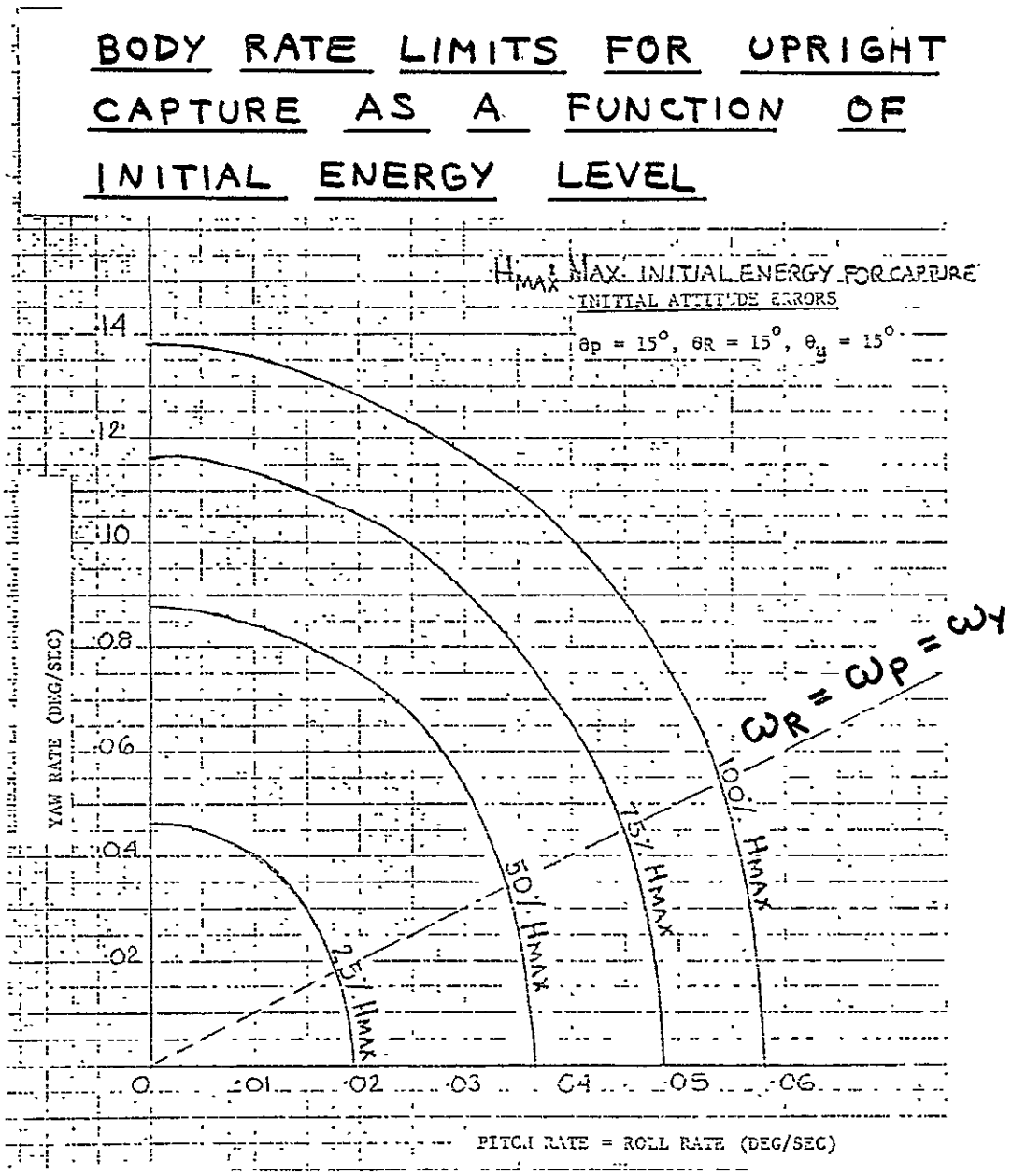
BODY RATE LIMITS FOR UPRIGHT CAPTURE AS A FUNCTION OF INITIAL ENERGY LEVEL
H_{MAX} = MAX. INITIAL ENERGY FOR CAPTURE
INITIAL ATTITUDE ERRORS
$\theta_P = 15^\circ$, $\theta_R = 15^\circ$, $\theta_Y = 15^\circ$
YAW RATE (DEG/SEC)
.14
.12
.10
.08
.06
.04
.02
0
.01
.02
.03
.04
.05
.06
PITCH RATE = ROLL RATE (DEG/SEC)
$\omega_R = \omega_P = \omega_Y$
25% H_{MAX}
50% H_{MAX}
75% H_{MAX}
100% H_{MAX}

Fig. 3.4.1

BODY RATE LIMITS FOR UPRIGHT CAPTURE
AS A FUNCTION OF INITIAL ATTITUDE ERROR.

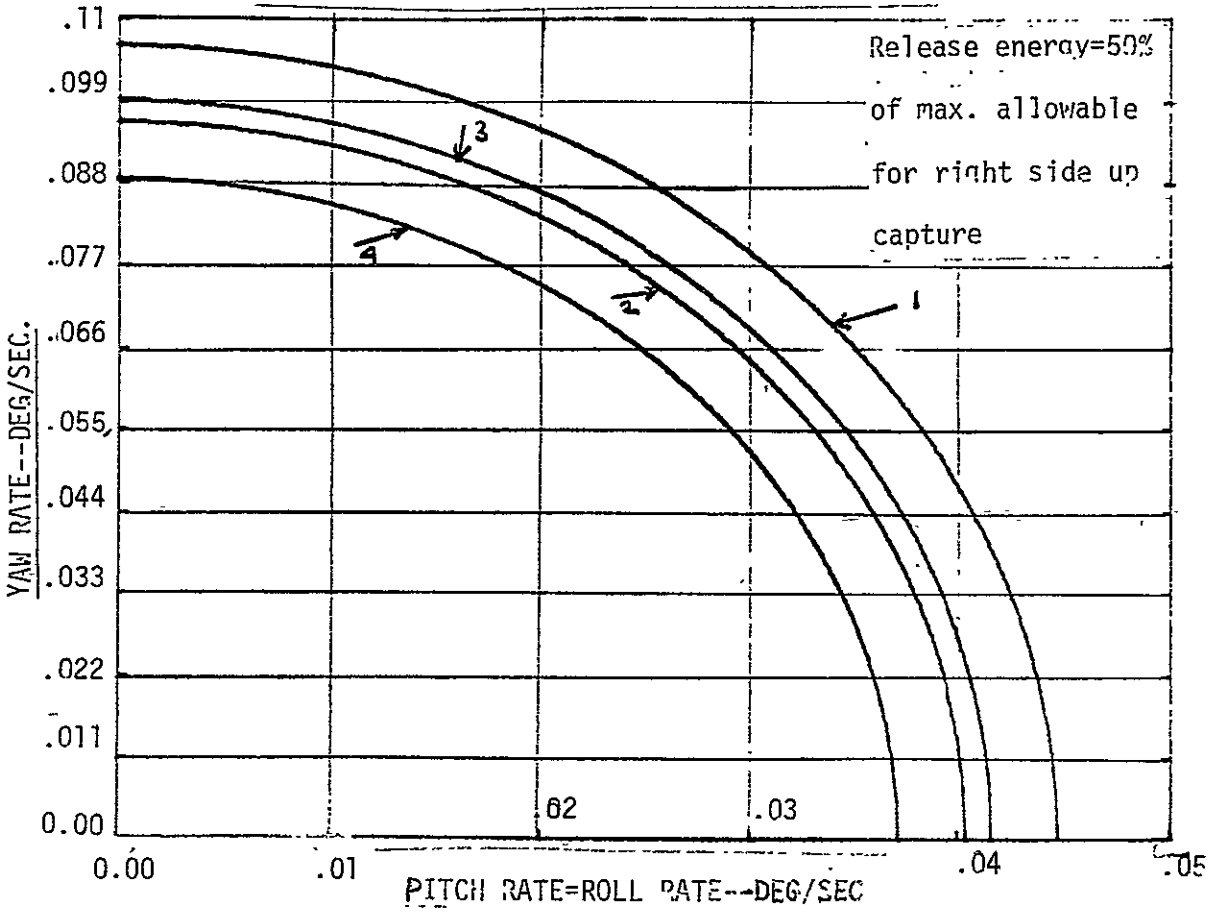

	INITIAL ATTITUDE ERROR (DEG)		
	θ_p	θ_r	θ_y
1.	0	0	0
2.	0	15	0
3.	15	0	0
4.	15	15	0

FIG. 3.4.2

3.5 Spacecraft Disturbances

The LDEF may be subjected to a number of disturbances such as plume impingement from the shuttle reaction control system nozzles, experiment outgassing, uncompensated momentum in tape recorders, moving parts in experiments, etc. These disturbances were divided into two classifications: impulse and constant momentum. An analysis was performed to determine their effects on LDEF attitude errors. The analysis is based on the first-flight LDEF configuration.

3.5.1 Impulsive Disturbances

An impulsive disturbance is defined to be a momentum caused by a torque acting for a time which is very small with respect to the period of the natural frequency in the axis of interest. (These are given in Table 3.1.3). If the spacecraft is assumed to be an undamped spring-mass system it can be shown (Appendix C) that the maximum error is given by

$$\theta_{MAX} = \frac{T\ t}{I\ Wn}$$

where T = disturbance torque

t = time of application of the torque

I = moment of inertia

Wn = natural frequency

These data are plotted in Figure 3.5.1.

DISTURBANCE MOMENTUM

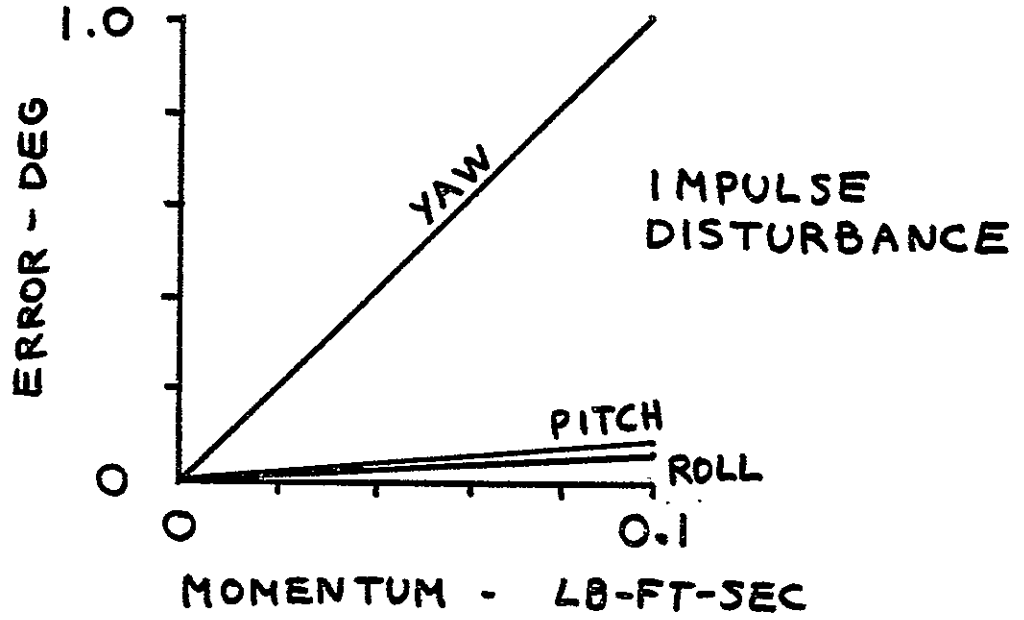

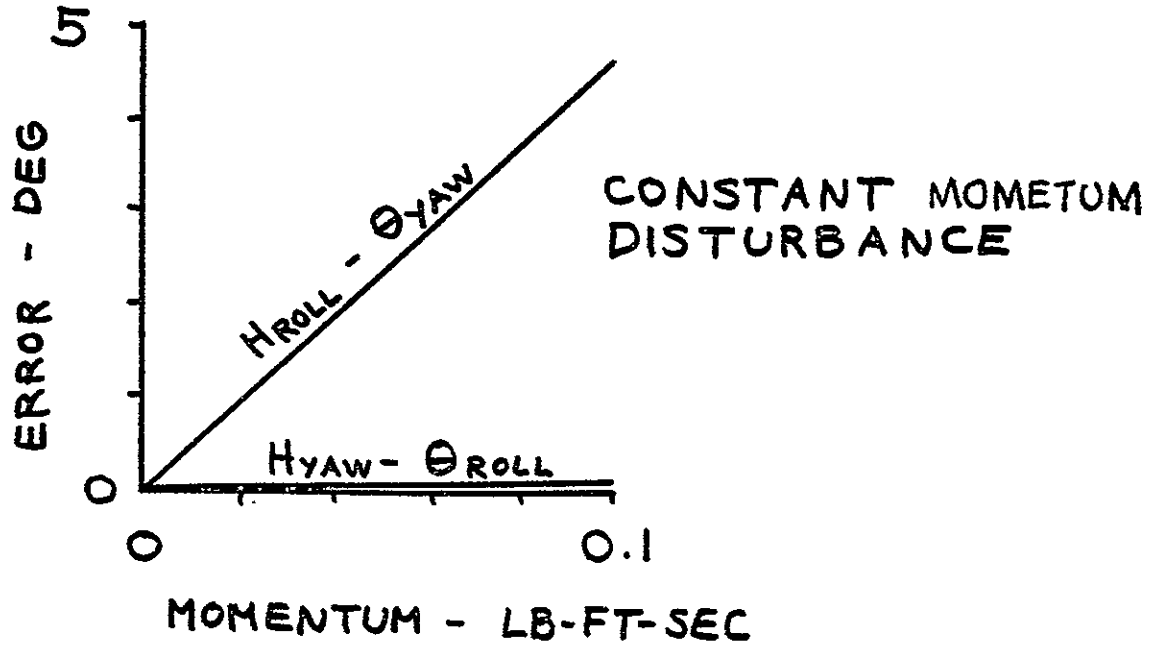

Fig 3.5.1

3.5.2 Constant Momentum

A constant momentum vector results from operation of a constant speed motor. If the disturbance momentum vector is located in the pitch axis, it remains fixed (approximately) with respect to an inertial reference frame. No steady-state error is caused. However, if the momentum vector is located in either roll or yaw a precession torque is produced as the spacecraft rotates in orbit. This is described by

$$\bar{T} = \bar{W} \times \bar{H}$$

where T = precession torque

W = orbit rate

H = disturbance momentum

At steady-state conditions the precession torque must be balanced by a gravity gradient torque. Thus the spacecraft will assume a bias corresponding to the required value of gravity gradient torque. Note that the precession torque is given by a vector cross product. Thus for a roll momentum the precession torque is about the yaw axis, and therefore a yaw bias results. Similarly a yaw momentum gives rise to a roll bias. These data are plotted in Figure 3.5.1.

3.6 Selection of Damping Constant

Selection of a damping constant requires consideration of three criteria. These are:

1. Garber stability. In the presence of a constant pitch bias (primarily caused by aerodynamic torque) the damping constant must be above a given value to avoid the region of instability.

2. Transient performance. At low values of damping the time constants are long. The time to decay from an initial transient to steady-state conditions may be excessive. Time constants decrease as damping increases up to the point at which the damper torques exceed the torque holding the damper magnet aligned with the earth's magnetic field. From this point on performance degrades rapidly as damping increases.
3. Steady-state performance. When the spacecraft reaches steady-state conditions the damper torques act as a disturbance torque. Attitude errors increase as damping constant exceeds a given value.

3.6.1 Garber Instability Criteria

The Garber instability limit proved to be the determining factor. The selection procedure involved determining a damping constant to avoid the region of instability, and then checking it against the other two criteria. The step-by-step procedure is given below.

1. Determine the maximum pitch bias. The only significant sources of pitch bias are aerodynamics and damper disturbances. The maximum values of these components of pitch bias are:

	Pitch Bias
Aerodynamic torque at 175 nm with a 2-inch yaw axis CP-CM offset (See Fig. 3.2.7)	2.0 deg.
Damper torque assuming a maximum value of damping constant of 9.0 lb-ft-sec. This is based on the constant component of the RSS error shown in Figure 3.2.3A	0.4 deg.
Total	2.4 deg.

2. Determine the minimum value of damping required to avoid Garber instability. Fig. 3.31 shows that for a pitch bias of 2.4 deg the damping constant must exceed 0.65 lb-ft-sec.
3. Select the minimum value of damping constant to be 0.9 lb-ft-sec. Since damping is proportional to the viscosity of the damping fluid which in turn is inversely proportional to the damper temperature, minimum damping occurs at the maximum temperature. Specify damping constant to be 0.95 ± 0.05 lb-ft-sec at 140 F.
4. Determine damping constant at nominal and minimum temperature. These are shown in Fig. 3.6.1. Approximate values shown are:

T (^{o}F)	B (lb-ft-sec)
0	5.5
70	2.0
140	1.0

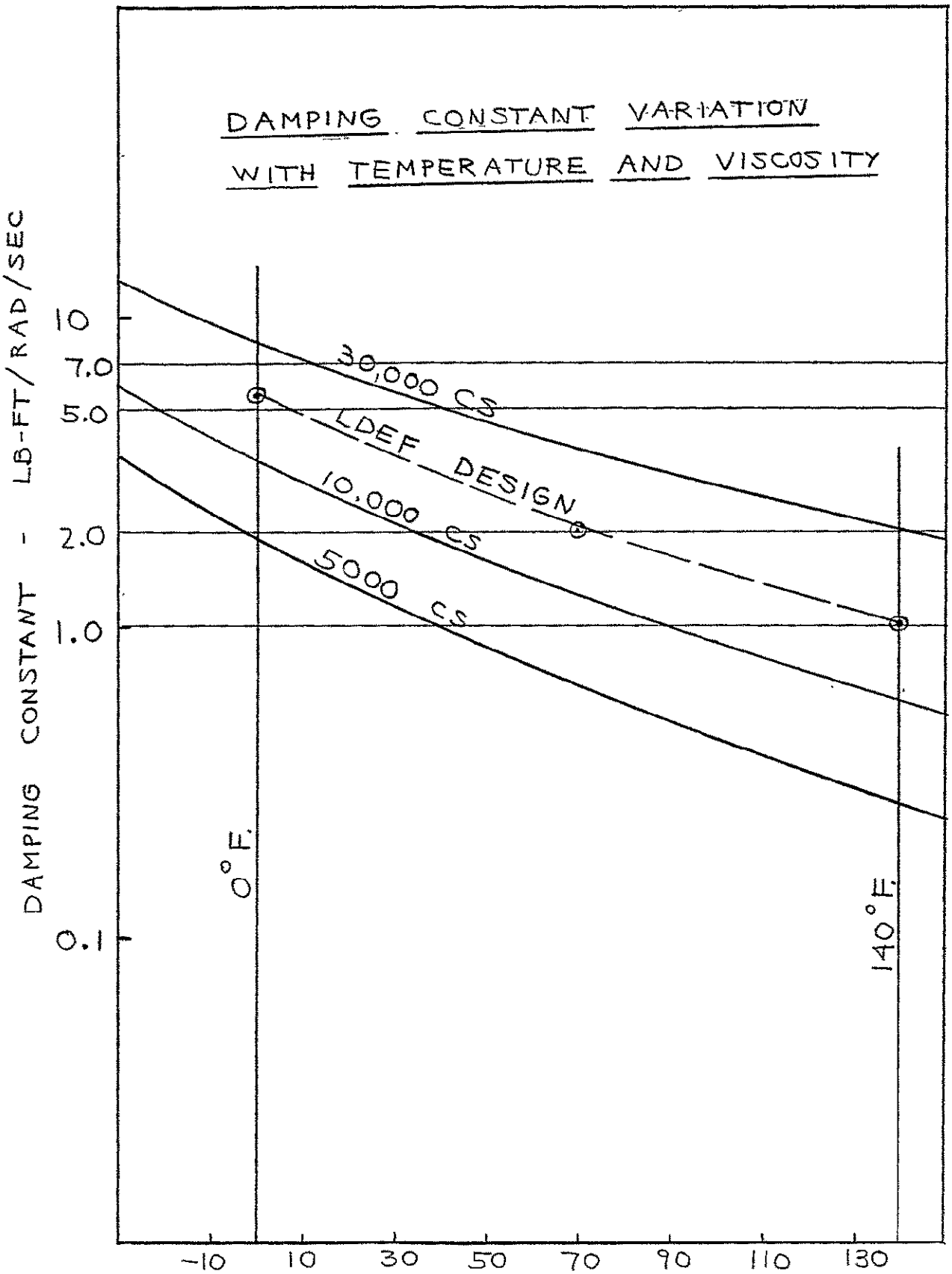
DAMPING CONSTANT VARIATION
WITH TEMPERATURE AND VISCOSITY
DAMPING CONSTANT - LB-FT/RAD/SEC
10
7.0
5.0
2.0
1.0
0.1
30,000 CS
LDEF DESIGN
10,000 CS
5000 CS
0° F.
140° F.
-10
10
30
50
70
90
110
130
TEMPERATURE - °F

Fig 3·6·1

3.6.2 Transient Performance

To determine the transient performance of the damper, the equations of motion of the damper and the spacecraft must be solved simultaneously. The normal analytical approach is to linearize the equations, but because the magnetic field orientation changes as a function of orbit position, several simplifying assumptions must be made. This derivation is presented in Appendix A. The result of this analysis is the damping time constant as a function of the damping constant. These data are plotted in Figures 3.6.2 to 3.6.6.

Figure 3.6.2 is representative of these data. For low values of damping the spacecraft is lightly damped and the time constant is large (for example 40 orbits when B = 0.4 lb-ft-sec). As damping is increased, the time constant decreases, reaching a minimum value of = 9 orbits at B = 3.5 lb-ft-sec. As damping constant is increased beyond 3.5 lb-ft-sec the time constant increases. The reason this occurs is that for large values of damping constant the damper torque on the magnet exceeds the magnetic torque orienting the magnet to the Earth's field. As the magnet is pulled away from the earth's field its effectiveness decreases. The extreme example of this occurs if the fluid viscosity is infinite. The magnet would be locked to the spacecraft, and there would be no damping at all despite a very high damping constant.

Figures 3.6.2 to 3.6.4 show these data for zero pitch bias. The pitch and roll curves show minimum time constants occur for damping constants of approximately 3-4 lb-ft-sec. The limit of effective operation is

approximately 6-9 lb-ft-sec. Thus the maximum damping constant of 5.5 lb-ft-sec is acceptable but with little margin. It is not known whether the sharp variations in the roll time constant plots are caused by physical phenomena or problems with the computer root-finding subroutine. It should be emphasized these results are only approximate. The simplifying assumptions used in this analysis are included in Appendix A.

Figures 3.6.5 and 3.6.6 show the roll and yaw time constants in the presence of a 2-degree pitch bias. With the bias present roll time constants are decreased slightly, yaw time constants are increased slightly.

This analysis is based on spacecraft and damper rates at or near orbital rate. For higher rates the damper torque is increased thus increasing the torque acting to drag the magnet away from the Earth's field. Damper parameters should be selected so that the damper magnet does not deviate more than approximately 40 degrees from the Earth's magnetic field. This is considered to be a conservative value. Fig. 3.6.7 shows the maximum allowable spacecraft angular rates as a function of the damping constant for 20, 40 and 90 degree deviations of the magnet from the Earth's field. Thus for a maximum damping value of 5.5 lb-ft-sec the maximum allowable rate for 40 degree deviation is 0.028 deg/sec. If the initial damper de-centering factor is included (See Section 4.1.1) damping constant is increased to 9 lb-ft-sec and

the allowable rate is reduced to 0.015 deg/sec. These values are exceeded by the initial separation rate of 0.04 deg/sec. This does not mean the spacecraft will not capture successfully. It does mean that initial damper effectiveness is reduced and acquisition time will be slightly increased. The non-linear simulation will be used to verify these conclusions.

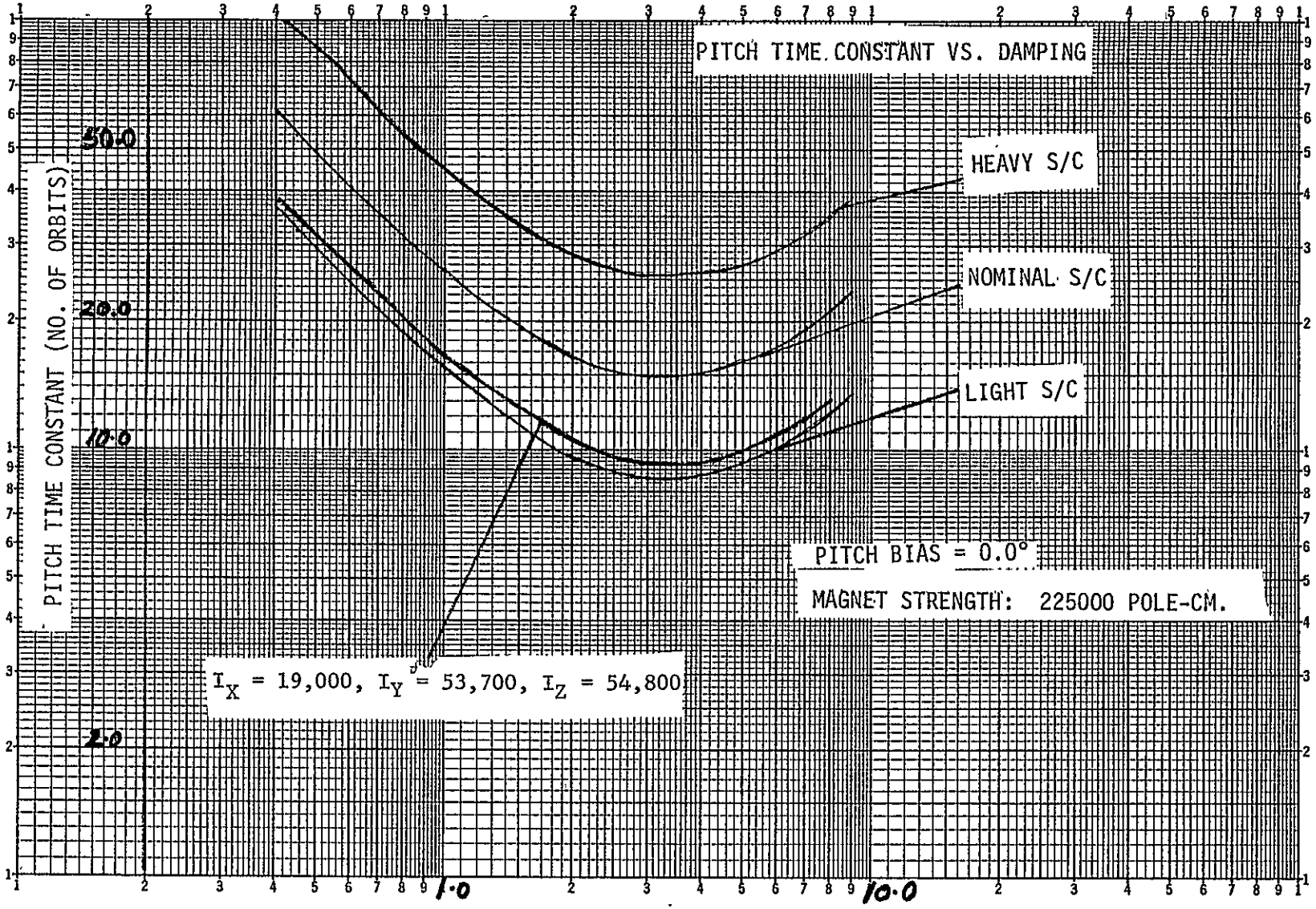
PITCH TIME CONSTANT VS. DAMPING
HEAVY S/C
NOMINAL S/C
LIGHT S/C
PITCH BIAS = 0.0°
MAGNET STRENGTH: 225000 POLE-CM.
I_X = 19,000, I_Y = 53,700, I_Z = 54,800
PITCH TIME CONSTANT (NO. OF ORBITS)
50.0
20.0
10.0
2.0
1.0
10.0
DAMPING COEFFICIENT (LB. FT. SEC/RAD)

fig 3.6.2

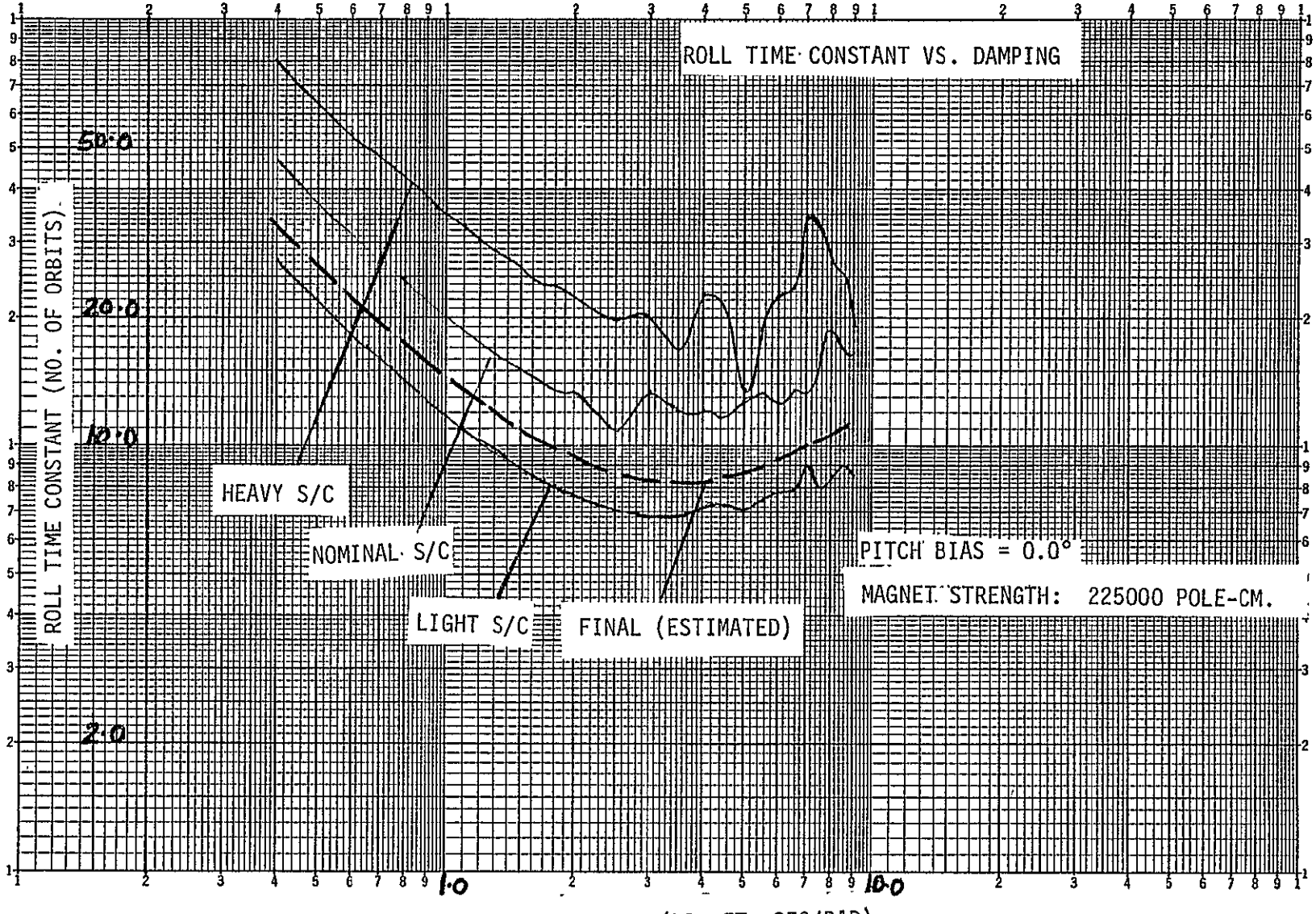
ROLL TIME CONSTANT VS. DAMPING
ROLL TIME CONSTANT (NO. OF ORBITS)
50.0
20.0
10.0
2.0
1.0
10.0
HEAVY S/C
NOMINAL S/C
LIGHT S/C
FINAL (ESTIMATED)
PITCH BIAS = 0.0°
MAGNET STRENGTH: 225000 POLE-CM.
DAMPING COEFFICIENT (LB. FT. SEC/RAD)

fig 3.6.3

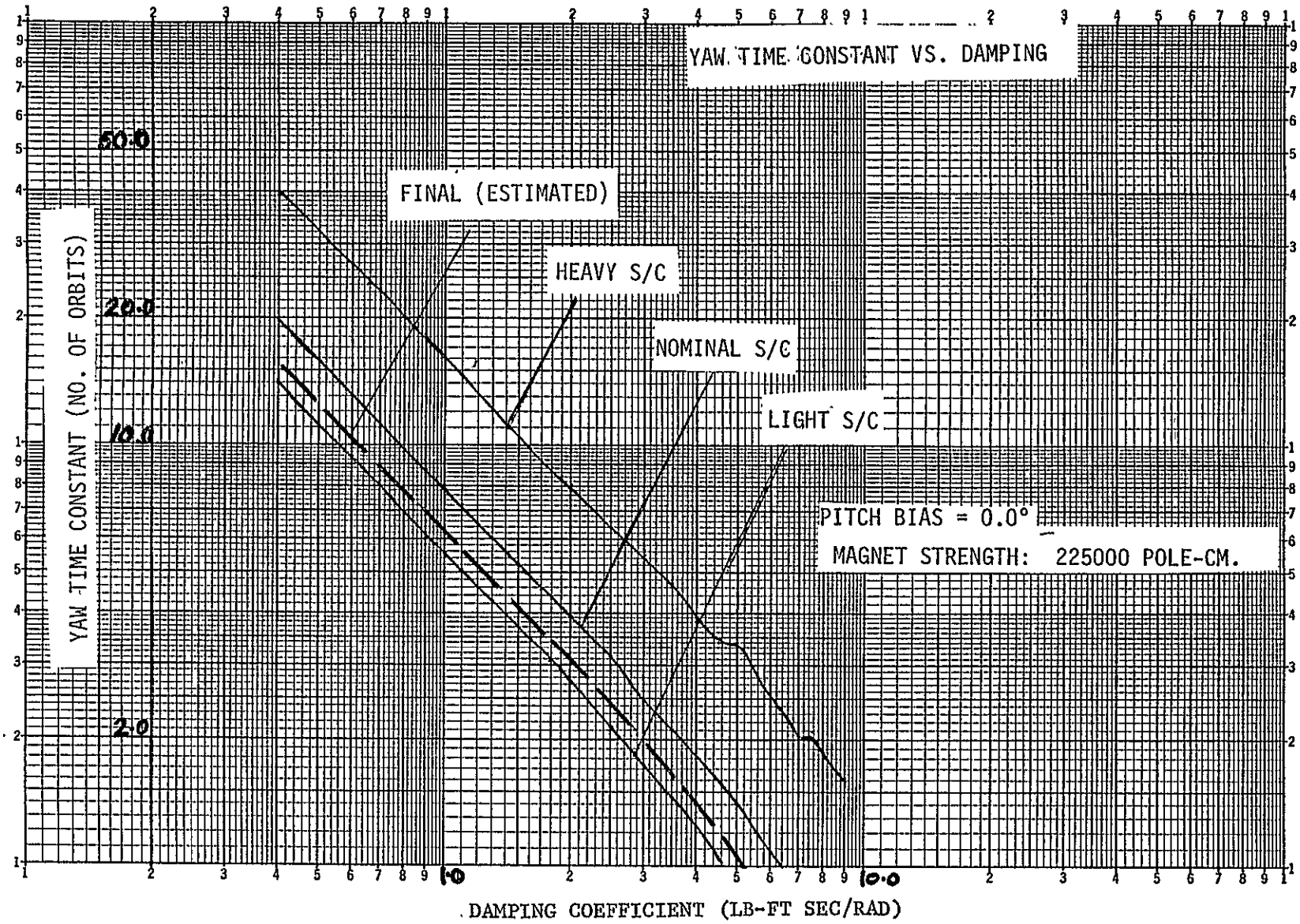
YAW TIME CONSTANT VS. DAMPING
FINAL (ESTIMATED)
HEAVY S/C
NOMINAL S/C
LIGHT S/C
PITCH BIAS = 0.0°
MAGNET STRENGTH: 225000 POLE-CM.
YAW TIME CONSTANT (NO. OF ORBITS)
50.0
20.0
10.0
2.0
1.0
10.0
DAMPING COEFFICIENT (LB-FT SEC/RAD)

Fig 3.6.4

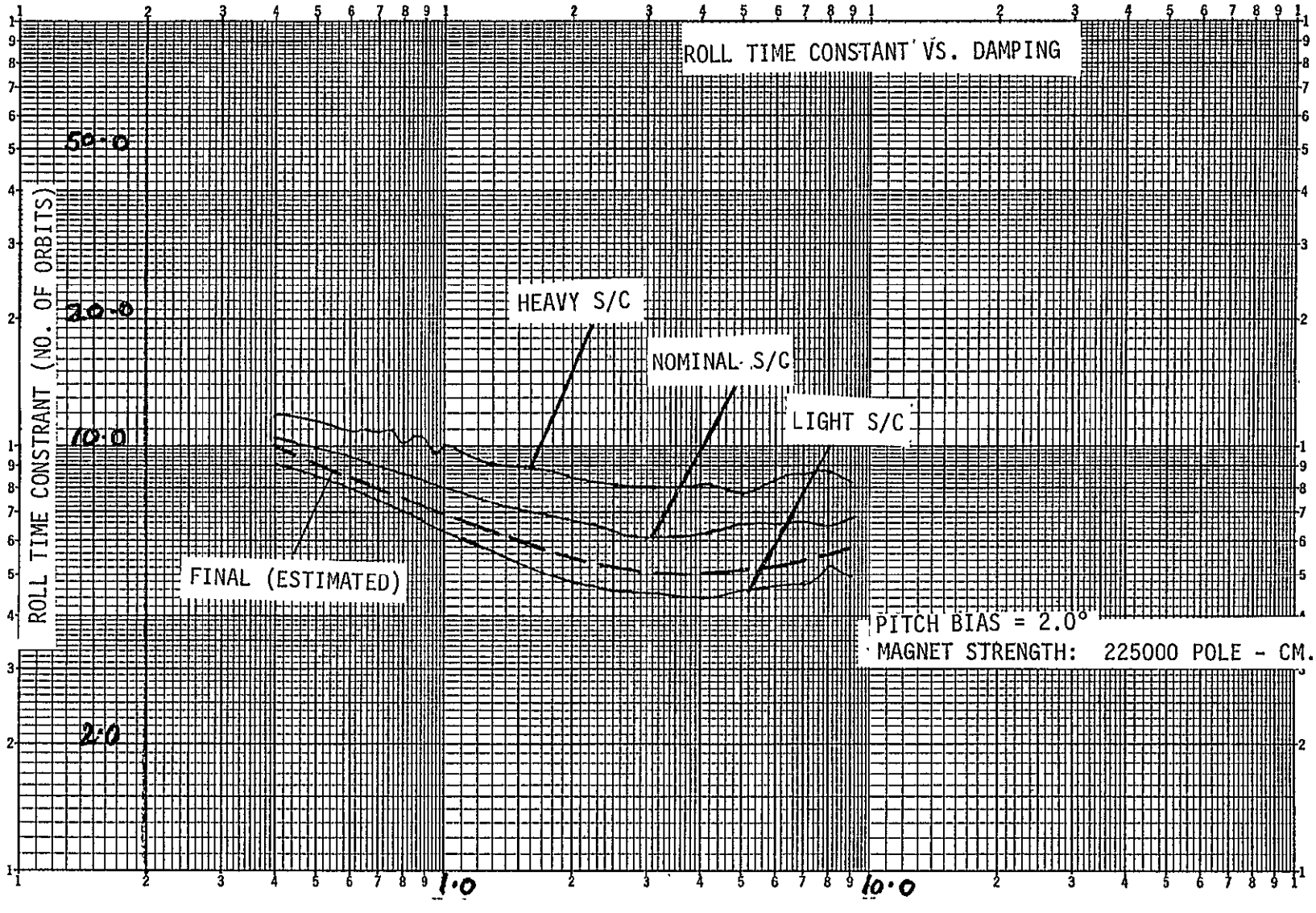
ROLL TIME CONSTANT VS. DAMPING
ROLL TIME CONSTRANT (NO. OF ORBITS)
50·0
30·0
10·0
2·0
HEAVY S/C
NOMINAL S/C
LIGHT S/C
FINAL (ESTIMATED)
PITCH BIAS = 2.0°
MAGNET STRENGTH: 225000 POLE - CM.
1·0
10·0
DAMPING COEFFICIENT (LB-FT SEC/RAD)

Fig 3.6.5

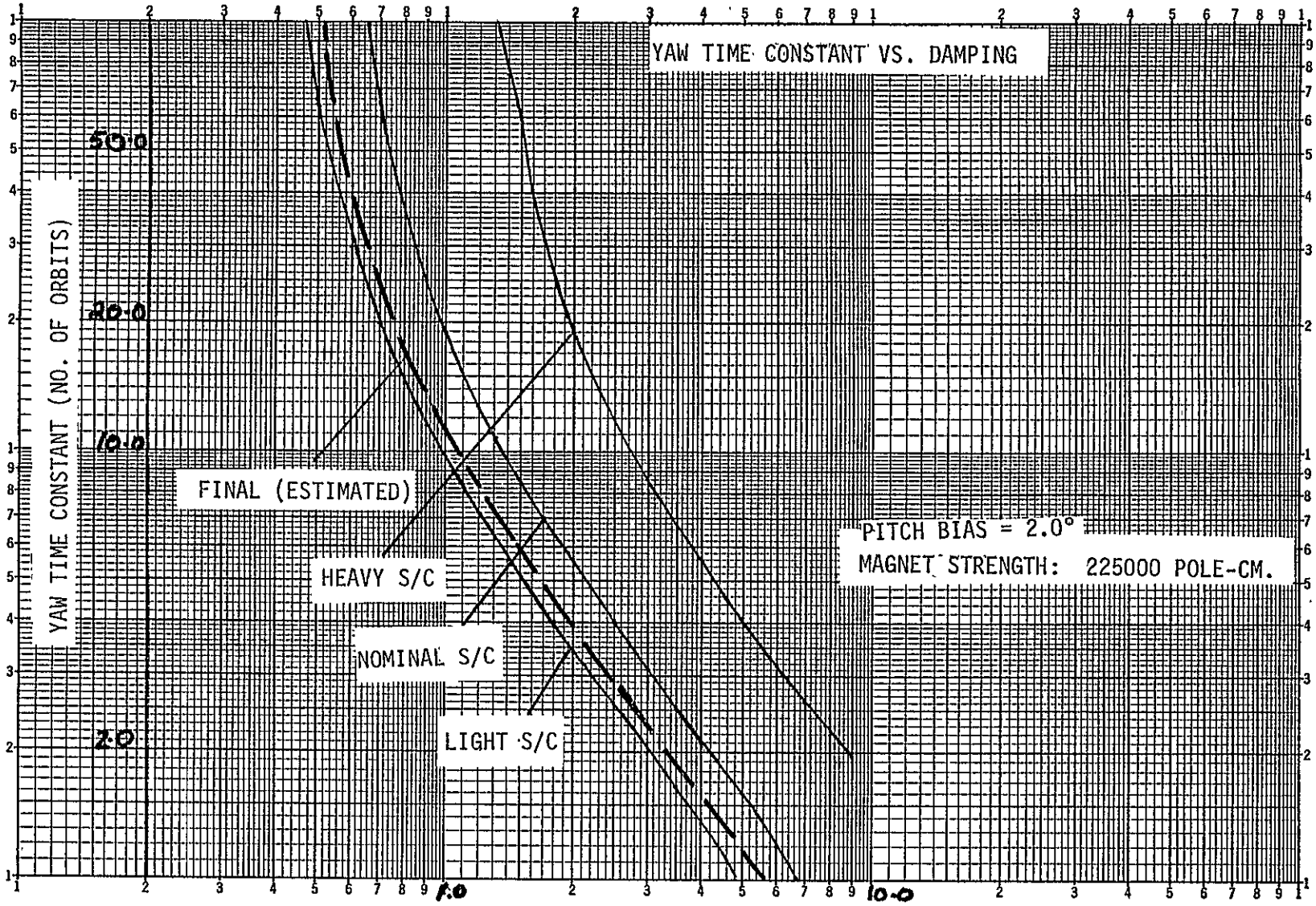
YAW TIME CONSTANT VS. DAMPING
YAW TIME CONSTANT (NO. OF ORBITS)
50.0
20.0
10.0
2.0
1.0
10.0
FINAL (ESTIMATED)
HEAVY S/C
NOMINAL S/C
LIGHT S/C
PITCH BIAS = 2.0°
MAGNET STRENGTH: 225000 POLE-CM.
DAMPING COEFFICIENT (LB. FT. SEC/RAD)

Fig 3.6.6

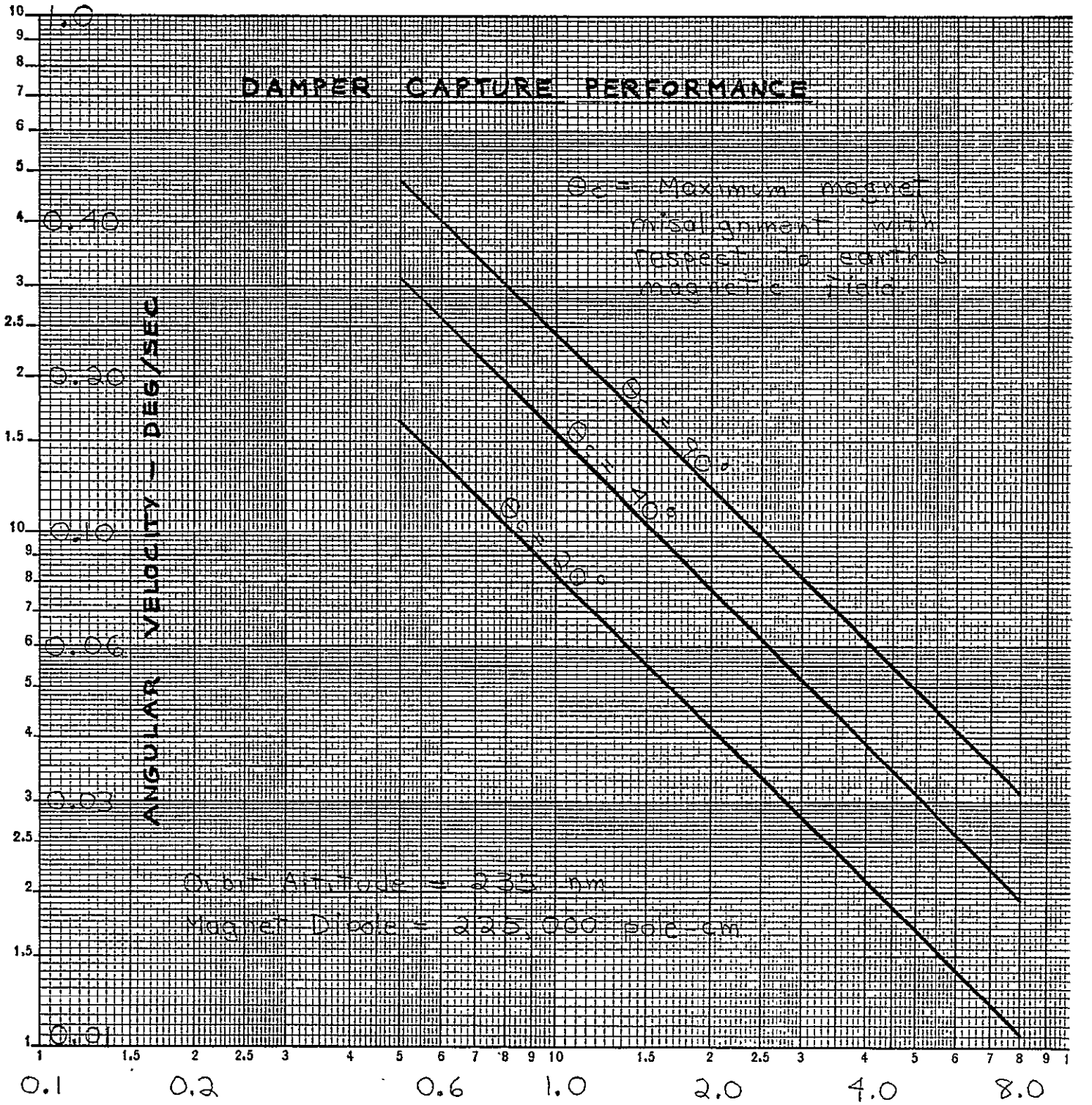
DAMPER CAPTURE PERFORMANCE
θ_c = Maximum magnet misalignment with respect to earth's magnetic field
$\theta_c = 30°$
$\theta_c = 20°$
$\theta_c = 10°$
Orbit Altitude = 235 nm
Magnet Dipole = 225,000 pole-cm
ANGULAR VELOCITY - DEG/SEC
1.0
0.40
0.30
0.10
0.06
0.03
0.01
10 9 8 7 6 5 4 3 2.5 2 1.5 10 9 8 7 6 5 4 3 2.5 2 1.5 1
1 1.5 2 2.5 3 4 5 6 7 8 9 10 1.5 2 2.5 3 4 5 6 7 8 9 1
0.1 0.2 0.6 1.0 2.0 4.0 8.0
DAMPING COEFFICIENT - LB-FT-SEC/RAD

Fig. 3.6.7

SECTION 4.0

SIMULATION

Performance predictions are made by simulating the LDEF configuration using a three-axis digital computer program. The purpose of the simulation is to verify the conclusions of the linear analysis while including non-linear dynamics and accurate models of all the disturbance torques.

The simulation program used is a large digital computer program called GOLD-N-ROD. The program simulates the dynamics of the spacecraft in three axes using Euler dynamical equations. The attitude of the spacecraft is specified by Euler parameters. Disturbance torques caused by solar pressure, aerodynamics, magnetics and the damper are included for both circular and eccentric orbits. Torques are calculated as a function of spacecraft attitude and orbit position. Damper magnet dynamics are also included. The equations of motion are integrated by a fifth order Adams-Moulton integration scheme with a fourth order Runge-Kutta starting routine.

The Earth's magnetic field is simulated by an eighth-order spherical harmonic model. The atmospheric density model is that of Jacchia (Reference 1). For aerodynamic and solar pressure torques, the spacecraft is modeled by 14 flat plates; twelve sides, one top and one bottom.

All simulation results are presented as plots of four angles versus time; THETA, PITCH, ROLL and YAW. THETA is the angle between the spacecraft yaw axis and the local vertical PITCH, ROLL and YAW are Euler angle rotations

in this specified order. Note that on some of the capture run plots the yaw angle appears to have sharp discontinuities. This is a peculiarity of the plot when the yaw angle is near 180 degrees. When the angle exceeds 180 degrees, it suddenly shifts to -180 degrees.

The simulation task is divided into two sections: Capture and Steady-State.

4.1 Capture Simulation

4.1.1 Initial Conditions

1.	Orbit altitude	235 nm
2.	Orbit inclination	28.5 deg
3.	Initial attitude	15 deg
4.	Initial rates	
	Nominal	0.04 deg/sec
	High	0.10 deg/sec
	Maximum	0.25 deg/sec
5.	Magnetic dipole	7300 pole-cm
6.	CP-CM offset	1 inch in pitch and roll
		2 inches in yaw

(Items 3, 4 Nominal, 4 High, 4 Maximum, and 5 apply on each axis.)

7. TEMPERATURE PROFILES:

1.	NOMINAL DAMPING	$T=70^{\circ}$ F.
2.	MINIMUM DAMPING	$T=80^{\circ}$ F. + 5°F./ORBIT $T_{max}=140^{\circ}$F.
3.	MAXIMUM DAMPING	$T=60^{\circ}$F - 5°F./ORBIT $T_{min}=0^{\circ}$ F.

Initial damper temperature at separation is specified to be 60-80°F. Maximum temperature variation is specified to be 5° F. per orbit. A plot of damping constant as a function of temperature is given in Figure 4.1.1. Also included are the linear approximations to this curve used in the simulation.

8.	DAMPER DECENTERING FACTOR	1.6 FOR NOMINAL AND MAXIMUM 1.0 FOR MINIMUM

The damper decentering factor results because the damper inner sphere after months in a 1-G field and a constant orientation is resting on the nylon separators. The gap between the inner and outer spheres is reduced to 0.060 inches from 0.100 inches. The gap on the other side of the sphere is increased to 0.14 inches. Under these conditions the damping constant is increased. The magnitude of the increase, called the decentering factor, is approximately

$$DCF \approx \frac{\text{Nominal gap}}{\text{Nominal gap - off-center distance}}$$

The DCF at launch is approximately 1.67. The diamagnetic force on the inner sphere gradually centers the sphere, reducing the DCF to 1.0. However, the time constant of this effect is approximately 11 days which is very long compared to capture times of less than four days. Thus for capture simulation runs, the DCF can be considered constant. A value of 1.6 was used which is the average value for a 60-hour period. This value was used for nominal and maximum damping constants. For minimum damping constants a factor of 1.0 was used to assure that an absolute minimum value was used.

VARIATION OF DAMPING CONSTANT WITH TEMPERATURE

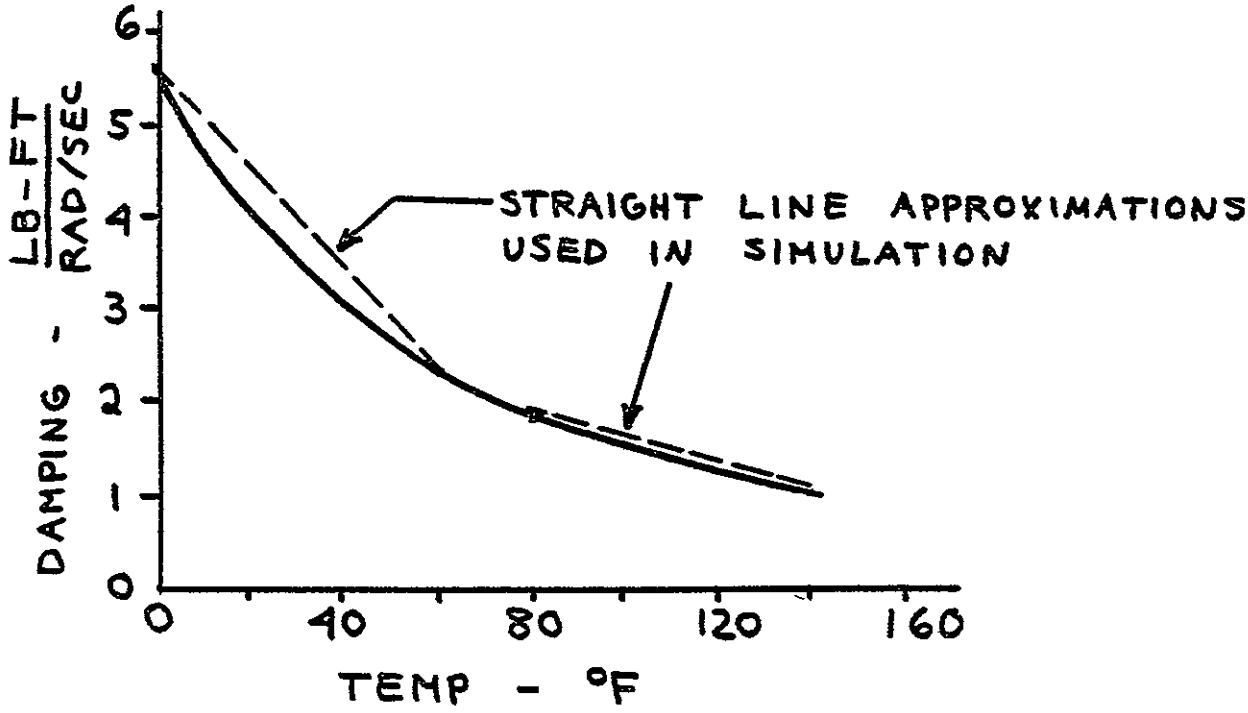

Fig 4.1.1

4.1.2 Simulation Capture Runs

Six capture runs were made. These are defined in Table 4.1.1

RUN NO.	INITIAL RATE/AXIS (deg/sec)	DAMPING CONSTANT
1	0.04	Nominal
2	0.04	Minimum
3	0.04	Maximum
4	0.10	Minimum
5	0.10	Maximum
6	0.25	Minimum

Capture Run Index

Table 4.1.1

The first three runs are for the maximum specified value of initial rate. This is less than the upright capture rate requirement (See Section 3.4) so that the spacecraft is captured upright after initial pitch and roll errors of about 40 degrees. However, in each case yaw is captured backwards. Acquisition time, arbitrarily defined as the time required to reduce pitch and roll errors to less than 10 degrees range from 85 hours down to 46 hours. Pitch and roll time constants have been calculated assuming an exponential decay characteristic. These results are listed in Table 4.1.2. Note that in roll the time constant increased sharply between nominal and maximum damping. This indicates the magnet is unable to maintain its orientation with respect to the earth's field. This is to be expected since

the maximum damping value is 8.8 lb-ft-sec (5.5 x the 1.6 DCF) and the roll rates are relatively high in the first half of the run (for example 0.02 deg/sec at 15 hours). Figure 3.6.7 shows the magnet will be about 50 degrees off the earth's field. This problem is much more severe in roll than in pitch because, for a low inclination orbit, the magnet is forced to rotate through larger roll angles than pitch angles to follow the earth's field.

Plots of these three capture runs are shown in Figures 4.1.1 to 4.1.7 inclusive. Each simulated a flight time of 80 hours. A second plot for each run is provided for the last 28 hours of each run with an expanded scale. Finally, Figure 4.1.3 shows the nominal damping case run for 200 hours, time to reach and maintain steady-state conditions.

	DAMPING		
	MIN	NOM	MAX
PITCH TIME CONSTANT (ORBITS)	43.	31.	21.
ROLL TIME CONSTANT (ORBITS)	20.	19.	56.
CAPTURE TIME (HOURS) ($\theta_p < 10^\circ$, $\theta_r < 10^\circ$)	85.	62.	46.

Results of Nominal Capture Runs

Table 4.1.2

Two capture runs were made with initial rates of 0.1 deg/sec and minimum and maximum damping. These are shown in Figures 4.1.8 and 4.1.9 respectively. Here the initial rate exceeds the upright capture requirement so that the spacecraft is tumbling following separation.

For minimum damping tumbling stops after 60 hours and a normal acquisition follows. However, for the maximum damping case while roll and yaw are captured, the spacecraft continues to tumble about the pitch axis. After 150 hours the spacecraft pitch rate is almost the initial value. The reason this occurs is that the magnet tends to seek a fixed position with respect to the pitch axis. As the spacecraft tumbles in pitch the magnet cones about the pitch axis, thus providing virtually no damping about this axis. This behavior is illustrated in Figure 4.1.10. This plot shows the following parameters in addition to THETA:

PRATE	-	pitch body rate with respect to a body-fixed reference frame, deg/sec.
GAMW BETW	-	these two angles describe the orientation of the damper magnet with respect to the orbiting reference frame. The magnet is initially aligned with the local vertical and then given the following two Euler rotations:

1. GAMW about the pitch axis
2. BET about the roll axis

It can be seen that GAMW is almost identical to the pitch attitude in the previous figure while BET varies relatively slowly. The pitch rate shows a very slight exponential decay in the last 50 hours of the plot. The time constant is roughly estimated to be 640 hours.

A final capture run with 0.25 deg/sec initial rates and minimum damping was run to estimate the time required to reduce the initial rates to 0.1 deg/sec (which was the approximate starting point for run #4) and this time proved to be 66 hours. This run was not performed for the maximum damping case since the 0.1 deg/sec case failed to capture.

CAPTURE RUN # 1 ATTITUDE ERROR HISTORY, ANGLES IN DEGS

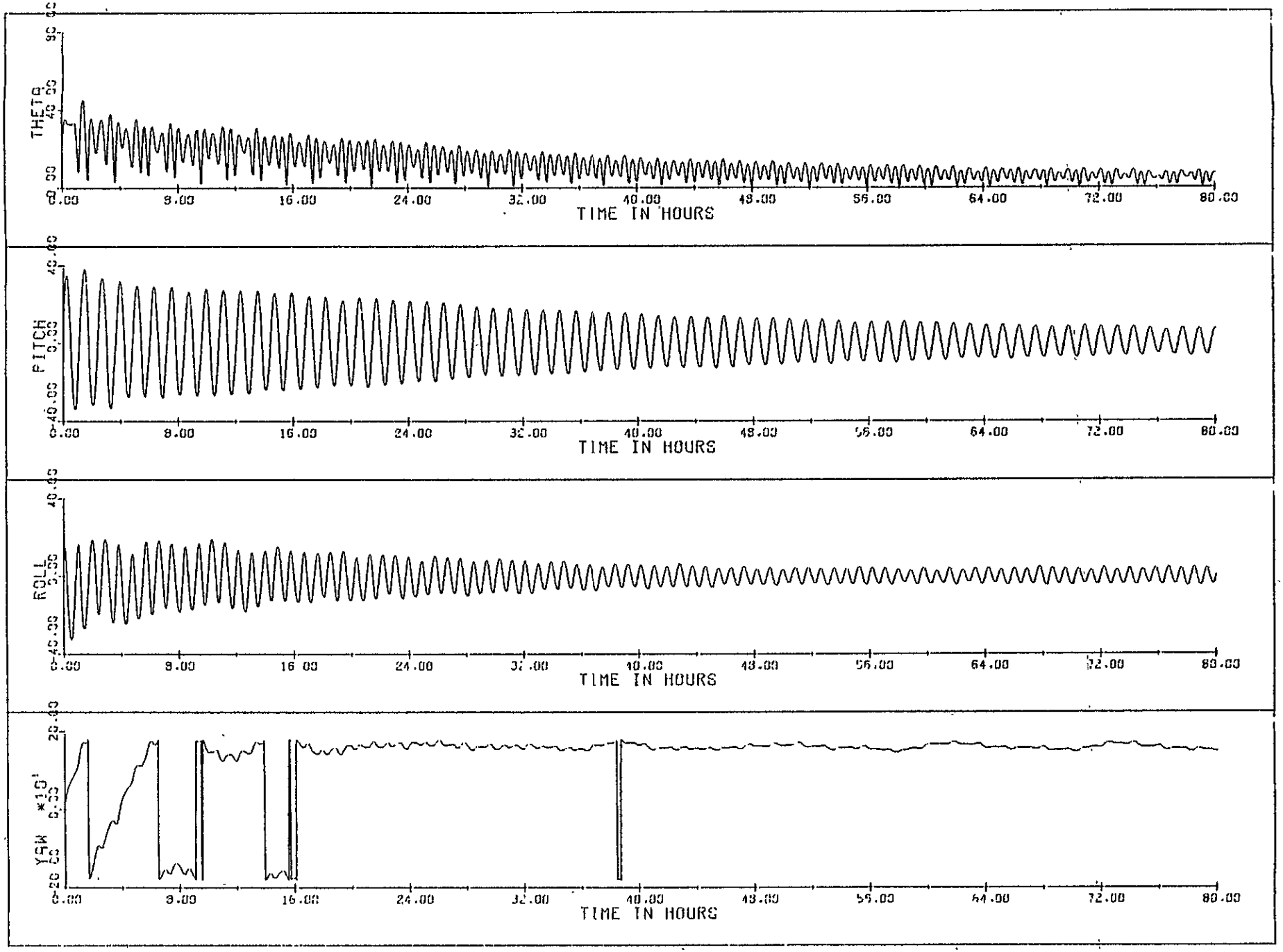

NOMINAL DAMPING .04 deg/sec per axis

CAPTURE #1 ATTITUDE ERROR HISTORY, ANGLES IN DEGS

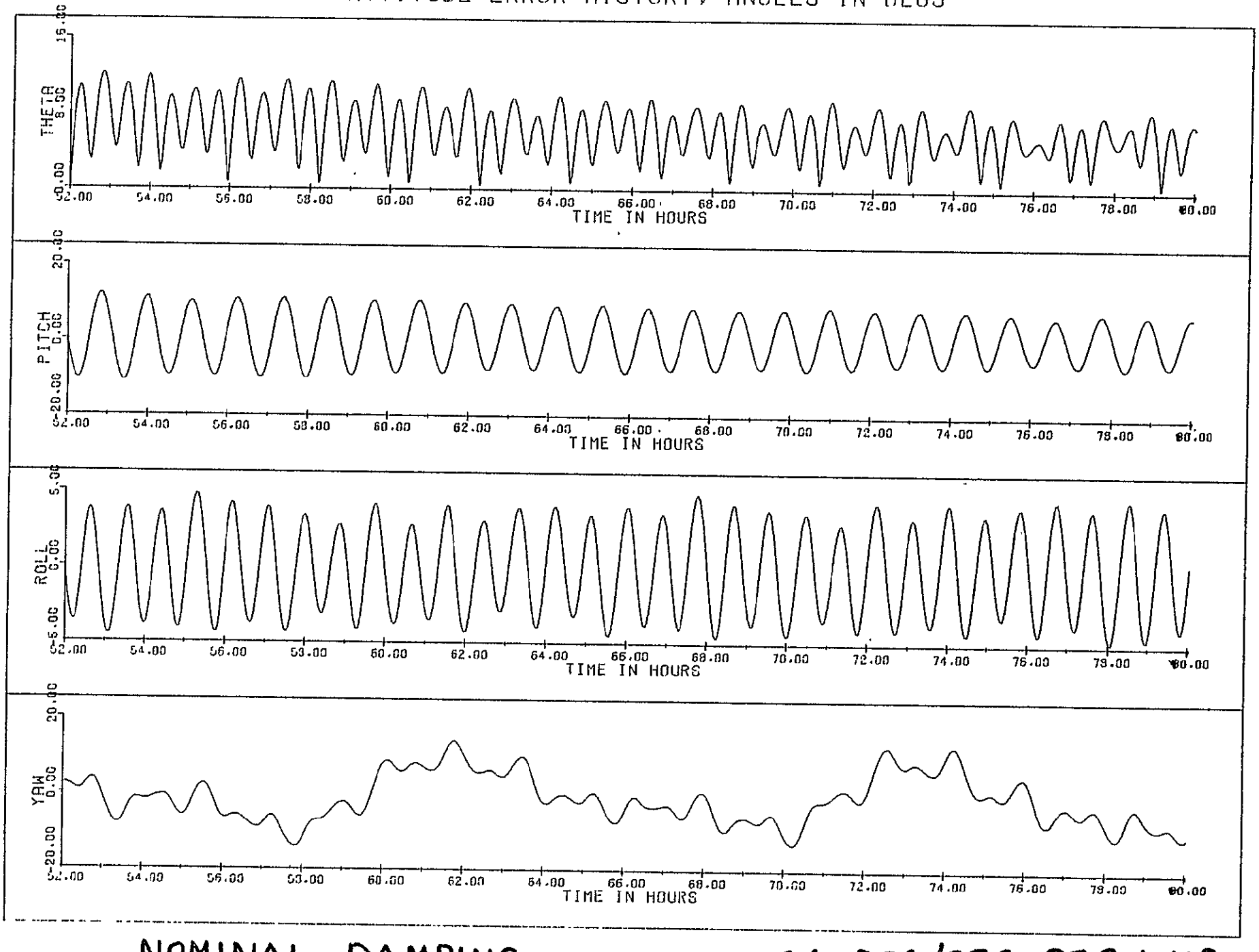

NOMINAL DAMPING .04 DEG/SEC PER AXIS

fig. 4.1.2

CAPTURE RUN #1 — ATTITUDE ERROR HISTORY

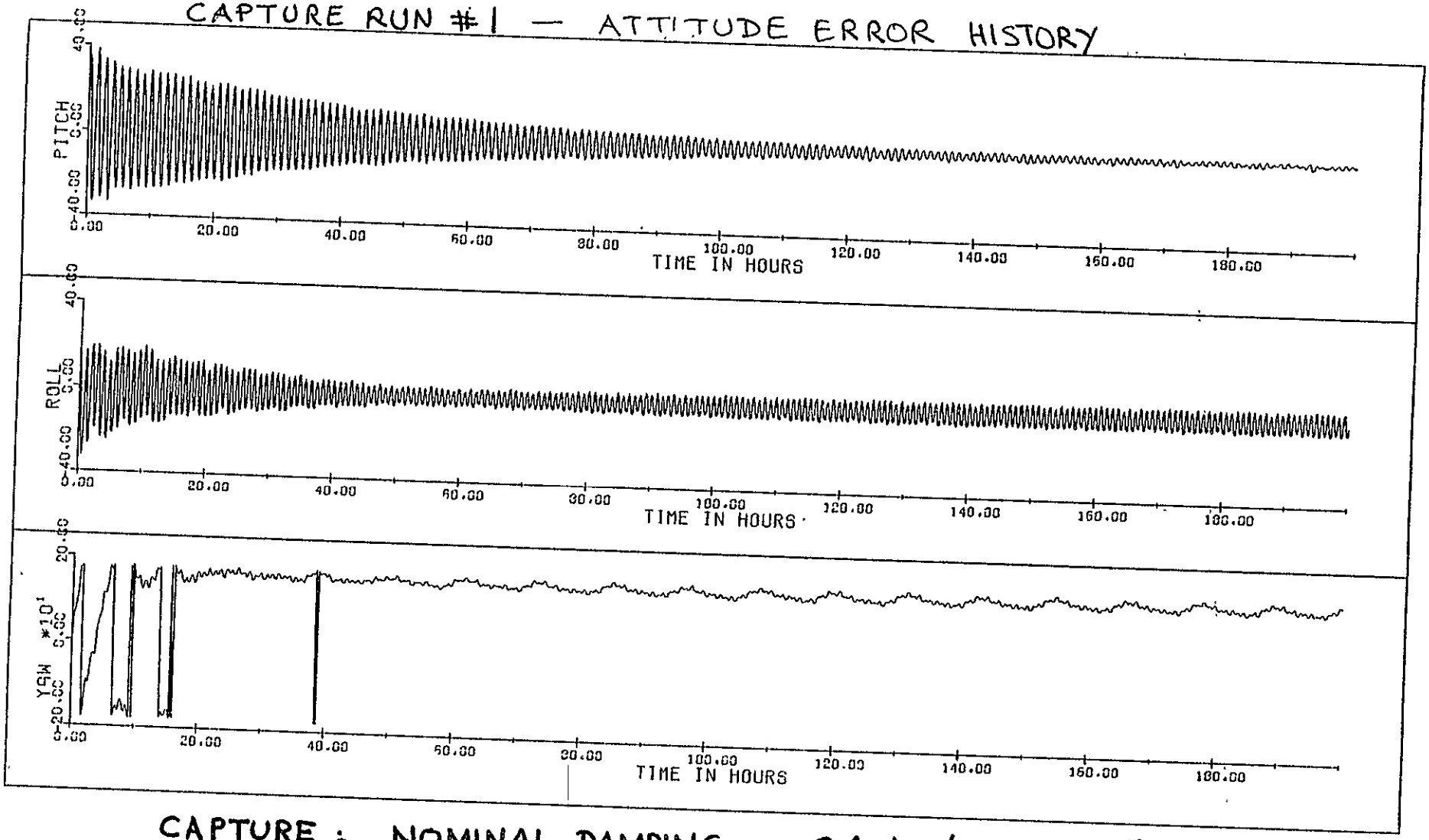

CAPTURE ; NOMINAL DAMPING ; .04 deg/sec on all axes.

fig. 4.1.3

CAPTURE RUN # 2 ATTITUDE ERROR HISTORY, ANGLES IN DEGS

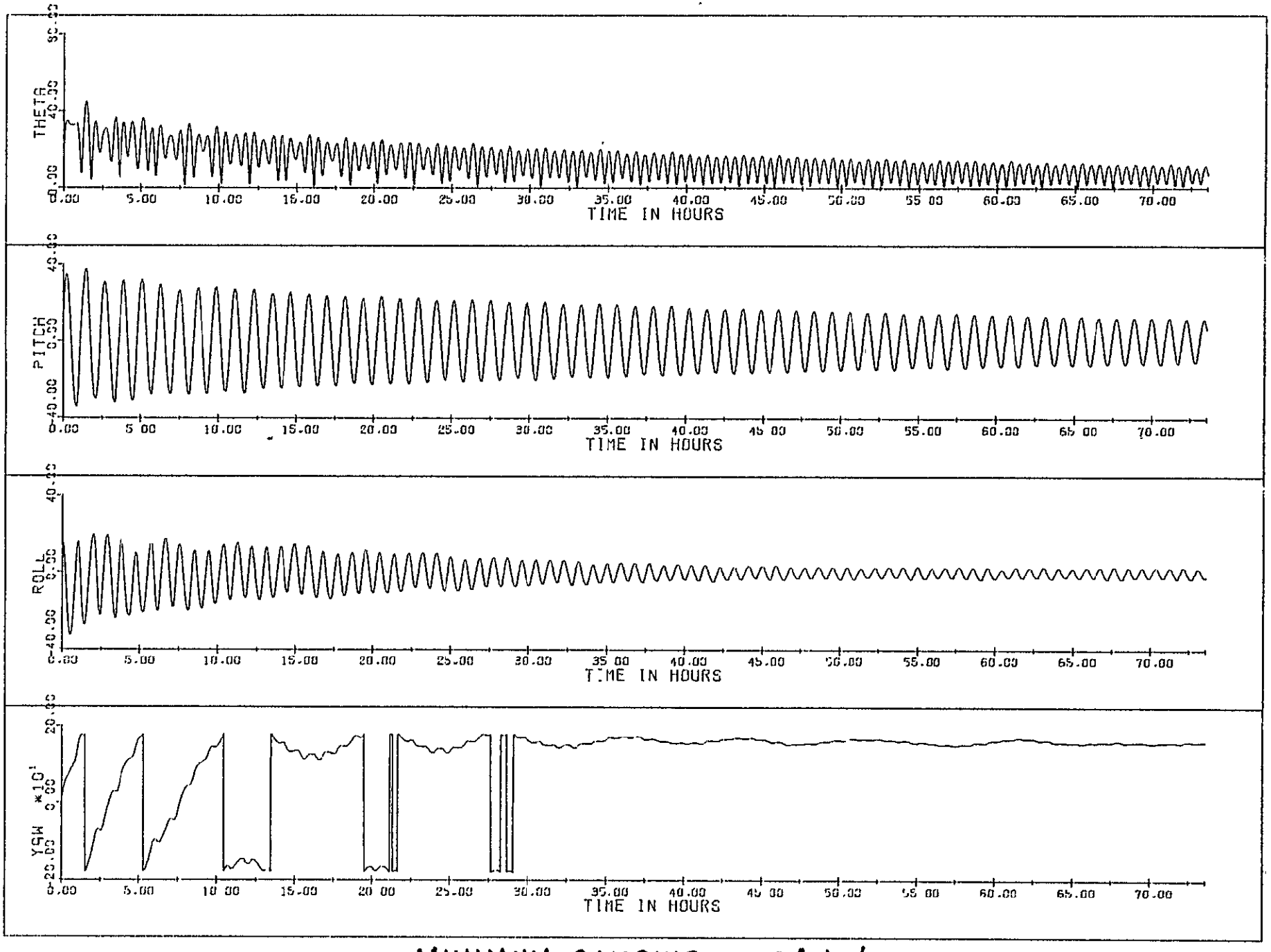

MINIMUM DAMPING ; ·04 deg/sec per axis

fig 4.1.4

CAPTURE # 2

ATTITUDE ERROR HISTORY, ANGLES IN DEGS

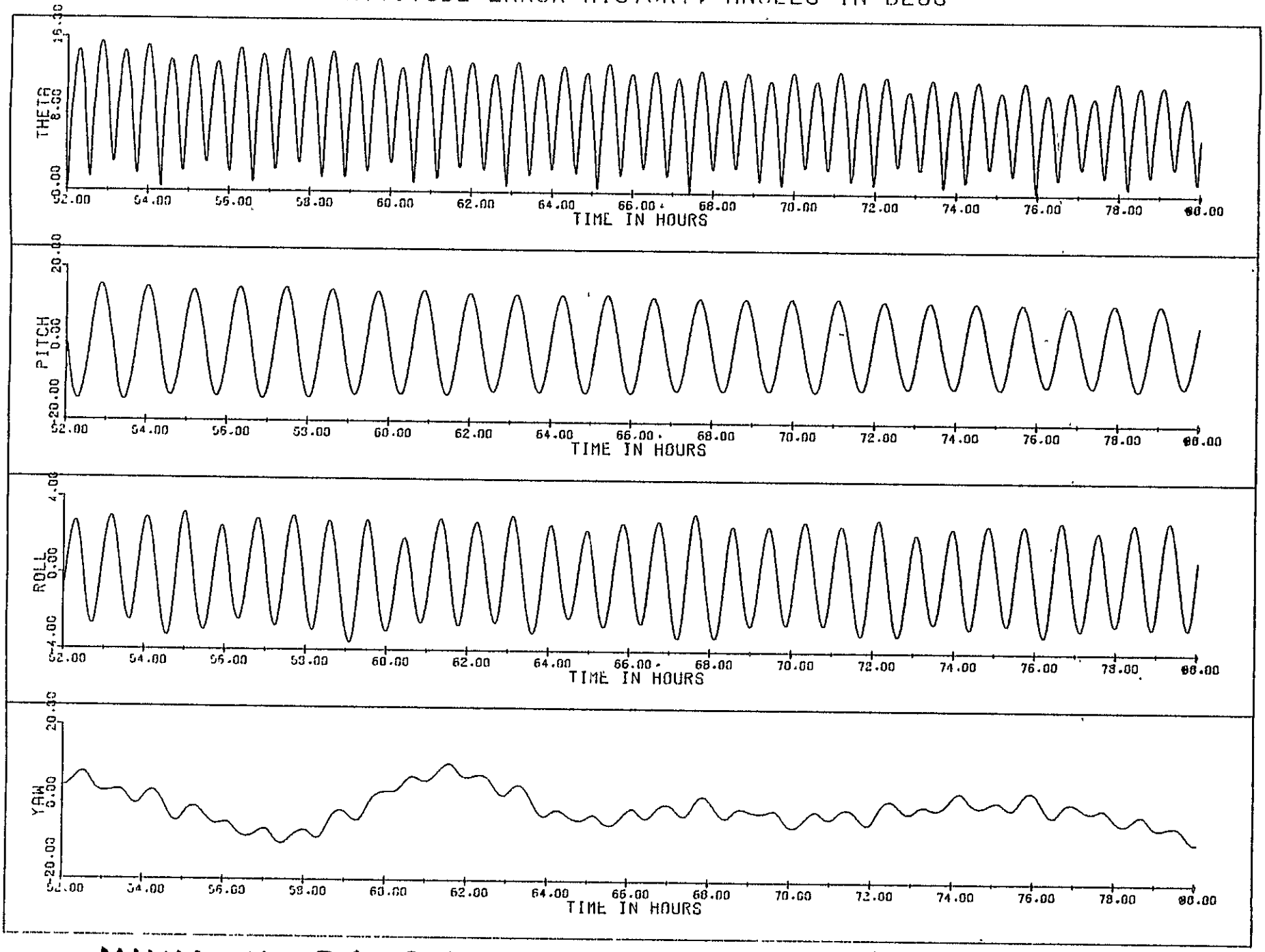

MINIMUM DAMPING .04 DEG/SEC PER AXIS

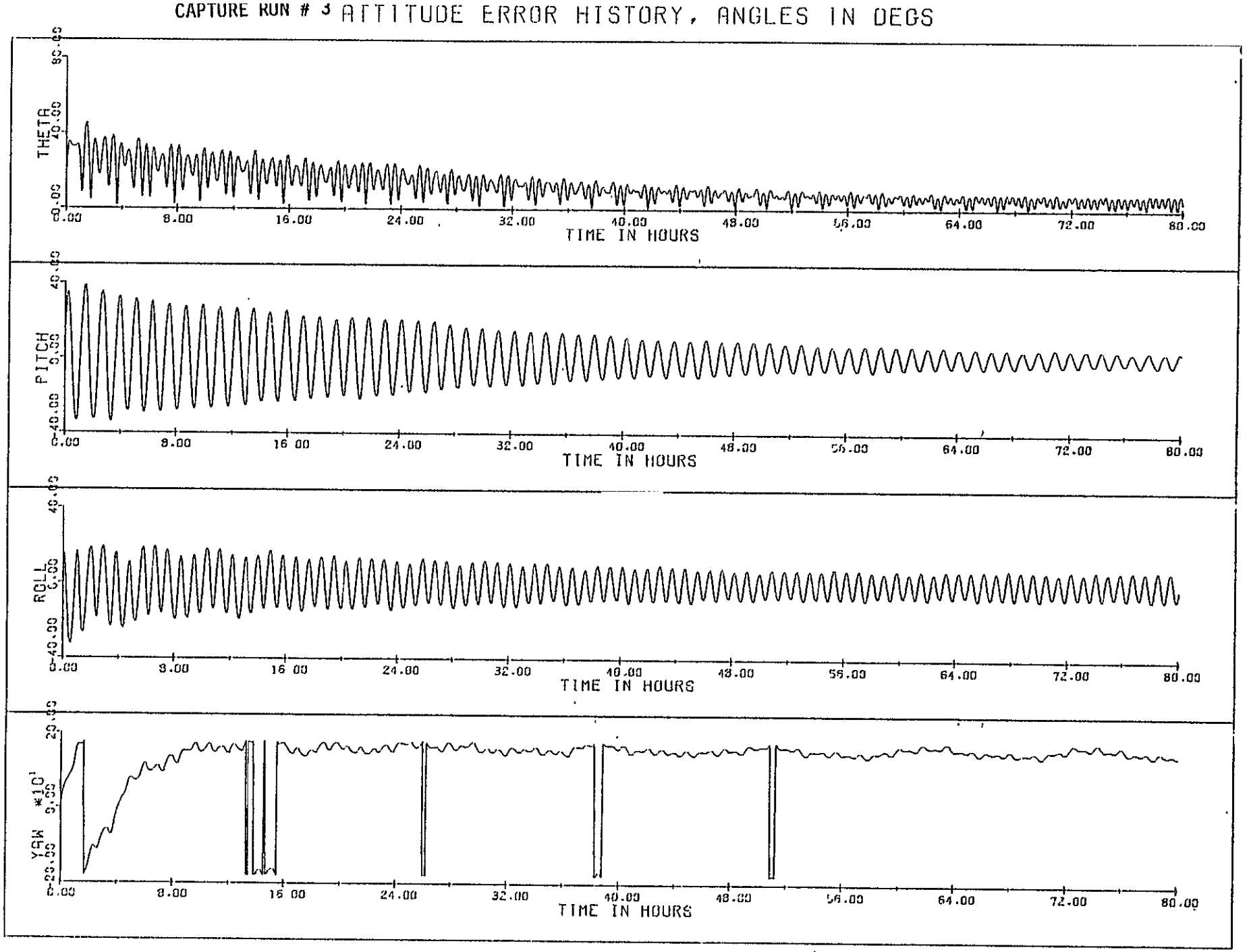

MAXIMUM DAMPING ; .04 deg/sec per axis

fig 4.1.6

CAPTURE #3 ATTITUDE ERROR HISTORY, ANGLES IN DEGS

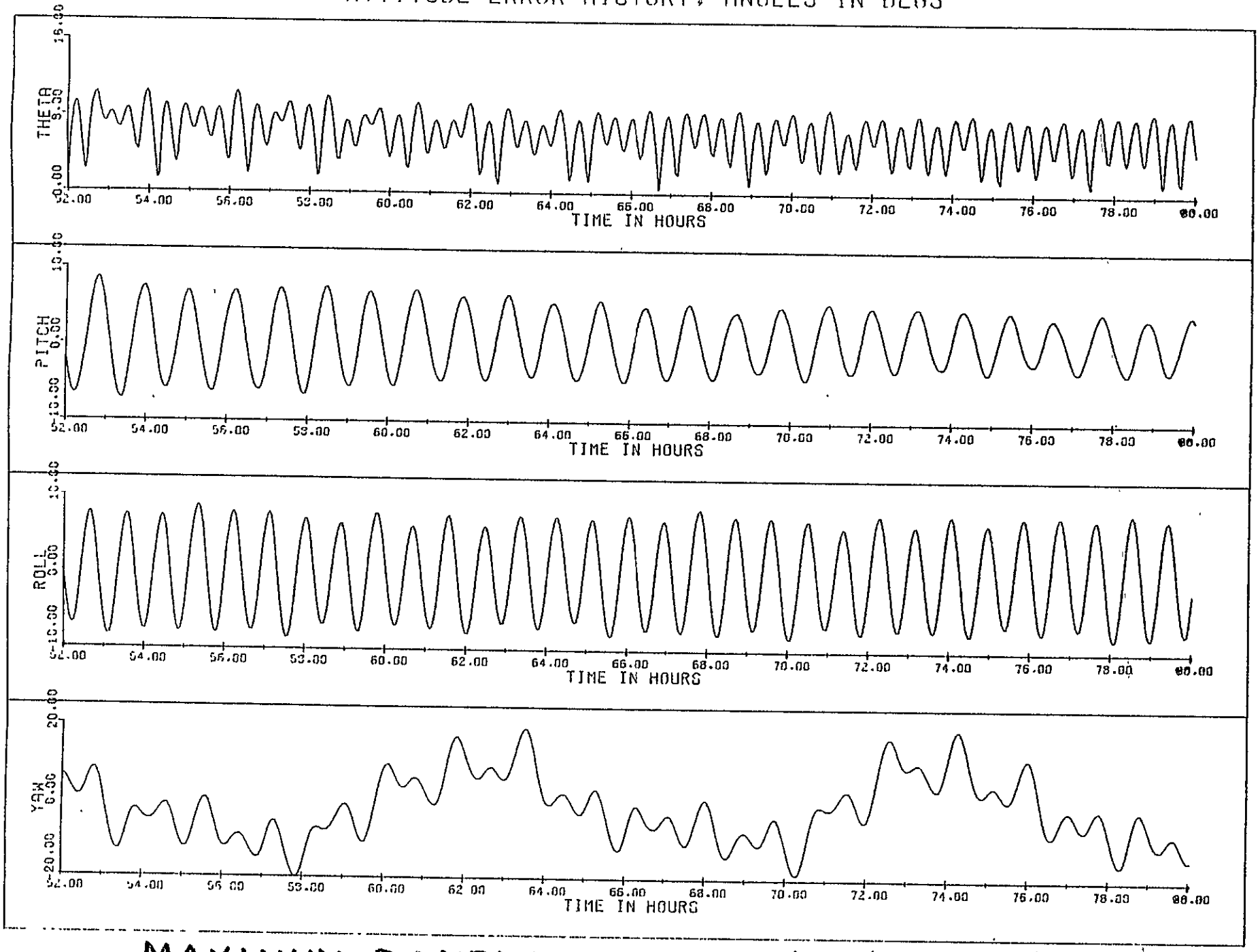

MAXIMUM DAMPING .04 DEG/SEC PER AXIS

CAPTURE #4 ATTITUDE ERROR HISTORY, ANGLES IN DEGS

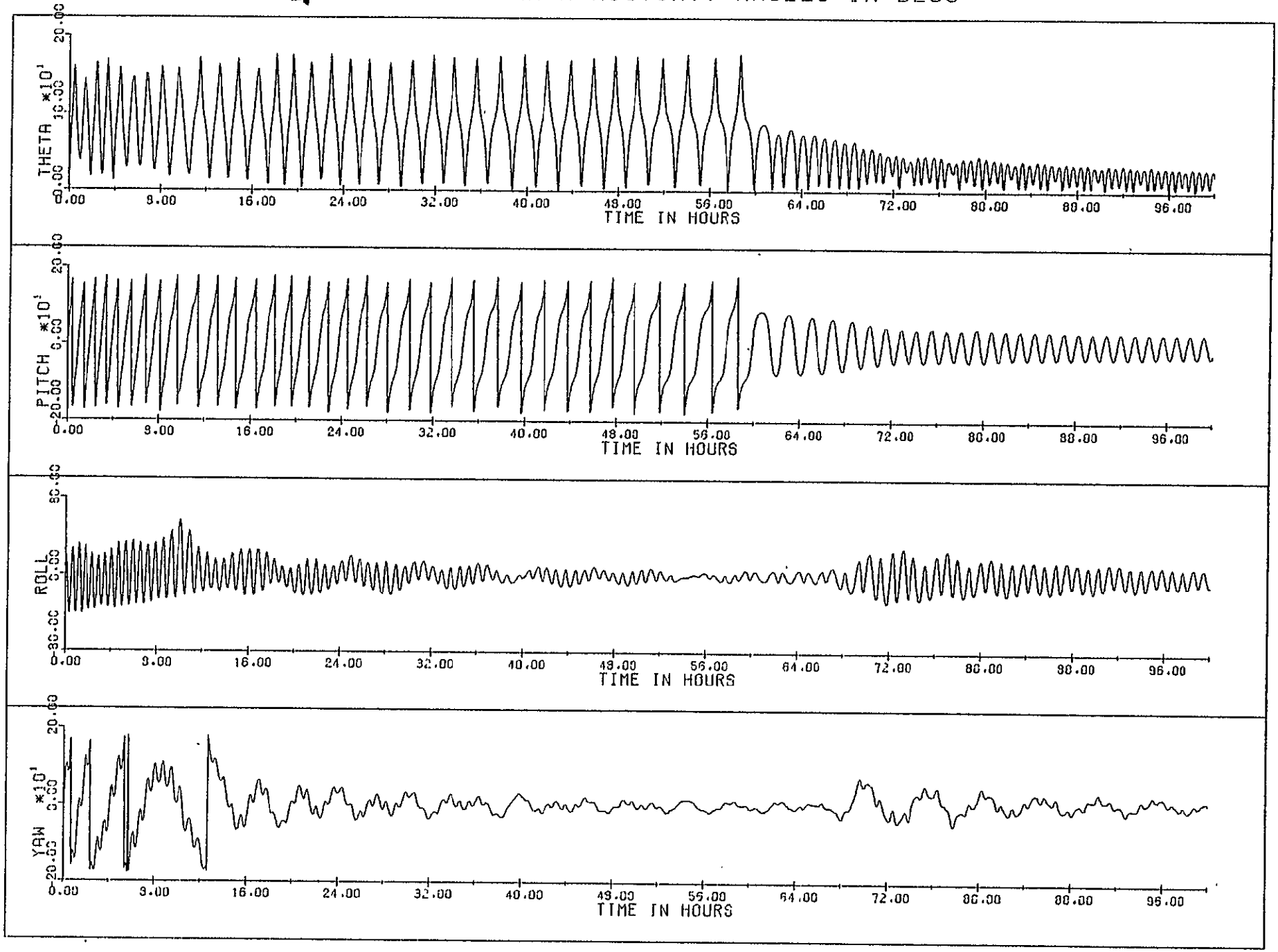

MINIMUM DAMPING ; •1 DEG/SEC PER AXIS.

fig 4.1.8

CAPTURE RUN #5 – ATTITUDE ERROR HISTORY

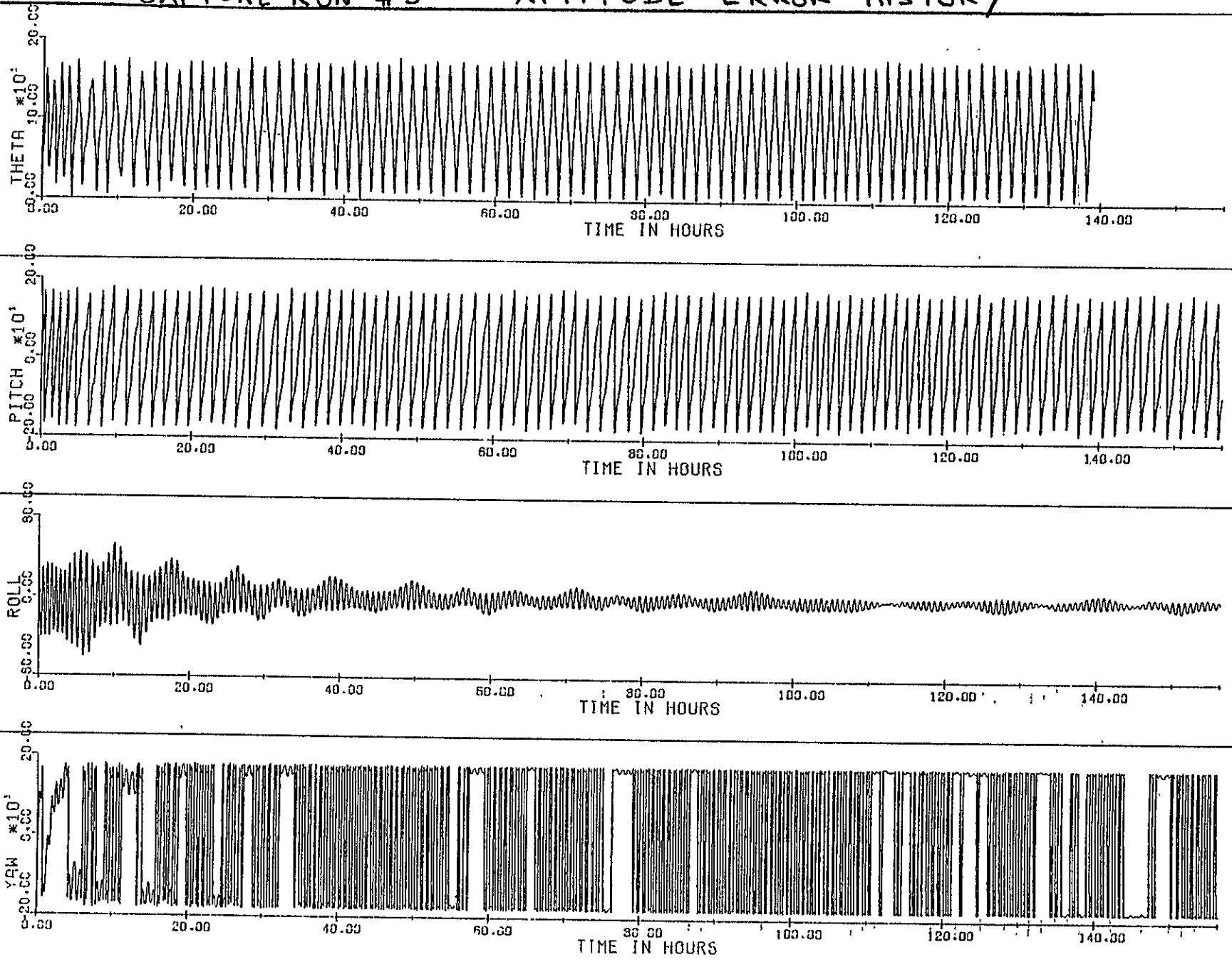

MAXIMUM DAMPING .1 DEG/SEC PER AXIS

CAPTURE RUN #5 ATTITUDE HISTORY. ANGLES IN DEG.

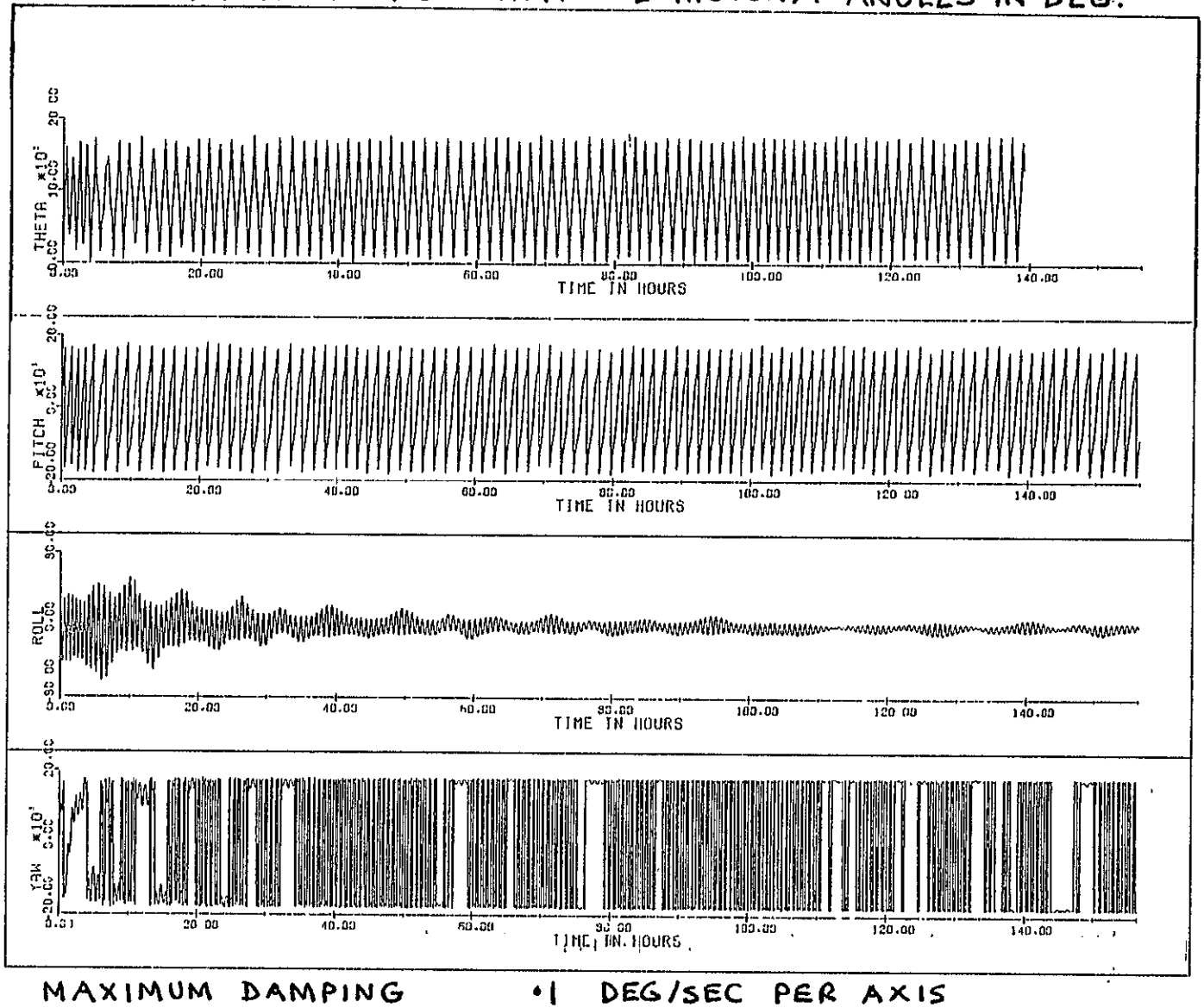

MAXIMUM DAMPING .1 DEG/SEC PER AXIS

fig 4.1.9

CAPTURE RUN #5 ATTITUDE ERROR HISTORY, ANGLES IN DEGS

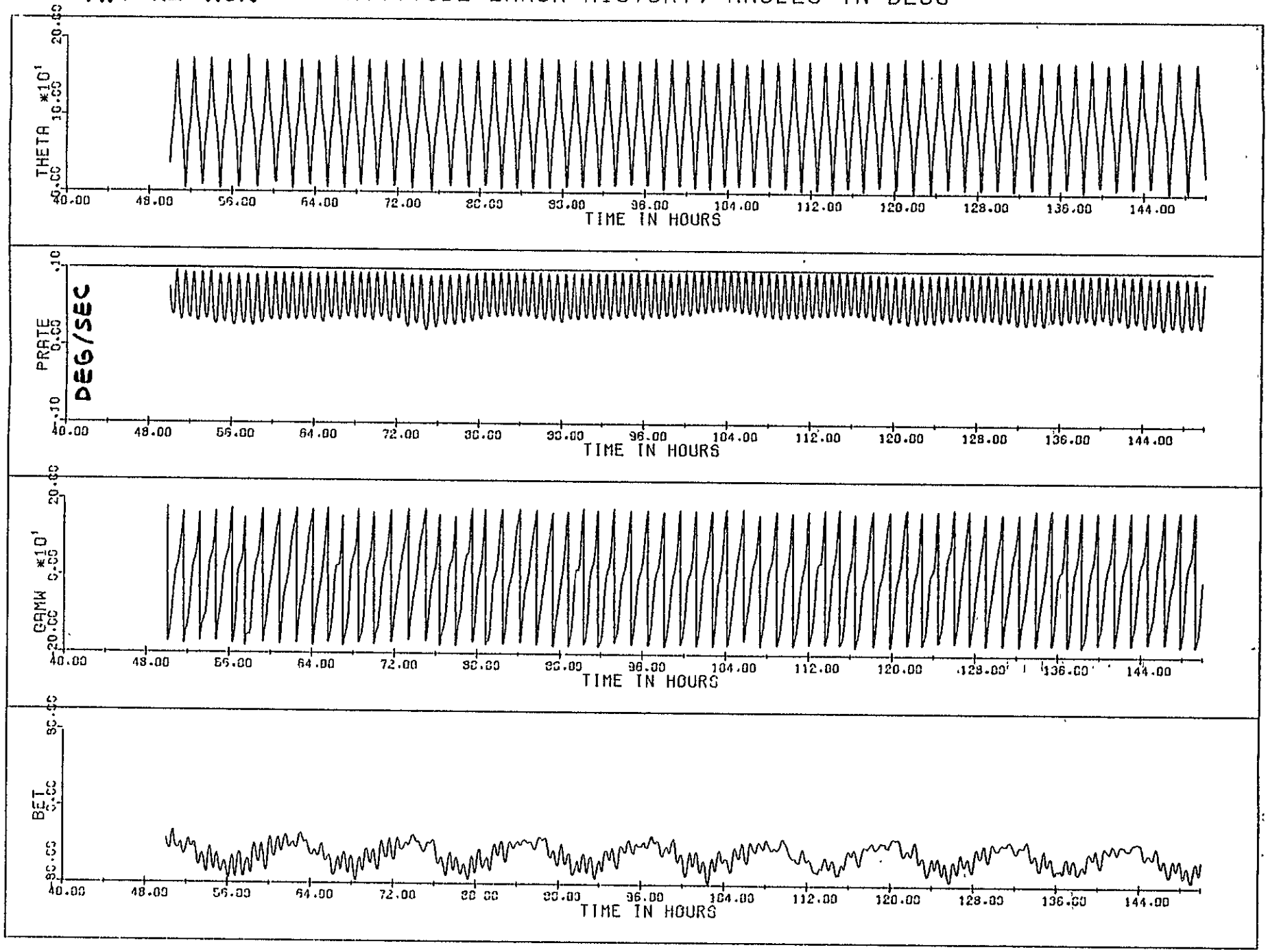

MAXIMUM DAMPING 0.1 DEG/SEC PER AXIS

4.2 Steady-State Simulation

Twelve computer simulations were made to determine the spacecraft attitude control performance when steady-state conditions have been reached. Three additional runs were made to demonstrate the effects of Garber instability and a damper malfunction. Table 4.2.1 is an index to the steady-state simulation runs. Appendix B lists the key parameter values used in these runs.

Two sets of disturbances were defined: nominal and worst-case. These are listed below. The worst-case set was obtained from the nominal set by doubling both the CP-CM offsets and the magnetic dipole.

	NOMINAL	WORST CASE
DIPOLE (pole-cm per axis)	7300	14600
CP-CM OFFSET (inches)		
ROLL	1.0	2.0
PITCH	1.0	2.0
YAW	2.0	4.0
ECCENTRICITY	.002	.002
10.7 CM SOLAR FLUX INDEX	200	200
AERODYNAMIC DRAG COEFFICIENT	2.2	2.2

The altitudes used were:

235 nm - separation

215 nm - retrieval

175 nm contingency

The damper temperature range was 0-140° F. which corresponds to a damping constant range of 5.5 to 1.0 lb-ft-sec respectively.

Polarities of CP-CM offsets and magnetic dipoles were selected to provide maximum errors. Perigee was located at the point of maximum atmospheric density to maximum aerodynamic torque.

The results of the steady-state simulation runs are presented in Tables 4.2.2 and 4.2.3. The first of these tables lists the maximum values of altitude error and rate. The second table gives altitude error as a bias plus a variation about the bias.

STEADY-STATE SIMULATION

RUN-SCHEDULE

RUN NO.	ALT (NM)	DISTURB-ANCES	DAMPING	COMMENTS
1	235	Damper	2.0	Nominal
2	↓	All	1.0	Disturbances
4	↓		5.5	
5	215	All	1.0	Nominal
7	↓		5.5	Disturbances
8	175	All	1.0	Nominal
10	↓		5.5	Disturbances
11	235	All	1.0	Worst-Case
13	175		1.0	Disturbances
14	235	All	5.5	Worst-Case
16	175		5.5	Disturbances
17	175	All	0.2	Exceed Garber
18	175	All	0.2	Limits
19	175	All	0.0	Locked Damper Magnet
20	215	All	2.0	CP-CM Offsets 10% of Maximum Dimensions from Spacecraft Center

TABLE 4.2.1

	(ERROR (DEG)			RATE (DEG/SEC)			ALT (NM)	DAMPING (LB-FT-SEC)	DISTURBANCES
	PITCH	ROLL	YAW	PITCH	ROLL	YAW			
1	0.9	4.3	10.3	<.001	.0074	.0015	235	2.0	DAMPER ONLY
2	1.2	3.3	22.2	<.001	.0064	.0026	235	1.0	NOMINAL
4	2.0	7.5	29.1	.0013	.0146	.0070	235	5.5	
5	1.4	3.3	29.0	.0015	.0061	.0042	215	1.0	
7	2.4	8.4	31.4	.0044	.0143	.0069	215	5.5	
8	3.1	2.4	35.1	.0022	.0040	.0014	175	1.0	
10	3.7	9.1	43.1	.0027	.0179	.0065	175	5.5	
11	1.7	3.7	32.8	<.001	.0064	.0047	235	1.0	WORST CASE
13	6.8	3.1	52.1	.0051	.0061	.0095	175	1.0	
14	2.8	7.9	35.7	.0017	.0153	.0050	235	5.5	
16	6.8	9.2	50.0	.0036	.0176	.0073	175	5.5	6-inch CP-CM x-axis OFFSET
17	DID NOT REACH STEADY-STATE						175	0.2	GARBER INSTABILI
18	UNSTABLE						175	0.2	LOCKED DAMPER
19	UNSTABLE						175	0.0	LARGE CP-CM OFFSETS
20	22.2	9.6	134.3	.0230	.0066	.0496	215	2.0	

LDEF Steady-State Simulation Results,
Maximum Attitude Errors and Rates

TABLE 4.2.2

RUN NO.	PITCH - DEG		ROLL - DEG		YAW - DEG	
	BIAS	VARIATION	BIAS	VARIATION	BIAS	VARIATION
1	+ 0.4	0.5	+ 0.1	4.2	+ 2.65	7.65
2	+ 0.45	0.75	- 0.05	3.25	+13.9	8.3
4	+ 0.95	1.05	- 0.15	7.35	+17.8	11.3
5	+ 0.55	0.85	+ 0.05	3.25	+18.25	10.75
7	+ 1.1	1.3	- 0.2	8.2	+21.0	10.4
8	+ 1.55	1.55	- 0.05	2.35	+31.75	3.35
10	+ 1.75	1.95	+ 0.1	9.0	+32.95	10.15
11	+ 0.6	1.1	0	3.7	+22.55	10.25
13	+ 2.6	4.2	0	3.1	+37.9	14.2
14	+ 1.4	1.4	- 0.15	7.75	+25.4	10.3
16	+ 3.25	3.55	- 0.30	8.9	+38.9	11.1
20	+ 4.0	18.2	- 0.95	8.65	+48.8	85.5

LDEF Steady-State Simulation Results,
Biases and Variations

TABLE 4.2.3

Simulation #1 has the magnetically anchored rate damper as its only disturbance source. The damping constant is the nominal value of 2.0 lb-ft-sec. Figure 4.2.1 shows the results of the simulation, and yields maximum errors in pitch, roll and yaw of 0.9, 4.3 and 10.3 degrees respectively. The roll and yaw errors are substantial, and they exceed the linear estimate by a factor of four. It is believed this discrepancy is caused by the damper dynamics. In the linear model the damper magnet is always aligned with the earth's magnetic field. In the simulation the damper magnet is acted upon by two torques; the magnetic torque and the damping torque. When the damping torque approaches the magnitude of the magnetic torque the magnet is dragged off of the earth's field. Damping torque is proportional to the relative rate between the spacecraft and the damper magnet. For a low inclination orbit roll and yaw rates are much higher (by a factor of approximately 10 and 4 respectively) than pitch rate. The key point here is that damper torques are a significant error source in roll and yaw.

Simulation runs 2-10 considered the spacecraft to be subject to the nominal set of disturbances. The results are shown in Figures 4.2.1 - 4.2.7 inclusive. Damping varied between minimum and maximum values, and altitude ranged from 235 to 175 nm. These runs show large increases in yaw error, primarily caused by aerodynamics. Note that in runs #5 and #8 where the damping is minimum the total roll error is less than in run #1, despite the effects of CP-CM offset and spacecraft magnetic dipole which are not included in run #1. This results because the roll error is caused primarily

by the damping torque. Pitch errors increase as the altitude drops due to the aerodynamic torque. Total pitch bias at the minimum altitude is 1.55 - 17.5 degrees. Table 4.2.4 presents a comparison between the linear estimates and the simulation results for two runs at the intermediate altitude. The pitch and yaw estimates are reasonably close to the simulation results. However, the roll error disagreement is significant. This is caused, as mentioned previously, by the roll damper torque error. This effect is not noticed in yaw because the yaw aerodynamic error is much larger than the damper error. All of the errors and rates are within specification with the exception of yaw attitude. The 30-degree requirement at 215 nm is slightly exceeded (31.4 degrees in run #7) and the 10-deg bias requirement is also slightly exceeded (11.3 deg in run #4).

	SIMULATION #5 (fig 4.2.5)			SIMULATION #7 (fig 4.2.7)		
Disturbance	Pitch	Roll	Yaw	Pitch	Roll	Yaw
Aero	.8	.1	35.0	.8	.1	35
Damper	0.	.5	1.2	.3	2.7	6.7
Magnetics	.2	.1	5.0	.2	.1	5.0
Eccentricity	.2	-	-	.2	-	-
RSS	.9	.5	35.4	0.9	2.7	36.0
Sum	1.2	.7	41.2	1.5	2.9	46.7
Simulation Results	1.4	3.3	29.0	2.4	8.4	31.4

Linear Estimate

TABLE 4.2.4

Simulation runs 11-16 were run with the worst-case set of disturbances. The results are shown in Figures 4.2.8 - 4.2.11 inclusive. Again, with the exception of the yaw axis, errors are within specification requirements. Yaw error exceeded the 30-degree requirement by 5.7 degrees (run #14) and the maximum variation about the bias reached 14.2 degrees (run #13). All rates remained within specification.

Simulation runs 17-19 were run to determine the effect of violating the Garber instability limits, and to determine performance when the damper magnet is locked. These are discussed in sections 4.3 and 4.4 respectively.

Simulation #20 shows the effect of large CP-CM offsets. Offsets were set at 10% of the maximum vehicle dimensions measured from the CM. This yields the following values of offset:

x - 1.5 feet
y - 0.7 feet
z - 0.7 feet

The results are shown in Fi. 4.2.12. Pitch and roll oscillations are relatively high (22 and 10 degrees respectively) while yaw oscillates ± 86 degrees about a bias position of 49 degrees. The nominal magnetic dipole and orbit eccentricity were present in this run. Yaw rate of 0.0496 deg/sec exceeded the rate specification of 0.034 deg/sec. Pitch and roll rates remained within specification.

4.3 Garber Instability

Simulation run #17 was run to show the effects of Garber instability. A 6-inch yaw axis CP-CM offset at 175 nm altitude should produce a pitch bias of 6 degrees. At this bias value a damping constant of 1.6 lb-ft-sec or higher is required to avoid the instability. Damping was set to 0.2, one-eighth of the limit value. The results are shown in Figure 4.3.1. Although steady-state conditions were not reached there is no sign of instability in the 120-hour run. This result is not understood at this time. One item which may contribute to this result is that the aerodynamic pitch torque is not a constant but varies by a factor of 1.5. Thus the bias is not constant but includes various frequency components.

Because of this result run #18 was made. The aerodynamic torque was eliminated and a constant pitch torque of 0.01 lb-ft applied. This torque will produce a steady-state pitch bias of 4.3 degrees. The damping constant of 0.2 was repeated (the stability limit is 1.15). The results are shown in Figure 4.3.2. The performance is obviously unstable. This confirms the existence of Garber instability, and demonstrates that its effects would be disastrous to the spacecraft.

Since the conflict between these two runs is not understood a conservative approach was taken. Although aerodynamic torques appear less likely to cause instability than a constant torque, this observation was ignored in selecting the damping constant. The LDEF damper, for the CP-CM offsets considered, is far inside the Garber instability limits. The penalty in performance is a slight increase in damper errors.

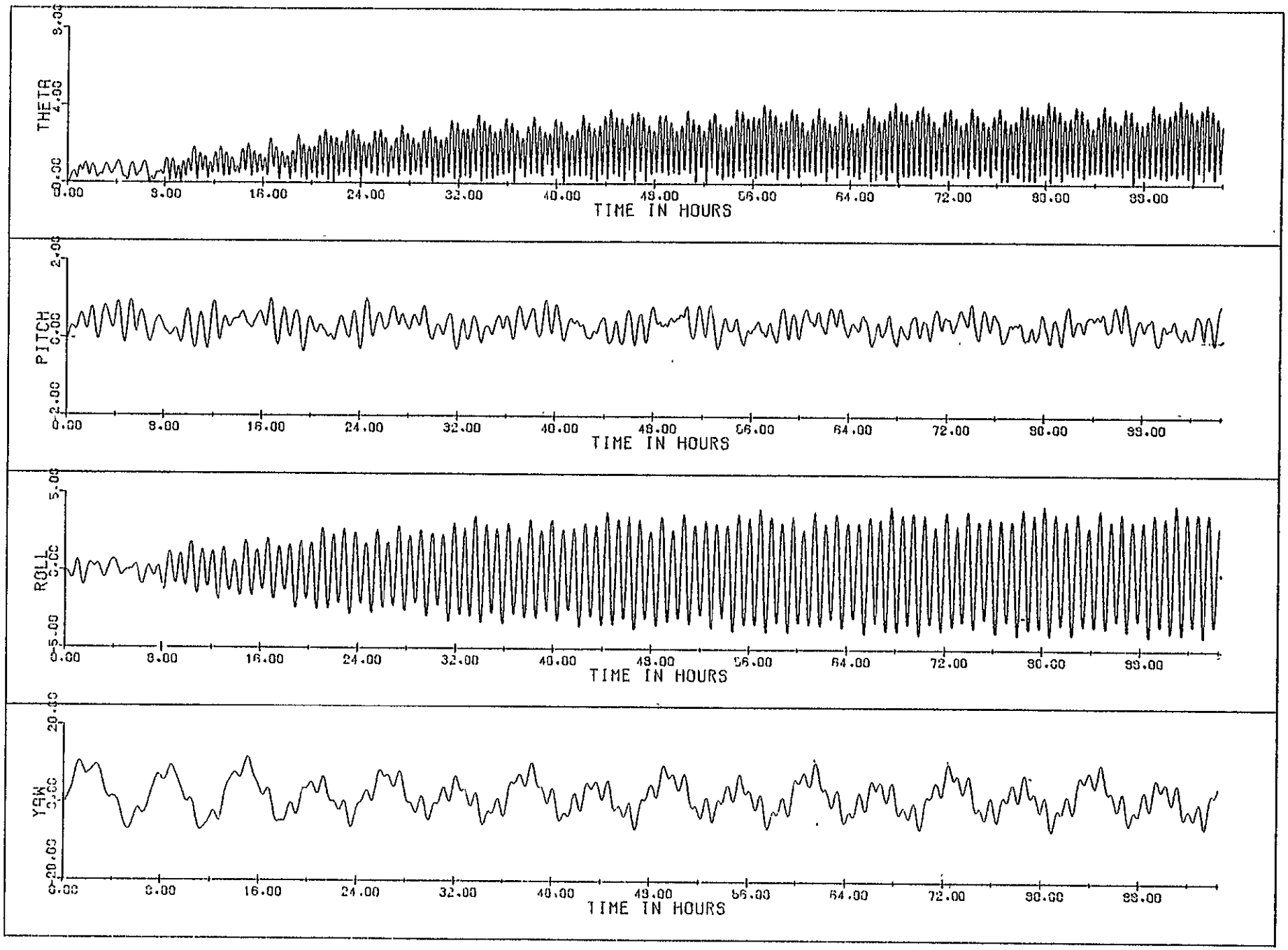

Fig. 4.2.1 – Damper Disturbance only· b=2.0; 235 n.

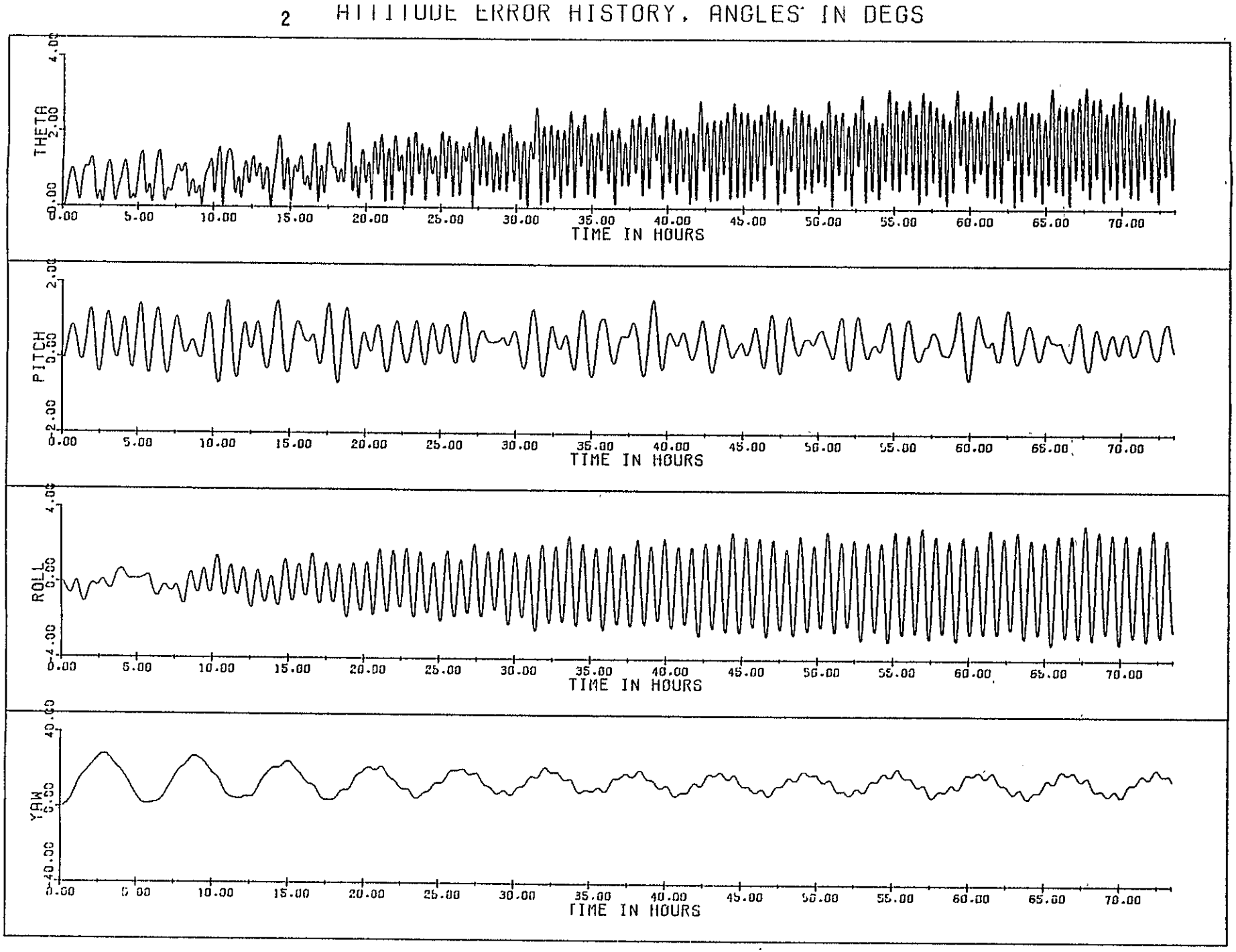

Fig. 4.2.2 - All disturbances; b=1.0; 235 mn

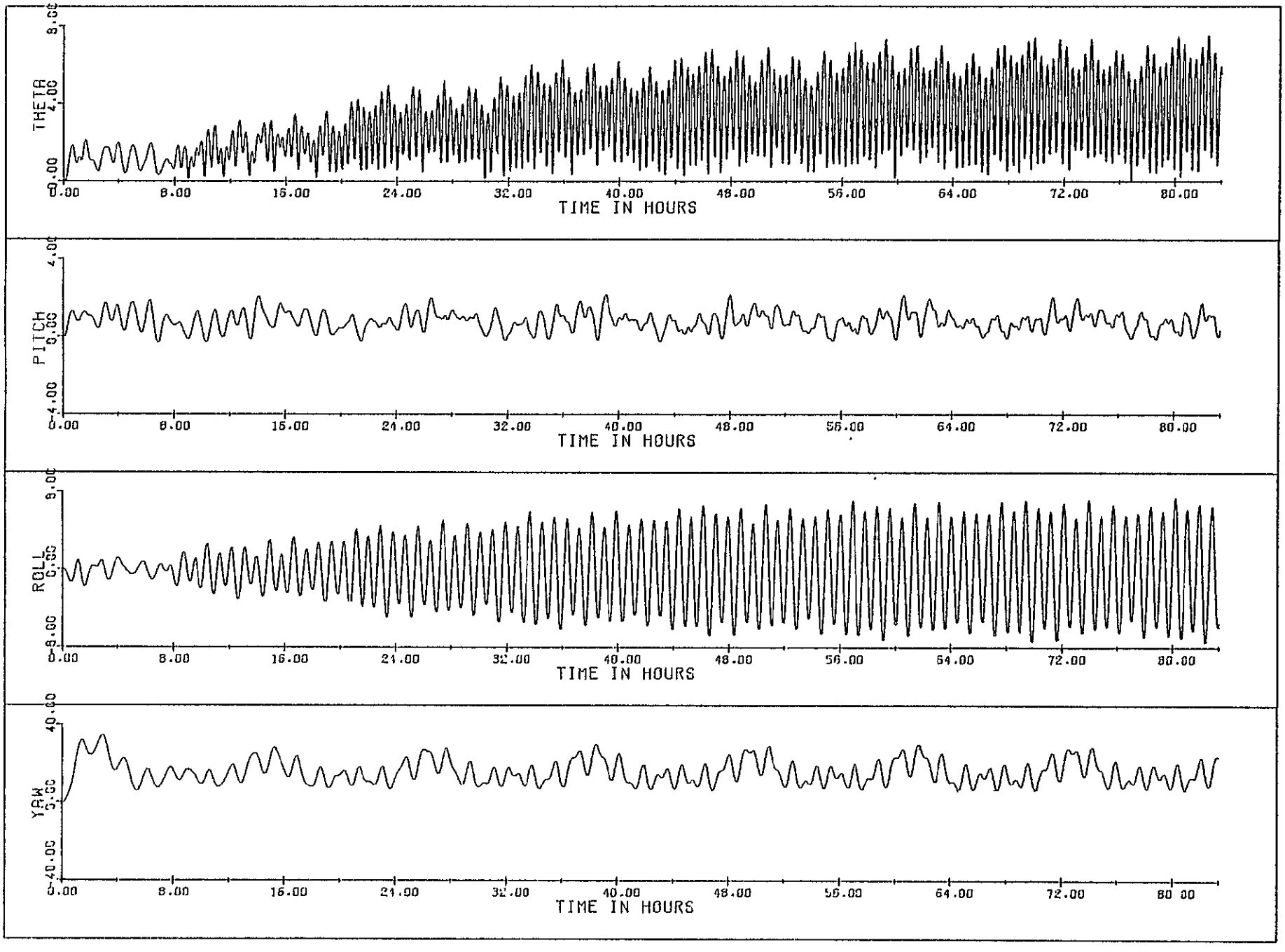

Fig. 4.2.3 - All disturbances; b=5.5; 235 nm

5 ATTITUDE ERROR HISTORY, ANGLES IN DEGS

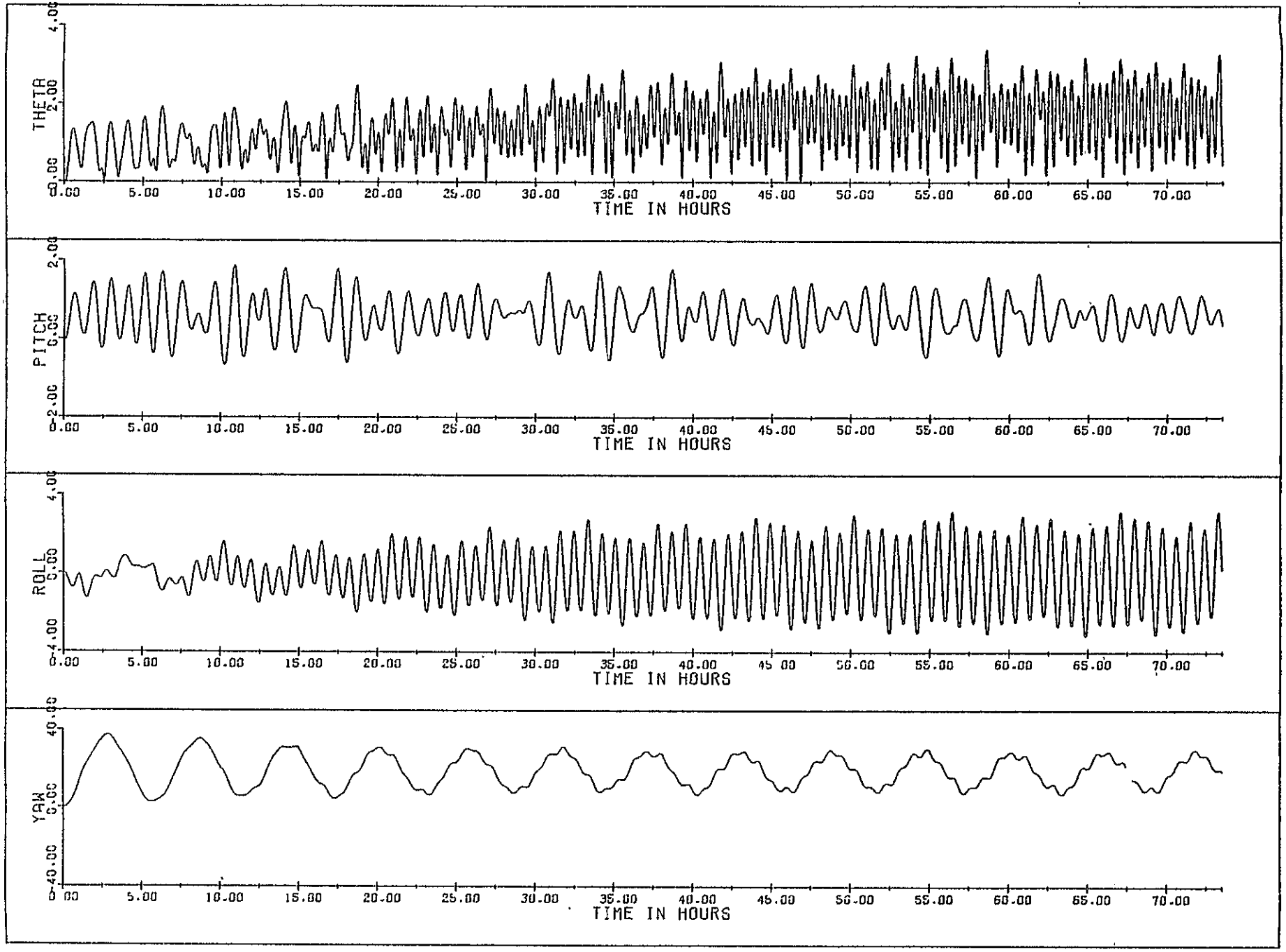

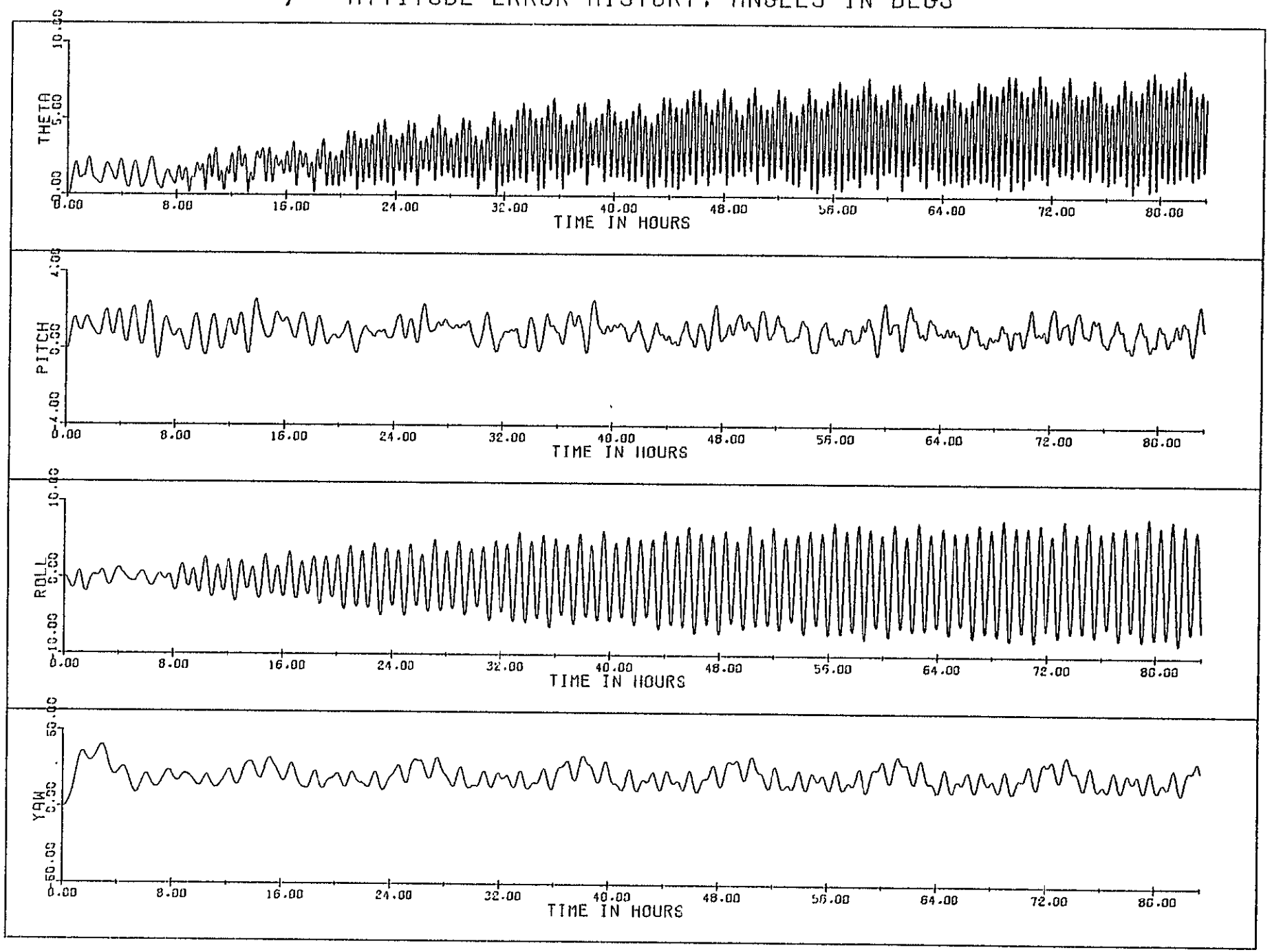

Fig. 4.2.5 - All disturbances; b=5.5: 215 nm

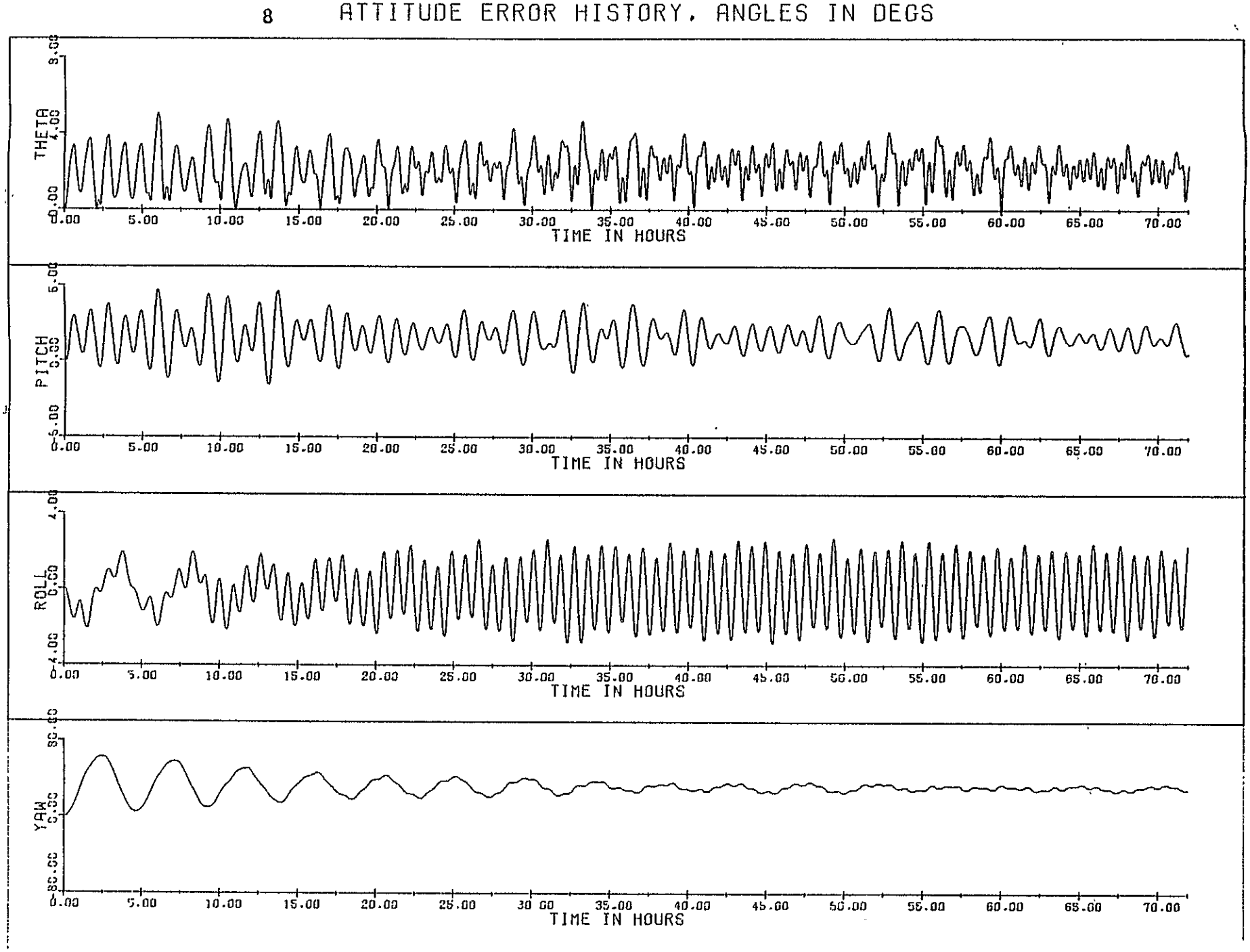

Fig. 4.2.6 - All disturbances; b=1.0; 175 nm

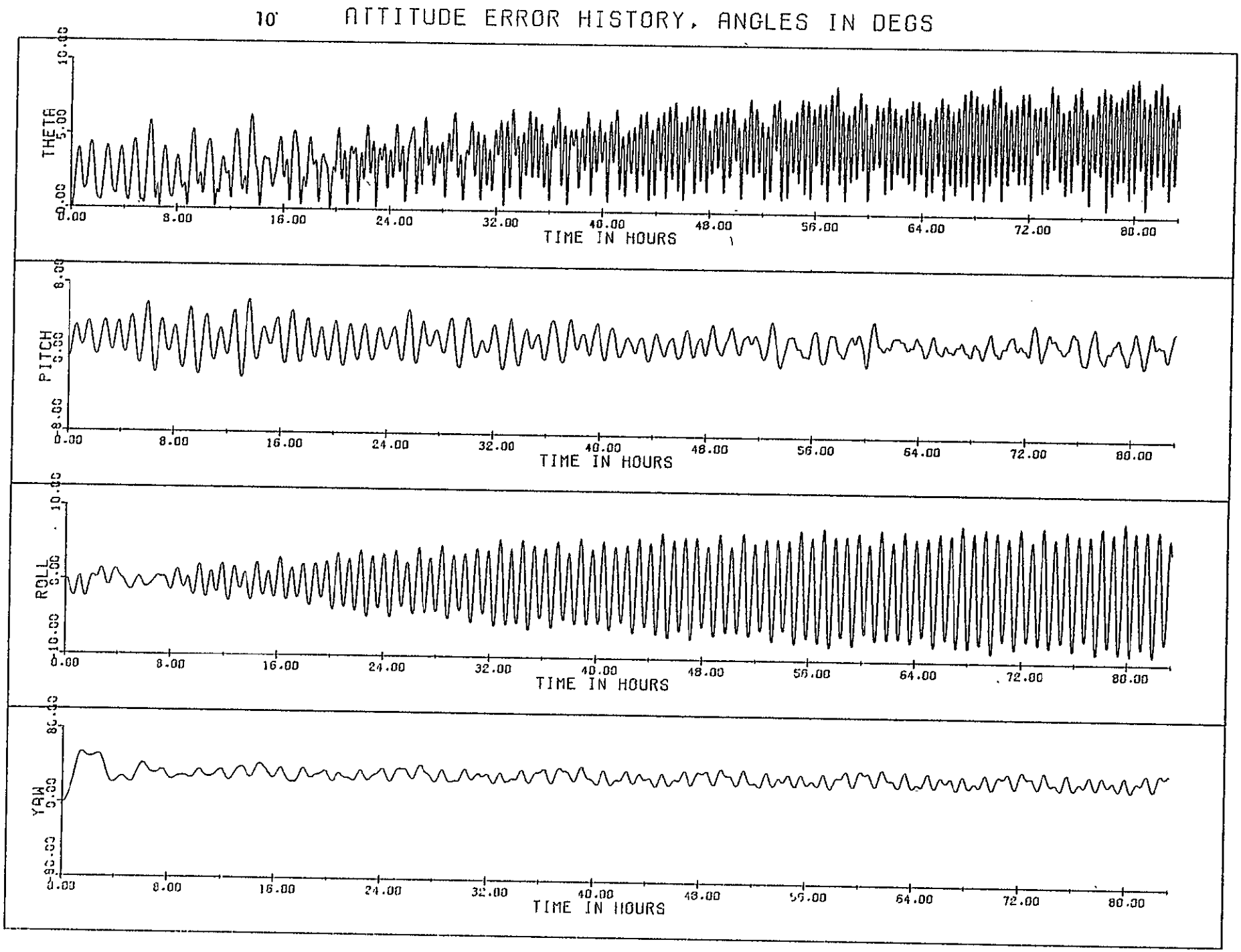

Fig. 4.2.7 - All disturbances; b=5.5; 175 nm

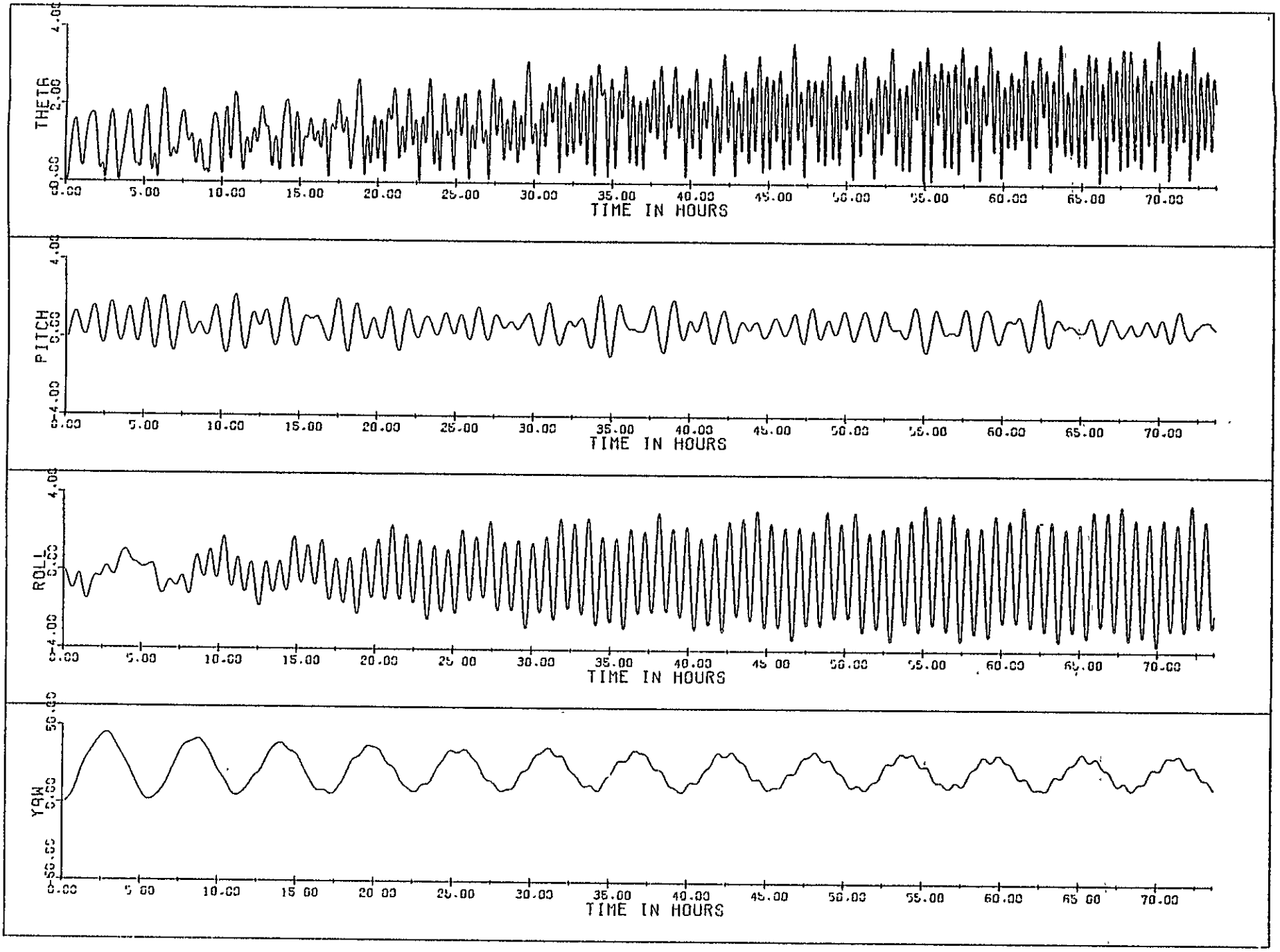

Fig. 4.2.8 - Worst Case disturbance; b=1.0; 235 nm

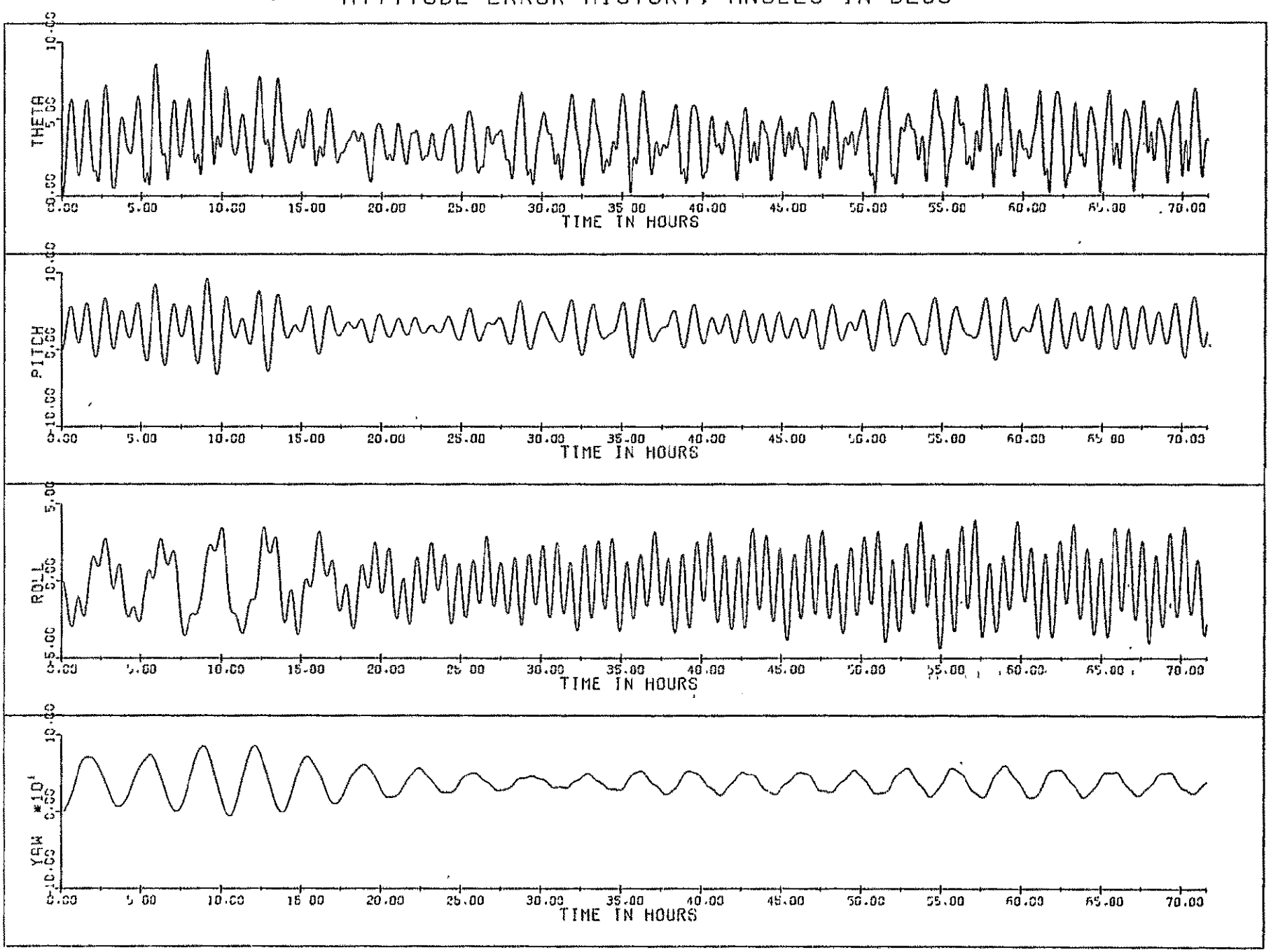

Fig. 4.2.9 - Worst Case disturbance; b=1.0; 175 nm

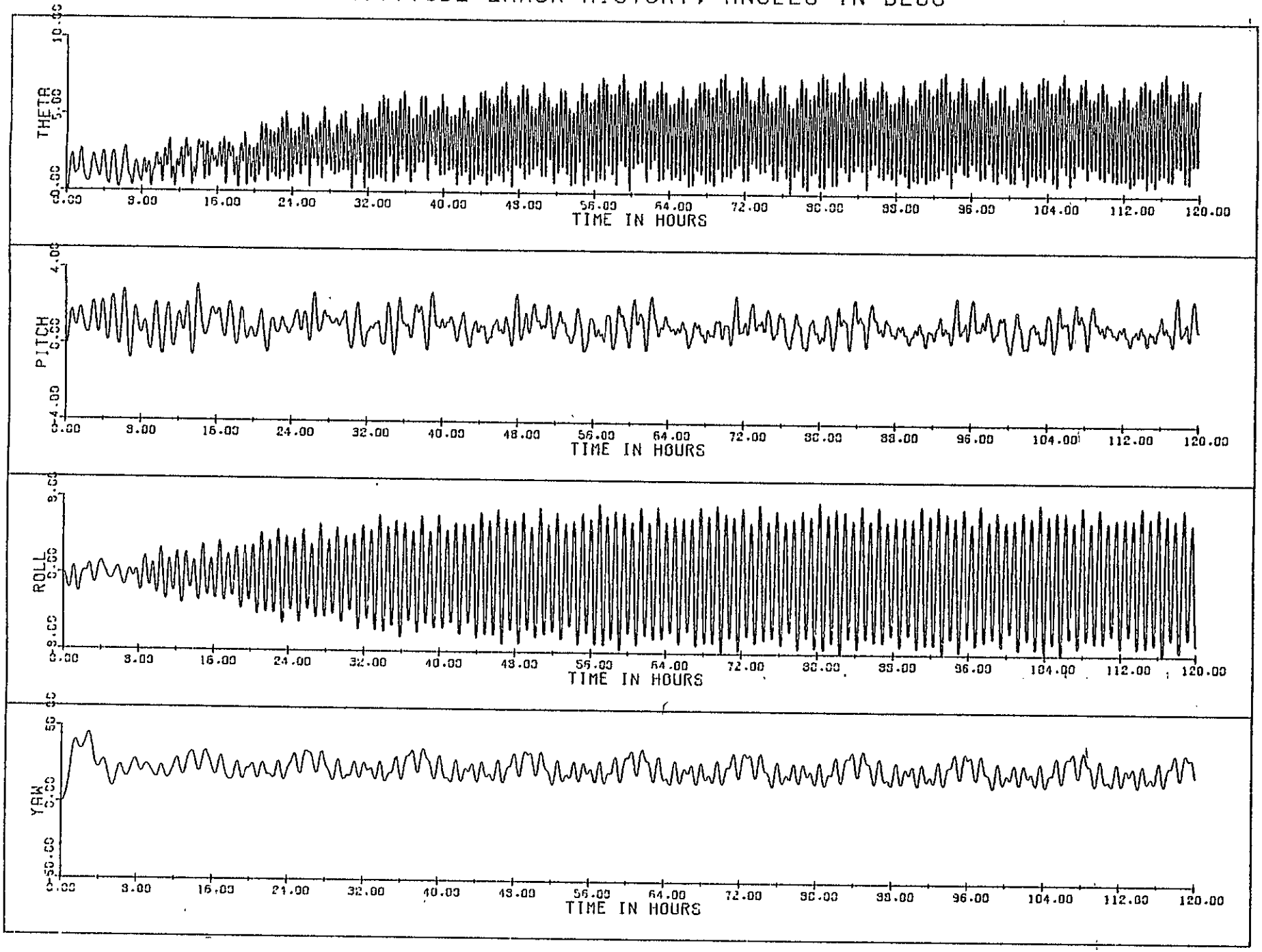

Fig. 4.2.10 - Worst Case disturbance; b=5.5; 235 nm

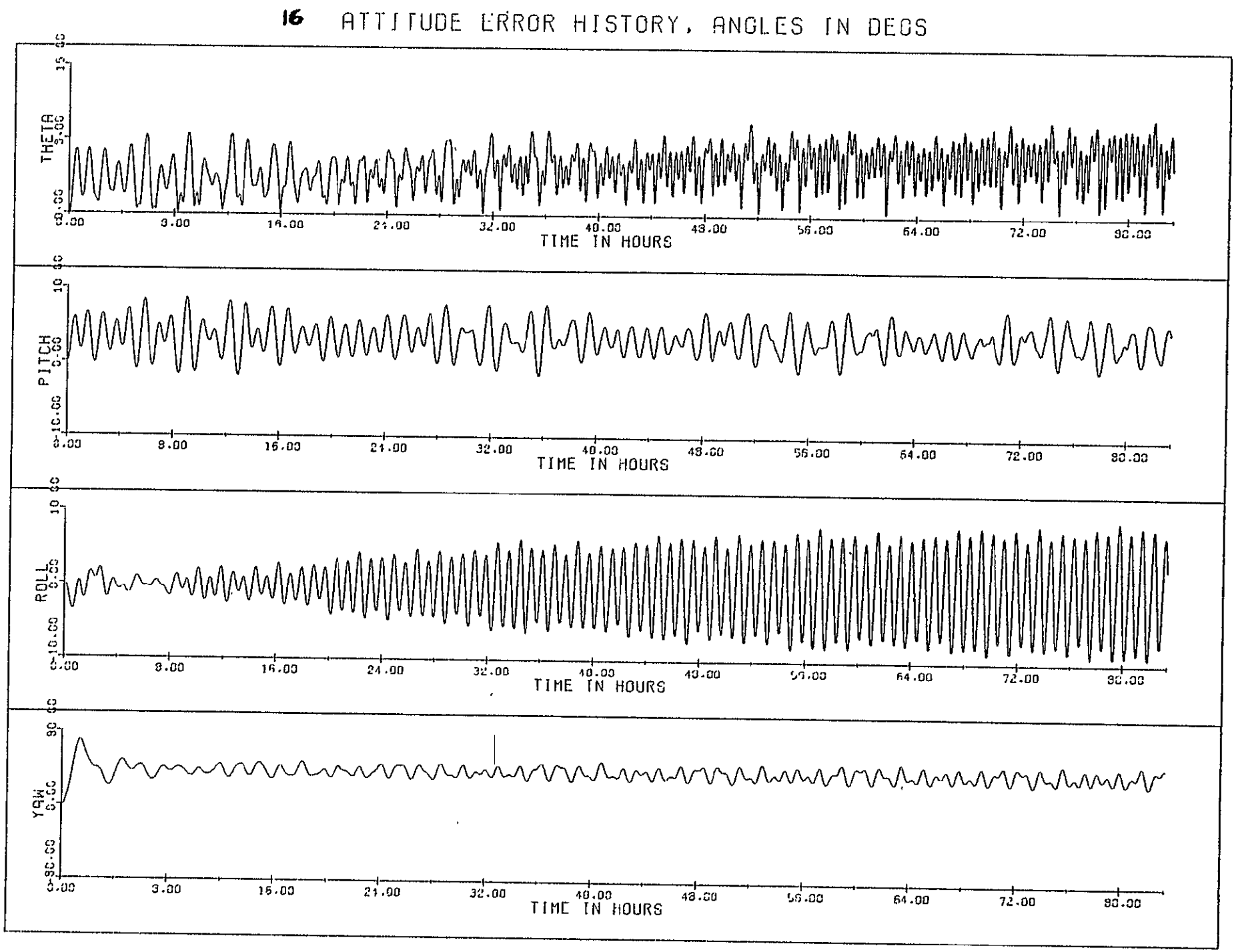

Fig. 4.2.11 - Worst Case disturbance; b=5.5: 175 nm

20 ATTITUDE ERROR HISTORY, ANGLES IN DEGS

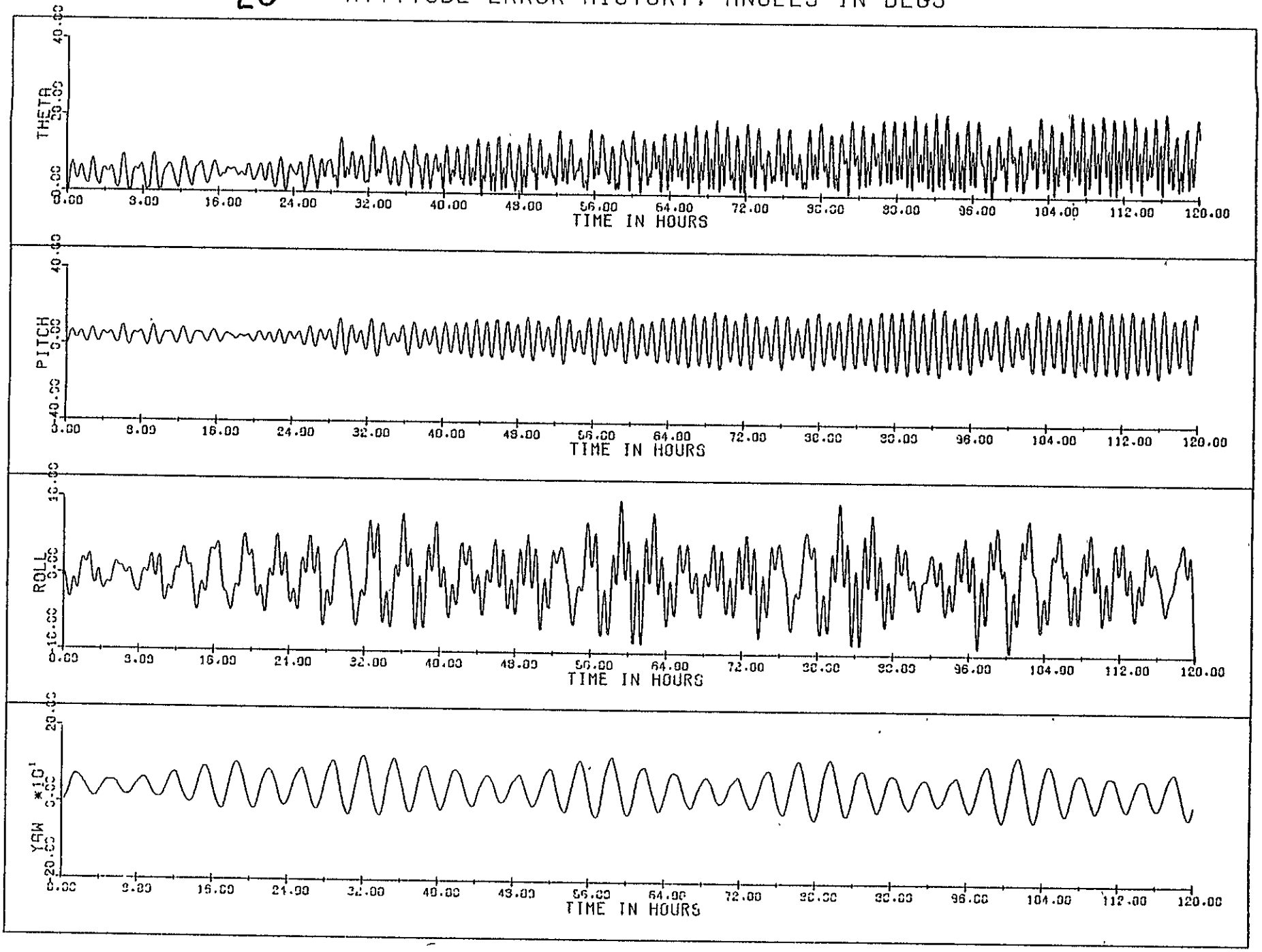

LARGE CP-CM OFFSETS B = 2.0 LB-FT-SEC ALT = 215 NM

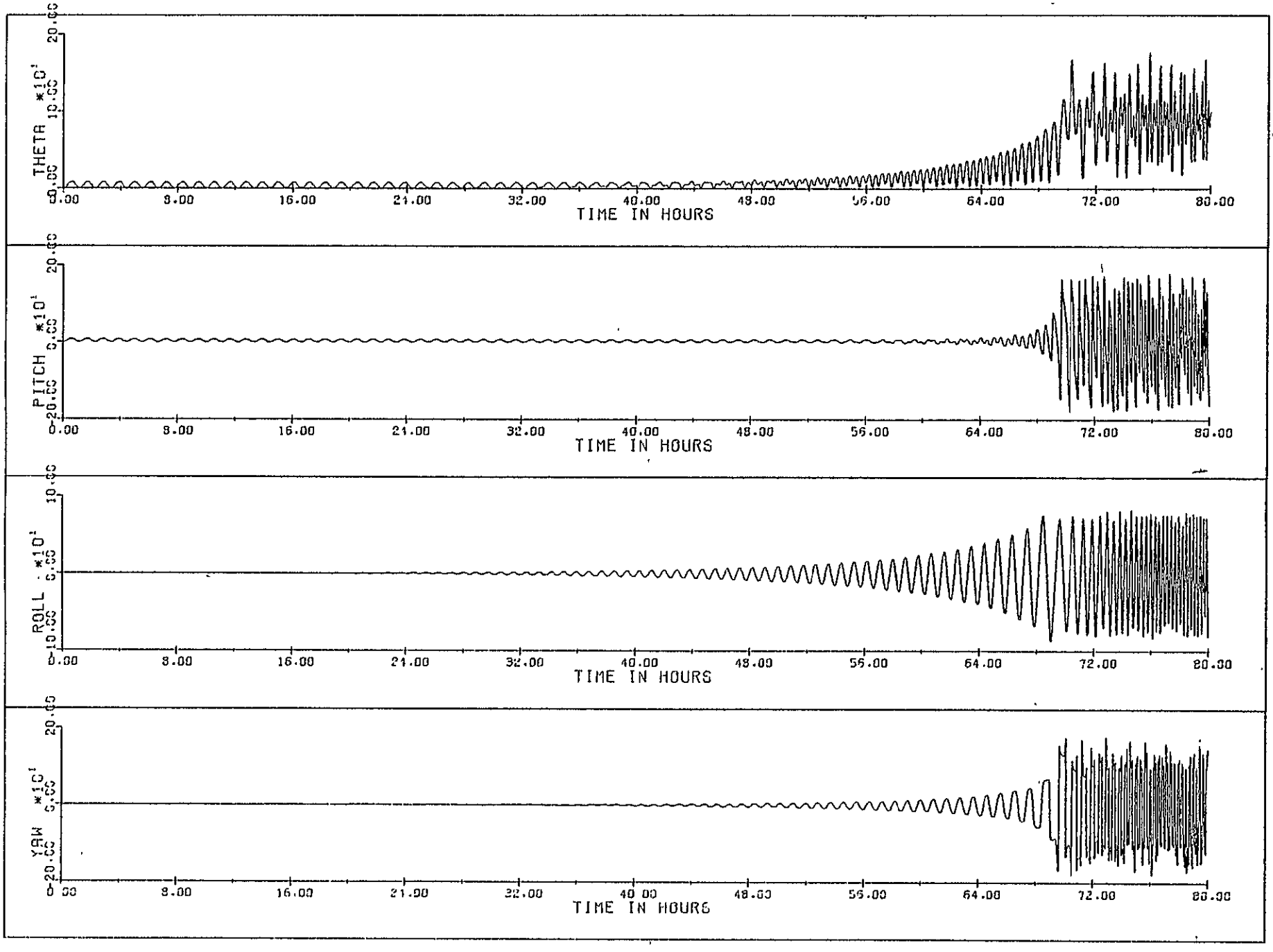

GARBER INSTABILITY B=0·2 T_z = ·01 LB-FT

Fig 4·3.2

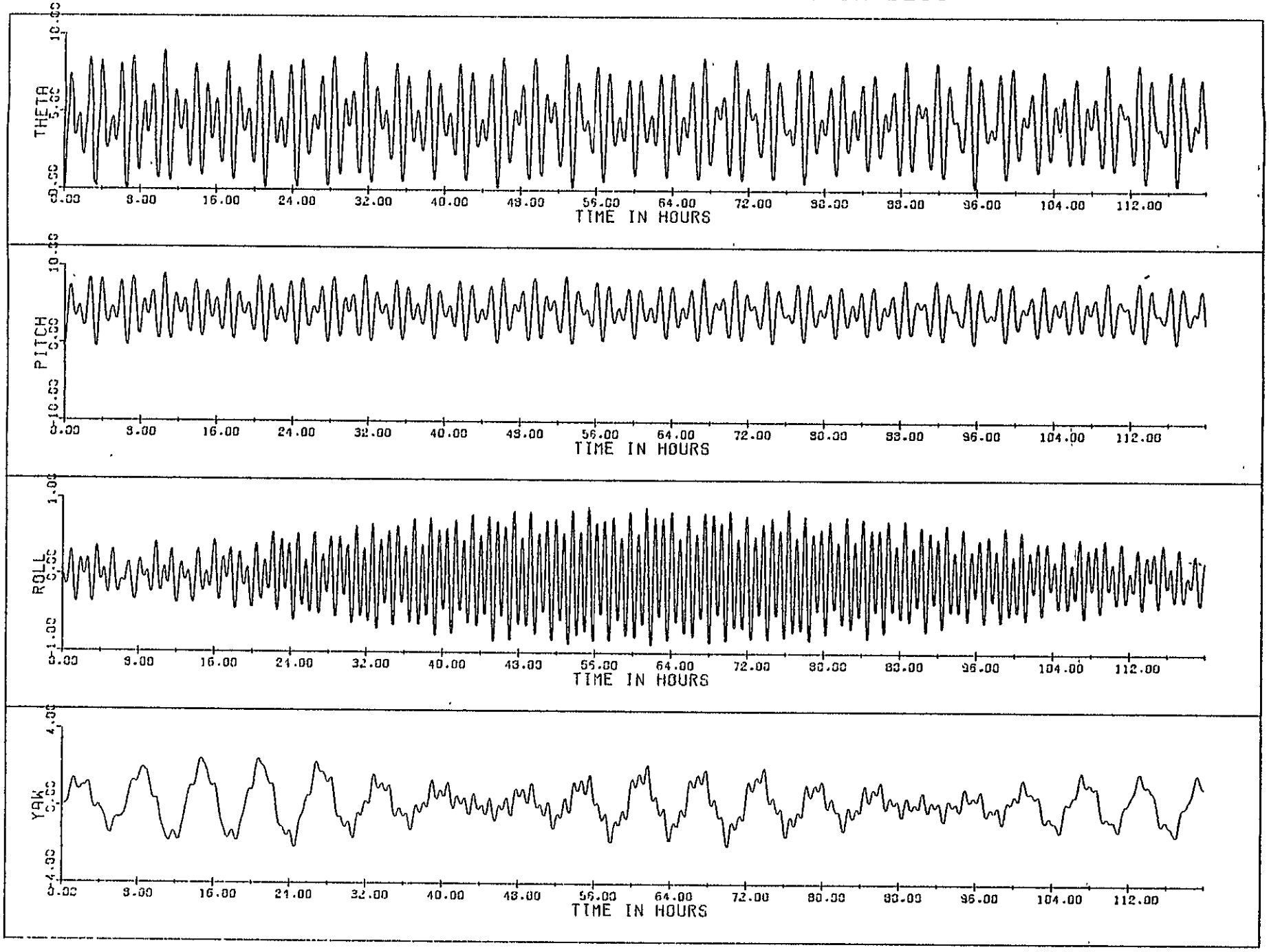

GARBER INSTABILITY B=·2 ALT= 175 nm. YAW CP-CM = 6 INCHES

Fig 4.3.1

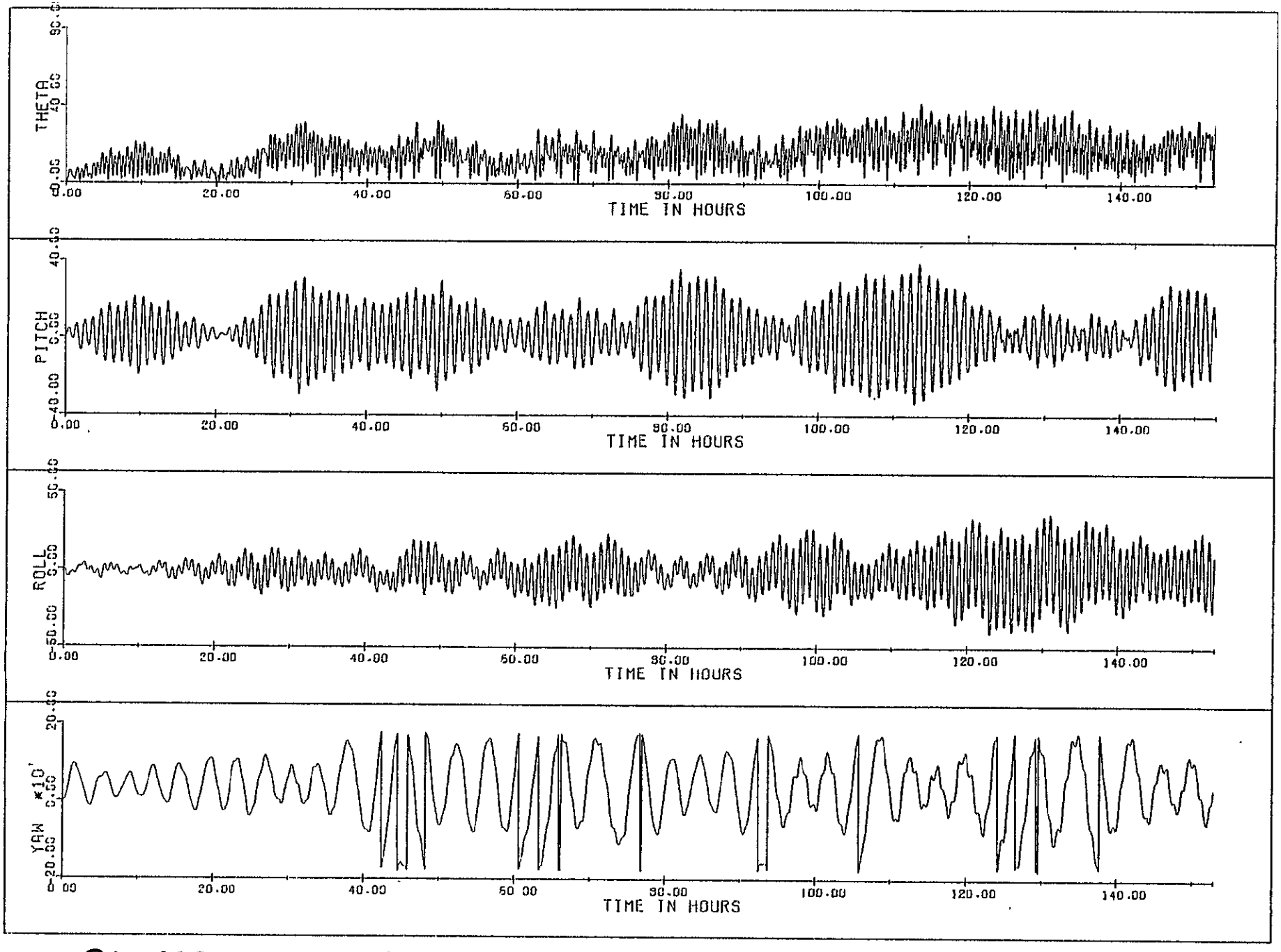

DAMPER MAGNET LOCKED ALT= 175 NM. NOMINAL DISTURBANCES

Fig 4.4.1

4.4 Locked Damper

One of the failure modes of the damper is for the inner sphere containing the magnet to become locked to the outer sphere. This might be caused by magnetic material on the outside of the damper or an obstruction between the inner and outer spheres. The effect of this is: 1) There is no damping torque since there is no relative rate between the inner and outer spheres, and 2) the 225,000 pole-cm magnet acts as a fixed spacecraft magnetic dipole. Note that for zero damping any pitch bias will cause the Garber instability limits to be exceeded.

Simulation run #19 was run to show the effects of this type of damper failure. The results are shown in Figure 4.4.1. As expected, the spacecraft is unstable.

5.0 REFERENCES

1. Models of the Earth's Atmosphere (90 to 2500 Km), NASA SP-8021, March 1973.

2. Solar Activity Indices, NASA - Marshall Space Flight Center, 16 November 1976.

3. Passive Aerodynamic Attitude Stabilization of Near Earth Satellites, Vol. II, Aerodynamic Analysis, Paul H. Davison, WADD - Technical Report, July 1961.

4. Influence of Constant Disturbing Torques on the Motion of Gravity Gradient Stabilized Spacecraft, T. B. Garber, AIAA Journal, Vol. 1 No. 4, April 1963.

5. Final Report; Passive Stabilization of the LDEF Facility, GE Document No. 74SD4264, November 1974.

6. Motion of an Artificial Satellite About Its Center of Mass, V. V. Beletskii, NASA TTF - 429, 1966.

APPENDICES

APPENDIX : A

DAMPER MAGNET DYNAMICS

NOMENCLATURE

$[A]$, $[B]$	State matrices; Eqs. (33), (34).
$[\hat{B}]$	Damping coefficient matrix; Eqs. (5), (6).
b	Scalar damping coefficient; Eq. (6).
$[C]$	State matrix; Eq. (35)
$[E]$	Coordinate transformation matrix; Eqs. (1), (8).
e_{ij} ; $i,j = 1,2,3$.	Elements of $[E]$; Eq. (2).
I_x , I_y , I_z	Principal moments of inertia of the spacecraft in the xyz coordinates; Eq. (3).
I'_x , I'_y , I'_z	Principal moments of inertia of the magnet in the $x'y'z'$ coordinates.
I_{ROLL} , I_{PITCH} , I_{YAW}	Roll, pitch and yaw moments of inertia of the spacecraft in the three-axis configuration.
$[\bar{I}]$	Identity matrix.
K	Universal gravitational constant multiplied by the mass of the Earth.
M	Strength of the magnet in pole-cms.
$[O]$	Null matrix.
p, q, r	Orbital frame of coordinates; Eq. (1).
r_o	Geocentric distance of the spacecraft.

$[S_i]$; $i = 1-4$.	Coefficient matrices of the magnet equations of motion; Eqs. (28), (29).
$S_{i,jk}$; $j,k = 1,2,3$.	Elements of $[S_i]$; Eq. (29).
T	Maximum yaw stiffness of a magnet; Eqs. (25), (30).
$\underline{T}_{ds}$	Damper torque on the spacecraft; Eq. (5).
$\underline{T}_g$	Gravity gradient torque vector on the spacecraft; Eqs. (4), (7).
T_{YAW} , T_{ROLL} , T_{PITCH}	Magnet stiffnesses; Eq. (23).
$\underline{T}_m$	Magnetic torque vector on the magnet; Eqs. (12), (15), (25).
$[\tau_i]$; $i = 1-4$.	Coefficient matrices of the spacecraft equations of motion; Eqs. (26), (27).
$\tau_{i,jk}$; $j,k = 1,2,3$.	Elements of $[\tau_i]$; Eq. (27)
t	Time from the ascending node.
$\underline{u}$	State vector; Eq. (31).
xyz	Body fixed coordinate system of the spacecraft; Eq. (1).
α	Local latitude.
ι	Orbit inclination.
$\dot{\eta}$	Orbital rate.
θ_p , θ_r , θ_y	Pitch, roll and yaw angles of the spacecraft.

θ_{ps} , θ_{rs} , θ_{ys}	Bias values of θ_p, θ_r and θ_y .
ϕ_p , ϕ_r , ϕ_y	Perturbed values of θ_p , θ_r and θ_y from the bias values.
$\underline{\phi}$	$[\phi_y , \phi_r , \phi_p]^T$.
$\underline{\omega}$	Spacecraft rate vector in $x\,y\,z$ - coordinates.
$\underline{\omega}_{ds}$	Damper rate vector referred to the axes fixed on the spacecraft.
$\underline{\omega}'_{sd}$	Spacecraft rate vector referred to the axes fixed on the damper.

SUPERSCRIPTS

$(\cdot)'$	Denotes variables which relate to the damper magnet.

SUBSCRIPTS

x , y and z	Denotes the elements of a vector in the corresponding axes.

OPERATORS

$[\cdot]^T$	Transpose
$\dot{(\,)}$	Derivative with respect to time.

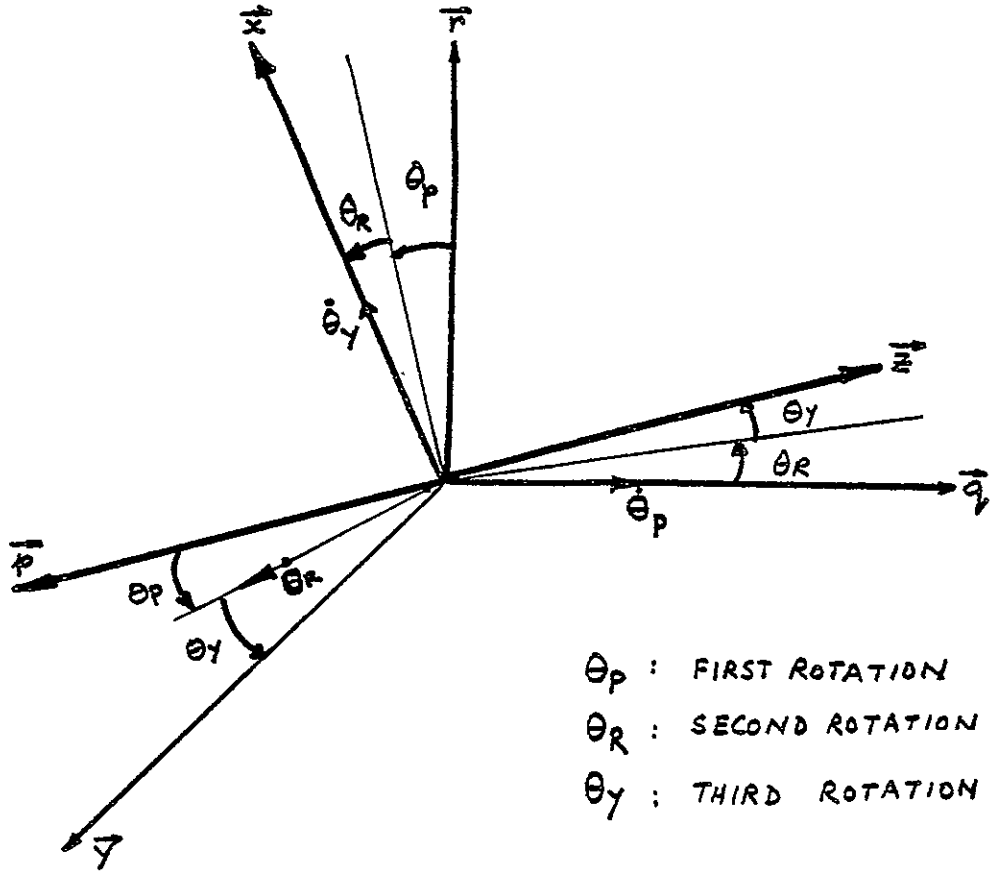

COORDINATE SYSTEM RELATIONSHIP

FIG. A 1.

EULER'S EQUATIONS OF MOTION

A coordinate system " x-y-z " is assumed to be attached to the orbiting spacecraft. Let "r-p-q" be the orbital coordinate system rotating at the orbital rate of the spacecraft about the q-axis. The relationship between the coordinate systems is defined as

$$\begin{Bmatrix} x \\ y \\ z \end{Bmatrix} = \left[E(\theta_p, \theta_r, \theta_y) \right] \begin{Bmatrix} r \\ p \\ q \end{Bmatrix} \qquad (1)$$

where the elements e_{ij}, $(i, j = 1, 2, 3)$ of the matrix $[E]$ are given by

$$\begin{aligned}
e_{11} &= \cos\theta_p \cos\theta_R \\
e_{12} &= \sin\theta_p \cos\theta_R \\
e_{13} &= -\sin\theta_R \\
e_{21} &= \cos\theta_p \sin\theta_R \sin\theta_y - \sin\theta_p \cos\theta_y \\
e_{22} &= \cos\theta_p \cos\theta_y + \sin\theta_p \sin\theta_R \sin\theta_y \\
e_{23} &= \cos\theta_R \sin\theta_y \\
e_{31} &= \sin\theta_p \sin\theta_y + \cos\theta_p \sin\theta_R \cos\theta_y \\
e_{32} &= \sin\theta_p \sin\theta_R \cos\theta_y - \cos\theta_p \sin\theta_y \\
e_{33} &= \cos\theta_R \cos\theta_y
\end{aligned} \qquad (2)$$

The angles θ_P, θ_R, θ_Y are the pitch, roll and yaw angular displacements, respectively, of the spacecraft and define the rotation of the x-y-z coordinates with respect to the r-p-q coordinates. Fig A-1 shows this angular relationship between the coordinate systems.

The x-axis is taken along the vertical local and the y-axis is parallel to the trajectory in the direction of motion of the center of mass of the spacecraft. The z-direction is the orbit plane forming a right-handed coordinate frame. With this convention, and assuming that the system is coincident with the axes of principal moment of inertia of the spacecraft, these moments of inertia are given by

$$I_x = I_{YAW} \quad ; \quad I_y = I_{ROLL} \quad ; \quad I_z = I_{PITCH} \tag{3}$$

With the preceding assumptions, the gravity gradient torque vector $\underline{T}_g$, in the x-y-z coordinate system is given by

$$T_{gx} = \frac{3K}{r_o^3}\left[(I_z - I_y)\, e_{21}\, e_{31}\right]$$

$$T_{gy} = \frac{3K}{r_o^3}\left[(I_x - I_y)\, e_{11}\, e_{31}\right] \tag{4}$$

$$T_{gz} = \frac{3K}{r_o^3}\left[(I_y - I_x)\, e_{11}\, e_{21}\right]$$

where the subscripts x, y, z refer to the corresponding axes, and

r_o = geocentric distance of the satellite

K = Universal gravitational constant multiplied by the mass of the earth.

Let $\underline{\omega}_{ds}$ be the angular velocity vector of the damper magnet expressed in the xyz coordinate system. Then, the damping torque vector $\underline{T}_{DS}$ on the space craft created by its motion relative to that of the damper magnet is

$$\underline{T}_{ds} = [\hat{B}] \{ \underline{\omega}_{ds} - \underline{\omega} \} \qquad (5)$$

where

$\underline{\omega}$ = angular velocity vector of spacecraft in xyz coordinates

$[\hat{B}]$ = the damping coefficient matrix of the damper assembly.

Due to the symmetry of the damper assembly, the matrix is a scalar matrix, and is of the form

$$[\hat{B}] = b\,[\hat{I}] \qquad (6)$$

where b is the scalar damping coefficient and $[\hat{I}]$ is the identity matrix.

Torques on the spacecraft from all other sources are neglected as the effects of only the damper are under investigation. Hence the equations of motion for the spacecraft are given by :

$$\begin{aligned} I_x \dot{\omega}_x + (I_z - I_y)\omega_y\omega_z + b(\omega_x - \omega_{dsx}) &= T_{gx} \\ I_y \dot{\omega}_y + (I_x - I_z)\omega_z\omega_x + b(\omega_y - \omega_{dsy}) &= T_{gy} \\ I_z \dot{\omega}_z + (I_y - I_x)\omega_x\omega_y + b(\omega_z - \omega_{dsz}) &= T_{gz} \end{aligned} \qquad (7)$$

where

$\dot{\underline{\omega}}$: angular acceleration vector of the s/c in x-y-z coordinates.

Let the principal moments of inertia of the magnet of the damper be along the axes of the $x'\,y'\,z'$ coordinate system. Let θ'_p, θ'_R, θ'_y be the pitch, roll and yaw angular displacements of the x'-y'-z' system with respect to the r-p-q axes. The relative orientations of the x'-y'-z' axes from the r-p-q axes are similar to those of the x-y-z axes from the r-p-q axes. Hence the r-p-q coordinates may be transformed to the x'-y'-z' in a manner analogous to that given by equation (1). Therefore

$$\begin{Bmatrix} x' \\ y' \\ z' \end{Bmatrix} = \left[E(\theta'_p, \theta'_R, \theta'_y) \right] \begin{Bmatrix} r \\ p \\ q \end{Bmatrix} \tag{8}$$

Let $\underline{\omega}'$ be the angular velocity vector of the magnet in the x'-y'-z' coordinates Then $\underline{\omega}'$ and $\underline{\omega}_{ds}$ are related by

$$\underline{\omega}_{ds} = \left[E(\theta_p, \theta_R, \theta_y)\right]\left[E(\theta'_p, \theta'_R, \theta'_y)\right]^{-1} \underline{\omega}' \tag{9}$$

for small angular displacements, eq(9) can be approximated by

$$\omega_{ds} = \left[E(\theta_p, \theta_R, \theta_y)\right]\left[\dot{\theta}'_y, \dot{\theta}'_R, (\dot{\theta}'_p + \dot{\eta})\right]^T \tag{10}$$

Hence, eqn.(7) becomes

$$\left\{ \begin{aligned} &I_x \dot{\omega}_x + (I_z - I_y)\left(\omega_y \omega_z - \tfrac{3K}{r_o^3} e_{21} e_{31}\right) + b\omega_x - b\omega_{dsx} = 0 \\ &I_y \dot{\omega}_y + (I_x - I_z)\left(\omega_x \omega_z - \tfrac{3K}{r_o^3} e_{11} e_{31}\right) + b\omega_y - b\omega_{dsy} = 0 \\ &I_z \dot{\omega}_z + (I_y - I_x)\left(\omega_x \omega_y - \tfrac{3K}{r_o^3} e_{11} e_{21}\right) + b\omega_z - b\omega_{dsz} = 0 \end{aligned} \right\} \tag{11}$$

Let I_x' , I_y' , I_z' be the principal moments of inertia along the x'-y'-z' coordinate axes. Also , let $\underline{\omega}'_{sd}$ be the angular velocity vector of the spacecraft expressed in x'-y'-z' coordinates. Then the equations of motion for the damper magnet is given by

$$\left\{ \begin{array}{l} I_x' \dot{\omega}_x' + (I_z' - I_y')\omega_y'\omega_z' + b(\omega_x' - \omega_{sdx}') = T_{mx} \\ I_y' \dot{\omega}_y' + (I_x' - I_z')\omega_x'\omega_z' + b(\omega_y' - \omega_{sdy}') = T_{my} \\ I_z' \dot{\omega}_z' + (I_y' - I_x')\omega_x'\omega_y' + b(\omega_z' - \omega_{sdz}') = T_{mz} \end{array} \right\} \qquad (12)$$

where $\dot{\underline{\omega}}'$ is the angular acceleration vector of the magnet in the x', y', z' coordinates and $\underline{T}_m$ is the Earth's magnetic torque vector on the damper magnet

$\underline{\omega}$ and ω_{sd}' are related by the expression

$$\underline{\omega}_{sd}' = [E(\theta_p', \theta_R', \theta_Y')][E(\theta_p, \theta_r, \theta_Y)]^{-1}\underline{\omega} \qquad (13)$$

Approximating eq$_n$ (13) by the relation

$$\underline{\omega}_{sd}' = [E(\theta_p', \theta_R', \theta_Y')][\dot{\theta}_Y, \dot{\theta}_R, (\dot{\theta}_p + \dot{\eta})]^T \qquad (14)$$

Eqns. (11) and (12) constitute the approximate coupled set of Euler's equations for the spacecraft and ~~magnet~~ magnet.

LINEARIZED EQUATIONS

Let a circular orbit be assumed such that

$$\dot{\eta} = \text{orbit rate} = \text{rate about } q_y \text{ axis} = \sqrt{\frac{K}{r_0^3}} \tag{16}$$

In terms of the Euler angle rates, the angular velocities of the spacecraft are given by

$$\begin{aligned} \omega_x &= \dot{\theta}_y - (\dot{\theta}_p + \dot{\eta}) \sin\theta_R \\ \omega_y &= \dot{\theta}_R \cos\theta_y + (\dot{\theta}_p + \dot{\eta}) \sin\theta_y \cos\theta_R \\ \omega_z &= -\dot{\theta}_R \sin\theta_y + (\dot{\theta}_p + \dot{\eta}) \cos\theta_y \cos\theta_R \end{aligned} \tag{17}$$

If $\theta_p, \theta_R, \theta_y$ have a non-zero bias such that

$$\begin{aligned} \theta_p &= \theta_{ps} + \phi_p \\ \theta_R &= \theta_{RS} + \phi_R \\ \theta_y &= \theta_{ys} + \phi_y \end{aligned} \tag{18}$$

where $\theta_{ps}, \theta_{RS}, \theta_{ys}$ = the bias angles

ϕ_p, ϕ_R, ϕ_y = small changes of the attitude angles from their bias values.

Let it also be assumed that θ_{ps} and θ_{ys} are constants but θ_{RS} is a variable.

The expressions for ω as given by (17) are linearised about the bias position to yield

$$\begin{aligned} \omega_x &= \dot{\phi}_y - \dot{\phi}_p \sin\theta_{RS} - \dot{\eta}\,\phi_R \cos\theta_{RS} - \dot{\eta} \sin\theta_{RS} \\ \omega_y &= \dot{\phi}_R \cos\theta_{ys} + \dot{\phi}_p \sin\theta_{ys} \cos\theta_{RS} - \dot{\eta}\,\phi_R \sin\theta_{ys} \sin\theta_{RS} + \dot{\eta}\phi_y \cos\theta_{RS} \cos\theta_{ys} \\ &\quad + \dot{\eta} \sin\theta_{ys} \cos\theta_{ys} \\ \omega_z &= -\dot{\phi}_R \sin\theta_{ys} + \dot{\phi}_p \cos\theta_{ys} \cos\theta_{RS} - \dot{\eta}\,\phi_y \sin\theta_{ys} \cos\theta_{RS} - \dot{\eta}\,\phi_R \cos\theta_{ys} \sin\theta_{RS} \\ &\quad + \dot{\eta} \cos\theta_{ys} \cos\theta_{RS} \end{aligned} \tag{19}$$

Similarly, the linearised form of the angular acceleration vector is given by

$$\dot{\omega}_x = \ddot{\phi}_y - \ddot{\phi}_p \sin\theta_{RS} - \dot{\eta}\dot{\phi}_R \cos\theta_{RS} + \dot{\theta}_{RS}\left(\dot{\eta}\phi_R \sin\theta_{RS} - \dot{\phi}_p \cos\theta_{RS} - \dot{\eta}\cos\theta_{RS}\right)$$

$$\dot{\omega}_y = \ddot{\phi}_R \cos\theta_{ys} + \ddot{\phi}_p \sin\theta_{ys}\cos\theta_{RS} - \dot{\eta}\dot{\phi}_R \sin\theta_{ys}\sin\theta_{RS} + \dot{\eta}\dot{\phi}_y \cos\theta_{RS}\cos\theta_{ys} - \dot{\theta}_{RS}\left(\dot{\phi}_p \sin\theta_{ys}\sin\theta_{RS} + \dot{\eta}\phi_R \sin\theta_{ys}\cos\theta_{RS} + \dot{\eta}\phi_y \sin\theta_{RS}\cos\theta_{ys} + \dot{\eta}\sin\theta_{ys}\sin\theta_{RS}\right) \quad (20)$$

$$\dot{\omega}_z = -\ddot{\phi}_R \sin\theta_{ys} + \ddot{\phi}_p \cos\theta_{ys}\cos\theta_{RS} - \dot{\eta}\dot{\phi}_R \cos\theta_{ys}\sin\theta_{RS} - \dot{\eta}\dot{\phi}_y \cos\theta_{RS}\sin\theta_{ys} - \dot{\theta}_{RS}\left(\dot{\phi}_p \cos\theta_{ys}\sin\theta_{RS} + \dot{\eta}\phi_R \cos\theta_{ys}\cos\theta_{RS} - \dot{\eta}\phi_y \sin\theta_{RS}\sin\theta_{ys} + \dot{\eta}\cos\theta_{ys}\sin\theta_{RS}\right)$$

Similarly, writing

$$\begin{aligned} \theta_p' &= \theta_{ps}' + \phi_p' \\ \theta_R' &= \theta_{RS}' + \phi_R' \\ \theta_y' &= \theta_{ys}' + \phi_y' \end{aligned} \quad (21)$$

equations for the damper magnet rates and accelerations are analogous to eqns (19) and (20).

It should be noted that although $\dot{\theta}_{RS}$ can be set equal to zero without too much error, $\dot{\theta}_{RS}'$ can not be. This is because the magnet continuously follows the Earth's magnetic field Expressions for θ_{RS}' and θ_{ys}' (which are time dependent) and the magnet stiffness in roll, pitch, yaw are found as follows:

Define an Earth-centered coordinate system I-J-K such that

- I is in the equatorial plane and contains the ascending node
- J is in the equatorial plane and is perpendicular to I
- K is the earth's spin axis

Let ν be the inclination of the orbit and η be the orbit angle. Errors are assumed small so that the r-p-q orbital axes are same as the x-y-z spacecraft axes.

The relationship between the x-y-z and I-J-K axes is defined by

$$\begin{Bmatrix} x \\ y \\ z \end{Bmatrix} = \begin{Bmatrix} \cos\eta & \sin\eta\cos\nu & \sin\eta\sin\nu \\ -\sin\eta & \cos\eta\cos\nu & \cos\eta\sin\nu \\ 0 & -\sin\eta & \cos\nu \end{Bmatrix} \begin{Bmatrix} I \\ J \\ k \end{Bmatrix} \qquad (21)$$

The Earths field is s/c coordinates is given by

$$\begin{Bmatrix} H_x \\ H_y \\ H_z \end{Bmatrix} = \begin{Bmatrix} -2\sin\eta\sin\nu \\ \cos\eta\sin\nu \\ \cos\nu \end{Bmatrix} \qquad (22)$$

Consider the magnet to be aligned with the pitch axis of the spacecraft. The roll and yaw rotations by the magnet in order to align itself with the Earths magnetic field is found as follows

$$\frac{1}{K} \begin{Bmatrix} H_x \\ H_y \\ H_z \end{Bmatrix} : \left\{ \begin{array}{l} \text{Euler Angle transformation} \\ \text{for roll, yaw} \end{array} \right\} \begin{Bmatrix} 0 \\ 0 \\ 1 \end{Bmatrix} \qquad (23)$$

where $K = \{(-2\sin\nu\sin\eta)^2 + (\cos\nu)^2 + (\cos\eta\sin\nu)^2\}^{1/2}$ (24)

$= [1 + 3\sin^2\eta\sin^2\nu]^{1/2}$ is a scaling factor to normalise the Earth's field vector.

The Euler Angle transformation for roll and yaw of the magnet is given by

$$\begin{Bmatrix} 1 & 0 & 0 \\ 0 & \cos\theta'_{ys} & \sin\theta'_{ys} \\ 0 & -\sin\theta'_{ys} & \cos\theta'_{ys} \end{Bmatrix} \begin{Bmatrix} \cos\theta'_{RS} & 0 & -\sin\theta'_{RS} \\ 0 & 1 & 0 \\ \sin\theta'_{RS} & 0 & \cos\theta'_{RS} \end{Bmatrix}$$

$$= \begin{Bmatrix} \cos\theta'_{RS} & 0 & -\sin\theta'_{RS} \\ \sin\theta'_{RS}\sin\theta'_{ys} & \cos\theta'_{ys} & \sin\theta'_{ys}\cos\theta'_{RS} \\ \cos\theta'_{ys}\sin\theta'_{RS} & -\sin\theta'_{ys} & \cos\theta'_{ys}\cos\theta'_{RS} \end{Bmatrix} \qquad (25)$$

Eqn (23) reduces to

$$\frac{1}{K} \begin{Bmatrix} -2\sin\nu\sin\eta \\ \cos\eta\sin\nu \\ \cos\nu \end{Bmatrix} = \begin{Bmatrix} -\sin\theta'_{RS} \\ \sin\theta'_{ys}\cos\theta'_{RS} \\ \cos\theta'_{ys}\cos\theta'_{RS} \end{Bmatrix} \qquad (26)$$

From eqn (26)

$$\boxed{\sin\theta'_{RS} = \tfrac{1}{K}(2\sin\nu\sin\eta)} \qquad (27)$$

$$\sin\theta'_{ys}\cos\theta'_{RS} = \cos\eta\sin\nu \qquad (28)$$

$$\cos\theta'_{ys}\cos\theta'_{RS} = \cos\nu \qquad (29)$$

From (28) and (29)

$$\boxed{\tan\theta'_{ys} = \cos\eta\tan\nu} \qquad (30)$$

Eqns (27) and (30) show the expressions for θ'_{RS} and θ'_{ys}. These values are time dependent and their average value over an entire orbit must be used wherever applicable.

Magnet Stiffness

Assuming that the magnet is aligned with the Earths field, the stiffness in axis i is found by rotating the spacecraft about axis i and evaluating $dT/d\theta_i$; where T is the torque.

The field due to the magnet is

$$\bar{M} = \begin{Bmatrix} M_x \\ M_y \\ M_z \end{Bmatrix} = K_1 \begin{Bmatrix} -2\sin\nu\sin\eta \\ \cos\eta\sin\nu \\ \cos\nu \end{Bmatrix} \qquad (31)$$

where $K_1 = \dfrac{M}{\sqrt{1+3\sin^2\eta\sin^2\nu}}$; M = magnet strength in pole-cm

The Earths field is given by

$$\bar{B} = \begin{Bmatrix} B_x \\ B_y \\ B_z \end{Bmatrix} = K_2 \begin{Bmatrix} -2\sin\nu\sin\eta \\ \cos\eta\sin\nu \\ \cos\nu \end{Bmatrix} \qquad (32)$$

where $K_2 = \dfrac{M_0}{r_0^3} \dfrac{1}{(1+3\sin^2\nu\sin^2\eta)^{1/2}}$ where M_0 = Earth's field strength in gauss.

Torque due to magnet misalignment = $\bar{T} = \bar{M} \times \bar{B}$

Roll Stiffness

If the magnet rotates in roll by an angle θ_R which is small, the magnet field in x-y-z coordinates is

$$\bar{M}_{\theta_R} = \begin{Bmatrix} 1 & 0 & \theta_R \\ 0 & 1 & 0 \\ -\theta_R & 0 & 1 \end{Bmatrix} [\bar{M}] \qquad (33)$$

The torque due to this mis-alignment is :

$$\bar{T} = \bar{M}_{\theta R} \times \bar{B} = \begin{vmatrix} x & y & z \\ M_{\theta Rx} & M_{\theta Ry} & M_{\theta Rz} \\ B_x & B_y & B_z \end{vmatrix}$$

The roll torque is given by

$$T_{ROLL} = -2K_1K_2\theta_R \left[\sin^2\eta \sin^2\nu + \cos^2\nu\right]$$

Therefore the roll stiffness due to Magnetic roll torque is

$$T_{yy} = -2K_1K_2 \left[\sin^2\eta \sin^2\nu + \cos^2\nu\right] \quad (34)$$

Proceeding in a similar manner the yaw & pitch stiffness are found to be

$$T_{xx} = K_1K_2 \cos\nu + \cos^2\eta \sin\nu \quad (35)$$

$$T_{zz} = K_1K_2 \sin^2\nu \left[1 + \sin^2\eta\right] \quad (36)$$

Hence at any arbitrary inclination the magnetic torques on the damper may be expressed as

$$\begin{aligned} T_{mx} &= -[T_{xx}]\,\phi'_x \\ T_{my} &= -[T_{yy}]\,\phi'_y \\ T_{mz} &= -[T_{zz}]\,\phi'_z \end{aligned} \quad (37)$$

Substituting the expressions for $\underline{\omega}$ and $\dot{\underline{\omega}}$ from (19) and (20) together with similar expressions for $\underline{\omega}'$ and $\underline{\omega}'$ into eqn (11) the linearised homogenous form of eqn (11) can be expressed as

$$[T_1]\ddot{\underline{\Phi}} + [T_2]\dot{\underline{\Phi}} + [T_3]\underline{\Phi} + [T_4]\dot{\underline{\Phi}}' = [\underline{0}] \qquad (38)$$

The elements of the [3x3] matrices $[T_i]$, $i = 1,4$ are as follows:

$$T_{1,11} = I_X$$

$$T_{1,12} = 0$$

$$T_{1,13} = -I_X \sin\theta_{RS}$$

$$T_{1,21} = 0 \qquad 39(a)$$

$$T_{1,22} = I_Y \cos\theta_{YS}$$

$$T_{1,23} = I_Y \sin\theta_{YS} \cos\theta_{RS}$$

$$T_{1,31} = 0$$

$$T_{1,32} = -I_Z \sin\theta_{YS}$$

$$T_{1,33} = I_Z \cos\theta_{YS} \cos\theta_{RS}$$

$$T_{2,11} = b$$

$$T_{2,12} = [(I_Z - I_Y)\cos 2\theta_{YS} - I_X]\dot{\eta}\cos\theta_{RS}$$

$$T_{2,22} = \dot{\eta}(I_Z - I_Y)\sin 2\theta_{YS}\cos^2\theta_{RS} - b\sin\theta_{RS}$$

$$T_{2,21} = (I_X + I_Y - I_Z)\,\dot{\eta}\cos\theta_{ys}\cos\theta_{RS}$$

$$T_{2,22} = (I_X - I_Y - I_Z)\,\dot{\eta}\sin\theta_{ys}\sin\theta_{RS} + b\cos\theta_{ys}$$

$$T_{2,23} = (I_Z - I_X)\,\dot{\eta}\cos\theta_{ys}\sin 2\theta_{RS} + b\sin\theta_{ys}\cos\theta_{RS} \qquad 39(b)$$

$$T_{2,31} = (I_Y - I_X - I_Z)\,\dot{\eta}\sin\theta_{ys}\cos\theta_{RS}$$

$$T_{2,32} = (I_X - I_Y - I_Z)\,\dot{\eta}\cos\theta_{ys}\sin\theta_{RS} - b\sin\theta_{ys}$$

$$T_{2,33} = (I_X - I_Y)\,\dot{\eta}\sin\theta_{ys}\sin 2\theta_{RS} + b\cos\theta_{ys}\cos\theta_{RS}$$

$$T_{3,11} = \dot{\eta}^2(I_Z - I_Y)\Big[\cos^2\theta_{RS}\cos 2\theta_{ys} - 3(\sin\theta_{ps}\cos\theta_{ys} - \sin\theta_{ys}\cos\theta_{ps}\sin\theta_{RS})\cdot (\sin\theta_{ys}\cos\theta_{ps}\sin\theta_{RS} - \sin\theta_{ps}\cos\theta_{ys}) - 3(\sin\theta_{ps}\sin\theta_{ys} + \cos\theta_{ys}\cos\theta_{ps}\sin\theta_{RS})(\cos\theta_{ys}\cos\theta_{ps}\sin\theta_{RS} + \sin\theta_{ps}\sin\theta_{RS})\Big]$$

$$T_{3,12} = \dot{\eta}^2(I_Y - I_Z)\Big[\tfrac{1}{2}\sin 2\theta_{RS}\sin 2\theta_{ys} + 3\cos\theta_{ys}\cos\theta_{RS}\cos\theta_{ps}(\sin\theta_{ys}\cos\theta_{ps}\sin\theta_{RS} - \sin\theta_{ps}\cos\theta_{ys}) + 3\sin\theta_{ys}\cos\theta_{RS}\cos\theta_{ps}(\sin\theta_{ps}\sin\theta_{ys} + \cos\theta_{ps}\sin\theta_{RS}\cos\theta_{ys})\Big]$$

$$T_{3,13} = \dot{\eta}^2(I_Z - I_Y)\Big[-3(\cos\theta_{ps}\sin\theta_{ys} - \cos\theta_{ys}\sin\theta_{ps}\sin\theta_{RS})(\sin\theta_{ys}\cos\theta_{ps}\sin\theta_{RS} - \sin\theta_{ps}\cos\theta_{ys}) + 3(\sin\theta_{ps}\sin\theta_{RS}\sin\theta_{ys} + \cos\theta_{ps}\cos\theta_{ys})\cdot(\sin\theta_{ps}\sin\theta_{ys} + \cos\theta_{ys}\cos\theta_{ps}\sin\theta_{RS})\Big] \qquad (39c)$$

$$T_{3,21} = \dot{\eta}^2(I_X - I_Z)\Big[\tfrac{1}{2}\sin\theta_{ys}\sin 2\theta_{RS} + 3\cos\theta_{ps}\cos\theta_{RS}(\sin\theta_{ps}\cos\theta_{ys} - \sin\theta_{ys}\cos\theta_{ps}\sin\theta_{RS})\Big]$$

$$T_{3,22} = \dot{\eta}^2(I_Z - I_X)\Big[\cos\theta_{ys}\cos 2\theta_{RS} + 3\cos\theta_{ys}\cos^2\theta_{ps}\cos^2\theta_{RS} - 3\cos\theta_{ps}\sin\theta_{RS}(\sin\theta_{ps}\sin\theta_{ys} + \cos\theta_{ys}\cos\theta_{ps}\sin\theta_{RS})\Big]$$

$$T_{3,23} = 3\dot{\eta}^2 (I_z - I_x)\left[\cos\theta_{ps}\cos\theta_{RS}\left(\cos\theta_{ps}\sin\theta_{ys} - \cos\theta_{ys}\sin\theta_{ps}\sin\theta_{RS}\right) - \sin\theta_{ps}\cos\theta_{RS}\left(\sin\theta_{ps}\sin\theta_{ys} + \cos\theta_{ys}\cos\theta_{ps}\sin\theta_{RS}\right)\right]$$

$$T_{3,31} = \dot{\eta}^2 (I_x - I_y)\left[\tfrac{1}{2}\cos\theta_{ys}\sin 2\theta_{RS} + 3\cos\theta_{ps}\cos\theta_{RS}\left(\sin\theta_{ys}\sin\theta_{ps} + \cos\theta_{ys}\cos\theta_{ps}\sin\theta_{RS}\right)\right]$$

$$T_{3,32} = \dot{\eta}^2 (I_x - I_y)\left[\sin\theta_{ys}\cos 2\theta_{RS} + 3\sin\theta_{ys}\cos^2\theta_{ps}\cos^2\theta_{RS} - 3\sin\theta_{RS}\cos\theta_{ps}\left(\sin\theta_{ys}\cos\theta_{ps}\sin\theta_{RS} - \sin\theta_{ps}\cos\theta_{ys}\right)\right]$$

$$T_{3,33} = 3\dot{\eta}^2 (I_y - I_x)\left[\sin\theta_{ps}\cos\theta_{RS}\left(\sin\theta_{ys}\cos\theta_{ps}\sin\theta_{RS} - \sin\theta_{ps}\cos\theta_{ys}\right) + \cos\theta_{ps}\cos\theta_{RS}\left(\sin\theta_{RS}\sin\theta_{ps}\sin\theta_{ys} + \cos\theta_{ps}\cos\theta_{ys}\right)\right]$$

$$T_{4,11} = -b_x\cos\theta_{ps}\cos\theta_{RS}$$

$$T_{4,12} = -b_x\sin\theta_{ps}\cos\theta_{RS}$$

$$T_{4,13} = b_x\sin\theta_{RS}$$

$$T_{4,21} = -b_y\cos\theta_{ps}\sin\theta_{RS}\sin\theta_{ys} + b_y\sin\theta_{ps}\cos\theta_{ys}$$

$$T_{4,22} = -b_y\cos\theta_{ps}\cos\theta_{ys} - b_y\sin\theta_{ps}\sin\theta_{RS}\sin\theta_{ys}$$

$$T_{4,23} = -b_y\cos\theta_{RS}\sin\theta_{ys}$$

$$T_{4,31} = -b_z\sin\theta_{ps}\sin\theta_{ys} - b_z\cos\theta_{ps}\sin\theta_{RS}\cos\theta_{ys}$$

$$T_{4,32} = -b_z\sin\theta_{ps}\sin\theta_{RS}\cos\theta_{ys} - b_z\cos\theta_{ps}\sin\theta_{ys}$$

$$T_{4,33} = -b_z\cos\theta_{RS}\cos\theta_{ys} \qquad \text{where} \quad b_x = b_y = b_z = b$$

39(d)

Proceeding similarly, the linearised homogeneous form of eqn (12) can be expressed as

$$[S_1]\ddot{\underline{\phi}}' + [S_2]\dot{\underline{\phi}}' + [S_3]\underline{\phi}' + [S_4]\underline{\phi} = [0] \qquad (40)$$

The element of the matrices $[S_i]$, $i = 1-4$ are as follows

$$\begin{aligned}
S_{1,11} &= I_x' \\
S_{1,12} &= 0 \\
S_{1,13} &= -I_x' \sin\theta_{RS}' \\
S_{1,21} &= 0 \\
S_{1,22} &= I_y' \cos\theta_{yS}' \\
S_{1,23} &= I_y' \sin\theta_{yS}' \cos\theta_{RS}' \\
S_{1,31} &= 0 \\
S_{1,32} &= -I_z' \sin\theta_{yS}' \\
S_{1,33} &= I_z' \cos\theta_{yS}' \cos\theta_{RS}'
\end{aligned} \qquad (41a)$$

$$\begin{aligned}
S_{2,11} &= b \\
S_{2,12} &= \dot{\eta}\left[(I_z' - I_y')\cos 2\theta_{yS}' - I_x'\right]\cos\theta_{RS}' \\
S_{2,13} &= \dot{\eta}\left[I_z' - I_y'\right]\cos^2\theta_{RS}'\sin 2\theta_{yS}' - b\sin\theta_{RS}' - \dot{\theta}_{RS}' I_x' \cos\theta_{RS}' \\
S_{2,21} &= \dot{\eta}\left(I_y' + I_x' - I_z'\right)\cos\theta_{RS}'\cos\theta_{yS}' \\
S_{2,22} &= \dot{\eta}\left(I_x' - I_z' - I_y'\right)\sin\theta_{yS}'\sin\theta_{RS}' + b\cos\theta_{yS}' \\
S_{2,23} &= \dot{\eta}(I_z' - I_x')\cos\theta_{yS}'\sin 2\theta_{RS}' + b\sin\theta_{yS}'\cos\theta_{RS}' \\
&\quad - \dot{\theta}_{RS}' I_y' \sin\theta_{yS}'\sin\theta_{RS}'
\end{aligned} \qquad (41b)$$

$$S_{2,31} = \dot{\eta}\,(I_y' - I_x' - I_z')\,\sin\theta_{ys}'\cos\theta_{RS}'$$

$$S_{2,32} = \dot{\eta}\,(I_x' - I_y' - I_z')\cos\theta_{ys}'\sin\theta_{RS}' - b\sin\theta_{ys}'$$

$$S_{2,33} = \dot{\eta}\,(I_x' - I_y')\sin 2\theta_{RS}'\sin\theta_{ys}' + b\cos\theta_{ys}'\cos\theta_{RS}' - \dot{\theta}_{RS}'\,I_z'\cos\theta_{ys}'\sin\theta_{RS}'$$

$$S_{3,11} = (\dot{\eta})^2(I_z - I_y)\cos^2\theta_{RS}'\cos 2\theta_{ys}' + T_{xx}$$

$$S_{3,12} = \tfrac{1}{2}\dot{\eta}^2\,(I_y' - I_z')\sin 2\theta_{ys}'\sin 2\theta_{RS}' + \dot{\theta}_{RS}'\,I_x'\dot{\eta}\sin\theta_{RS}'$$

$$S_{3,13} = 0$$

$$S_{3,21} = \tfrac{1}{2}\dot{\eta}^2\,(I_x' - I_z')\sin\theta_{ys}'\sin 2\theta_{RS}' - \dot{\eta}\,I_y'\,\dot{\theta}_{RS}'\sin\theta_{RS}'\cos\theta_{ys}' \qquad (41c)$$

$$S_{3,22} = \dot{\eta}^2\,(I_z' - I_x')\cos\theta_{ys}'\cos 2\theta_{RS}' + T_{yy}$$

$$S_{3,23} = 0$$

$$S_{3,31} = \tfrac{1}{2}\dot{\eta}^2\,(I_x' - I_y')\cos\theta_{ys}'\sin 2\theta_{RS}' + \dot{\theta}_{RS}'\,I_z'\dot{\eta}\sin\theta_{RS}'\sin\theta_{ys}'$$

$$S_{3,32} = \dot{\eta}^2\,(I_x' - I_y')\sin\theta_{ys}'\cos 2\theta_{RS}'$$

$$S_{3,33} = T_{zz}$$

$$S_{4,11} = -b_x\cos\theta_{ps}'\cos\theta_{RS}'$$

$$S_{4,12} = -b_x\sin\theta_{ps}'\cos\theta_{RS}' \qquad (41d)$$

$$S_{4,13} = b_x\sin\theta_{RS}'$$

$$S_{4,21} = -b_y\cos\theta_{ps}'\sin\theta_{RS}'\sin\theta_{ys}' + b_y\sin\theta_{ps}'\cos\theta_{ys}'$$

$$S_{4,22} = -b_y\cos\theta_{ps}'\cos\theta_{ys}' - b_y\sin\theta_{ps}'\sin\theta_{RS}'\sin\theta_{ys}'$$

$$S_{4,23} = -b_y\cos\theta_{RS}'\sin\theta_{ys}'$$

$$S_{4,31} = -b_z\sin\theta_{ps}'\sin\theta_{ys}' - b_z\cos\theta_{ps}'\sin\theta_{RS}'\cos\theta_{ys}'$$

$$S_{4,32} = -b_z\sin\theta_{ps}'\sin\theta_{RS}'\cos\theta_{ys}' - b_z\cos\theta_{ps}'\sin\theta_{ys}'$$

$$S_{4,33} = -b_z\cos\theta_{RS}'\cos\theta_{ys}' \qquad \text{where } b_x = b_y = b_z = b$$

In view of eqns (21) and (37), it is evident that the coefficient matrices $[T_i]$ and $[S_i]$, $i = 1,4$, of eqns (38) and (40) contain time dependent terms. Since these terms are small and since the time constant of the dependent variables are in the order of twenty or more orbits, these time dependent terms in eqns (38) and (40) are replaced by their average value over one orbit. This procedure converts the equations (38) and (40) into equations with constant coefficients.

Let the state vector be defined as

$$\underline{u}(t) = \left[\underline{\Phi}, \underline{\Phi}', \dot{\underline{\Phi}}, \dot{\underline{\Phi}}' \right]^T \tag{42}$$

Then eqns (38) and (40) can be combined to yield

$$[A]\,\dot{\underline{u}} + [B]\,\underline{u} = [\underline{0}] \tag{43}$$

The (12 x 12) matrices **A** and **B** are defined as

$$[A] = \begin{bmatrix} [I] & [0] & [0] & [0] \\ [0] & [I] & [0] & [0] \\ [0] & [0] & [T_1] & [0] \\ [0] & [0] & [0] & [S_1] \end{bmatrix} \tag{44}$$

$$[B] = \begin{bmatrix} [0] & [0] & -[I] & [0] \\ [0] & [0] & [0] & -[I] \\ [T_3] & [0] & [T_2] & [T_4] \\ [0] & [S_3] & [S_4] & [S_2] \end{bmatrix} \qquad (45)$$

where $[0]$ = the null matrix.

$[I]$ = the identity matrix.

Let $[C]$ be the 12×12 matrix defined by

$$C = -A^{-1} B \qquad [46]$$

The time constants and the Garber stability boundaries of the spacecraft-magnet system are obtained by computing the eigen values of the matrix C

APPENDIX B

The following is a list of inputs that were common to all the steady state simulation runs. Features differentiating one run from the other are discussed in Section 4.2.

Initial Attitude Error = 0 degrees on all axes

Initial Attitude Rates = Orbit rate in pitch; 0 degrees/sec in roll & yaw

Rt. ascension of ascending node = 210°

Time of the year = Winter Solstice

Orbit Inclination = 28.5°

Orbit Eccentricity = .002

Moments of Inertia of Spacecraft (Slug - ft^2)

I_{Roll} = 53700 ; I_{Pitch} = 54800 ; I_{Yaw} = 19200

(no products of inertia were considered)

Damper Magnet strength 225000 pole cm

F 10.7 Solar activity index 200

Geomagnetic Index K_p 3.54

No. of flat plates used to model the S/C: 14 (12 plates each 3.7736' by 30.166' and 2 end plates each 14.0833 ft. in diameter)

APPENDIX C

EFFECT OF A DISTURBANCE CAUSED BY A TORQUE IMPULSE

Consider the spacecraft to be an undamped torsional pendulum

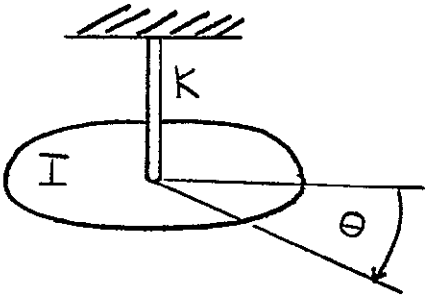

The equation of motion is

$$T = I\ddot{\Theta} + K\Theta \qquad (1)$$

where T = disturbance torque
I = moment of inertia
K = gravity gradient stiffness

Divide by I and let $\omega_n^2 = \frac{K}{I}$

$$\ddot{\Theta} + \omega_n^2 \Theta = \frac{T}{I} \qquad (2)$$

Take the Laplace transform assuming T is a step function

$$\Theta\,(s^2+\omega_n^2) = \frac{T}{Is} \qquad (3)$$

$$\Theta(s) = \frac{\frac{T}{I}}{s(s^2+\omega_n^2)} \qquad (4)$$

The inverse transform of eq. (4) yields

$$\theta(t) = \frac{T}{I\omega_n^2}\,(1-\cos\omega_n t) \qquad (5)$$

IF the torque is removed at time t_F the equation of motion is

$$\ddot{\theta} + \omega_n^2\,\theta = 0 \qquad (6)$$

Find the position and rate at time t_F. From eq (5)

$$\theta(t_F) = \frac{T}{I\omega_n^2}\,(1-\cos\omega_n t_F) \qquad (7)$$

Differentiating eq (7)

$$\dot{\theta}(t_F) = \frac{T}{I\omega_n}\,(\sin\omega_n t_F) \qquad (8)$$

The solution of eq (6) is

$$\theta(t) = A\,\sin(\omega_n t + \phi) \qquad (9)$$

$$\dot{\theta}(t) = A\,\omega_n\cos(\omega_n t + \phi) \qquad (10)$$

The maximum value of $\theta(t)$ is A. It is not necessary to find the value of ϕ.

Substitute the initial conditions from eqs. (7) and (8) into eqs. (9) and (10).

$$\frac{T}{I\omega_n^2}\left(1-\cos\omega_n t_F\right) = A\sin\left(\omega_n t+\phi\right) \quad (11)$$

$$\frac{T}{I\omega_n}\sin\omega_n t_F = A\,\omega_n\cos\left(\omega_n t+\phi\right) \quad (12)$$

Divide eq (12) by ω_n and square

$$\left(\frac{T}{I\omega_n^2}\right)^2\sin^2\omega_n t_F = A^2\cos^2\left(\omega_n t+\phi\right) \quad (13)$$

Square eq. (11)

$$\left(\frac{T}{I\omega_n^2}\right)^2\left(1-\cos\omega_n t_F\right)^2 = A^2\sin^2\left(\omega_n t+\phi\right) \quad (14)$$

Add eqs (13) and (14)

$$\left(\frac{T}{I\omega_n^2}\right)^2\left[\sin^2\omega_n t_F+\left(1-\cos\omega_n t_F\right)^2\right] = A^2 \quad (15)$$

Simplifying

$$\frac{2T^2}{I^2\omega_n^4}\left(1-\cos\omega_n t_F\right) = A^2 \quad (16)$$

Solving for A

$$A = \frac{T}{I\omega_n^2}\left[2\left(1-\cos\omega_n t_F\right)\right]^{\frac{1}{2}} \quad (17)$$

The series expansion for $\cos\omega_n t_F$ is

$$\cos\omega_n t_F = 1-\frac{\left(\omega_n t_F\right)^2}{2!}+\frac{\left(\omega_n t_F\right)^4}{4!}-\ldots \quad (18)$$

For $\omega_n t_F \ll 1$

$$\cos \omega_n t_F \approx 1 - \frac{\omega_n^2 t_F^2}{2} \qquad (19)$$

Substituting eq (19) into eq. (17) yields

$$A = \frac{T}{I\omega_n^2}\left[2\left(1 - 1 + \frac{\omega_n^2 t_F^2}{2}\right]^{\frac{1}{2}} \qquad (20)$$

$$\boxed{A = \frac{T\, t_F}{I\, \omega_n}} \qquad (21)$$

GENERAL ELECTRIC

Space Division

Headquarters: Valley Forge, Pennsylvania ☐ Daytona Beach, Fla. ☐ Evendale, Ohio

☐ Huntsville, Ala. ☐ Bay St. Louis, Miss. ☐ Houston, Texas ☐ Sunnyvale, Calif.

☐ Beltsville, Md. ☐ Tacoma, Wash. ☐ Palmdale, Calif. ☐ Bedford, Mass.

☐ Washington, D.C. Area